Bank Runs and Market Value Solvency *

Lucas Belmudes† **Angelo Mendes**‡

Job Market Paper

November 1, 2026

Updated frequently, most recent version can be found here.

Abstract

Interest rate hikes lower long-duration government bond prices. Yet capital requirements treat government bonds as risk-free regardless of their maturity. Abrupt rate hikes were a determining factor during the 2023 regional banking crisis. We study a dynamic model in which banks choose dividends and a portfolio of short and long bonds. Long bonds hedge fluctuations of deposit spreads while depositors stay in the bank, but make banks exposed to runs when rates rise. Uninsured depositors play a coordination game that makes runs likely when banks are poorly capitalized. Deposit insurance is financed by taxes on surviving banks, and affects depositors' payoffs, changing their incentives to run. We use U.S. Call Reports for 2010–2025 to calibrate the model and match the cross-sectional demand for long-bond holdings. We then evaluate a capital requirement that assign risk weights to long-bond holdings and uninsured deposits. Along the observed rate path, a weight of 30% on uninsured deposits reduces deposits at failing banks by 15%. For at least half of the rate paths, however, the same rule increases deposits at failing banks, because it imposes losses after rates fall.

*We thank Manuel Amador, Marco Bassetto, and Tim Kehoe for their guidance during this project. We also thank Zach Bethune, Anmol Bhandari, Saki Bigio, Rafael Berriel, Hasan Cetin, Dean Corbae, Miguel Faria-e-Castro, Jason Hall, Kyle Herkenhoff, Illenin Kondo, Fernando Lopes, Guillermo Ordonez, Victor Orestes, Kjetil Storesletten, David Yang, and the participants in the Trade Workshop at the University of Minnesota, the UMN-UW Graduate Student Workshop, the Society for Advancements in Economic Theory (Rio de Janeiro, 2026), Rice University, and the Minnesota Jamboree for their comments and suggestions. All errors are our own.

†belmu002@umn.edu: University of Minnesota.

‡mende449@umn.edu: University of Minnesota.

1 Introduction

Banks face three main risks: credit risk, liquidity risk, and interest-rate risk. The last gained prominence with the 2023 regional banking crisis, marked by the failures of Silicon Valley Bank (SVB), Signature Bank, and First Republic. As interest rates rose, the market value of banks' long-duration securities fell, weakening their ability to meet withdrawals by uninsured depositors. Yet these same assets that were a source of fragility in 2023 also hedge against fluctuations in deposit spreads: when short-term rates fall, and deposit margins compress, long-bond valuations partly offset the loss. The SVB episode reignited the debate on bank regulation and raised concerns over the treatment of interest-rate risk. As emphasized by Metrick (2024), this risk was not adequately incorporated into the supervisory framework facing U.S. banks in 2023. Our goal is to understand how run risk shapes banks' demand for long-duration securities and to study the implications of imposing limits on U.S. banks' long-bond holdings.

We develop a model in which banks face fluctuations in deposit spreads from aggregate shocks to the Fed Funds rate, pay operating costs, pay taxes to fund the FDIC, choose dividend payouts and a portfolio of short- and long-duration bonds among their liquid assets, and are exposed to runs. We assume that in normal times deposits are sticky, and banks pay deposit rates below the Fed Funds rate, so deposit spreads comove with short-term interest rates. In this case, deposits behave as a long-term liability, and this comovement creates a hedging demand for long bonds: when rates fall, and deposit margins shrink, long bonds pay off (Di Tella and Kurlat, 2021).

Banks' portfolio and payout decisions determine the evolution of the bank's market-value net worth and can leave it poorly capitalized or insolvent, making it vulnerable to runs. We model runs as a coordination game among uninsured depositors. The resulting equilibrium in the depositors' game determines the run hazard rate and is affected by FDIC coverage: higher coverage reduces incentives for depositors to run, reducing the run risk banks face. When a bank has large amounts of uninsured deposits relative to its net worth, the run probability is high. When the bank is well capitalized, that is, it has enough net worth against its uninsured depositors, the run probability is small. When a run occurs, the bank loses its franchise value: it can no longer earn profits by leveraging its equity with low-cost deposits or by originating loans that earn a spread.

In our model, run risk interacts with banks' hedging demand for long bonds. Lower capitalization implies a higher risk of uninsured depositors running, which correspondingly shortens the duration of deposits and reduces the share of long bonds in a bank's portfo-

lio. Well-capitalized banks face almost no run risk and have a small share of their assets funded by deposits, so they demand fewer long bonds to hedge. The hedging motive is stronger for banks with intermediate solvency. For these banks, the marginal value of net worth is highly dependent on the rates: for high rates, deposit spreads are high, and the bank expects to move away from risk of runs, whereas when rates are low, compressed deposit spreads and operating costs drag the bank into a region where runs are more likely. Because long bonds pay precisely in these low-rate states, they insure intermediate solvency banks exactly when an additional dollar of net worth is most valuable. Therefore, intermediate banks hold more long bonds in a world where they face run risk.

Using quarterly Call Reports for U.S. commercial banks, we document that such a non-monotonic relationship between the share of long bonds and bank capitalization is also present in the data. We look at banks with more than $1.5 billion in assets from 2010 to 2025, and map the model's balance-sheet objects into their data counterparts. We measure market-value net worth as book equity plus unrealized gains and losses on held-to-maturity securities, and scale it by uninsured deposits to obtain a mark-to-market solvency ratio, a measure of the solvency buffer per dollar of runnable funding. The long-bond share is the fraction of liquid assets with some duration exposure, namely securities that mature or reprice after three months. This share is hump-shaped in the solvency ratio: it rises with solvency among fragile banks. It falls with solvency among well-capitalized banks, so long bonds are concentrated among banks with intermediate solvency buffers. The pattern survives time and bank fixed effects and standard balance-sheet controls, and it is the main target of our calibration.

Our model has two main sources of inefficiency that justify policy intervention. First, FDIC coverage generates a standard fiscal externality. Although banks internalize the effects of their portfolios on their probability of suffering runs, they do not internalize that this portfolio decision may expose the remaining banks to higher taxes, which may increase their run probability as well. Second, runs are a coordination failure among depositors, which destroys the franchise of banks that would have survived had depositors stayed.

We use the calibrated model to evaluate two policies. First, we study limits on long-bond holdings: at every date, each bank must hold enough net worth to absorb a 100 basis point rise in rates without falling below a floor proportional to its uninsured deposits. The rule caps the long-bond share, more tightly for less solvent banks, and is equivalent to a capital requirement that, unlike current rules, assigns a positive risk weight to long bonds and uninsured deposits. We impose the rule from 2010 onward, starting from the cross-

section of banks in the 2010Q1 Call Reports, and evaluate it along the observed path of short rates through 2025 and along the rate paths the model generates after 2021. Along the observed path, which includes the 2022–2023 hiking cycle, a floor of 30% of uninsured deposits reduces deposits at failing banks by 15%. *Ex-ante*, the policy would have reduced deposits involved in failures for half of the simulated rate paths. Still, it would have generated welfare losses to banks, which would be obliged to bear fluctuations in their deposit spreads. Second, we evaluate increasing FDIC coverage for uninsured depositors from 0 to 3.5%. This policy is more effective than a modified capital requirement that assigns risk weights to long-bonds. The increase in depositor protection reduces depositors' incentives to run, and the reduction in run probability generates welfare gains for banks. Banks would gladly pay the FDIC premium for this reduction in run probabilities.

Related Literature. Our paper relates to the literature on banks' exposure to interest rates. Di Tella and Kurlat (2021) show that banks' demand for long-duration assets reflects a dynamic hedging motive: banks accept losses when rates rise because higher deposit spreads improve their future profits. Other papers have studied how this mechanism leads to an increase in the duration held by US banks due to low interest rates, and low term-premium (Schneider, 2026; Mertens et al., 2026). Related work studies how low rates and deposit market power affect bank profitability, risk-taking, and monetary policy transmission (Wang, 2025; Whited et al., 2021; Wang et al., 2022). Abad et al. (2026) show that heterogeneity in interest-rate exposure matters for monetary transmission when banks approach their solvency constraints. Our calibration also reflects a low-rate environment and a low, average term premium. We add to this literature by studying how dynamic hedging interacts with run risk. Run exposure depends on net worth relative to uninsured deposits, and on deposit insurance coverage, shaping the demand for long bonds across the solvency distribution.

We contribute to the literature on the regulation of banks' interest-rate risk.[1] Begenau et al. (2026) study microprudential regulation in a model of heterogeneous banks choosing portfolios and funding under endogenous run risk. Miao et al. (2023) study long-term securities and banking crises in a DSGE model with a representative bank. Varraso (2025) is the closest to our paper, and studies maturity choice and regulation in a quantitative

[1]For broader quantitative models of heterogeneous banks and banking regulation, see Corbae and D'Erasmo (2021) on capital buffers and banking industry dynamics, Jamilov and Monacelli (2026) on bank heterogeneity and aggregate fluctuations, and Begenau and Landvoigt (2022) on regulation and the allocation of activity between commercial and shadow banks.

model of heterogeneous banks with endogenous leverage and default. As in our model, capitalization affects banks' willingness to hold long assets: poorly capitalized banks limit duration exposure to preserve franchise value. In his framework, maturity choices balance excess returns against default risk and balance-sheet constraints. We emphasize the additional role of long bonds as a hedge against fluctuations in deposit spreads, as in Di Tella and Kurlat (2021). The interaction between hedging and runs is what generates the hump-shaped portfolio pattern that we document in the data and disciplines our calibration and creates a trade-off to a policy that restricts long bond holdings: this restriction reduces valuation losses when rates rise but weakens banks' insurance against low deposit cash flows. Besides that, the fact our model features endogenous runs generates important welfare consequences, as those runs result from a coordination failure that policies can mitigate.

Our model also builds on the literature linking banks' ex ante choices and runs. Ennis and Keister (2003) embed runs in a dynamic growth model and study an equilibrium-selection rule under which banks' portfolios affect run probabilities. Ennis and Keister (2006) show that run risk can increase or decrease long-term investment, depending on liquidation costs. We study a distinct channel: the risk of runs alter banks' demand to hedge deposit-spread income against interest-rate shocks, generating non-monotonic securities holdings across the solvency distribution. Our quantitative model matches this pattern and allow us to evaluate the welfare consequences of policies that restrict banks' portfolio choices.

A related strand studies runs on banks' franchise value. Amador and Bianchi (2024) and Drechsler et al. (2026) emphasize that a bank's franchise is valuable while the bank operates but cannot be liquidated to meet withdrawals. Jiang et al. (2024) show how losses on long assets can expose banks to self-fulfilling solvency runs even when their balance-sheet assets are liquid. We share the view that a run destroys the bank's ability to earn future profits from deposit funding and lending. To microfound the runs we rely on the long tradition of the global games literature (Carlsson and Van Damme, 1993; Morris and Shin, 1998, 2003; Goldstein and Pauzner, 2005), and embed a coordination game among depositors in a dynamic model (De Groot, 2021; Ikeda and Matsumoto, 2026). To add to this literature, we bring the insights from Ennis and Keister (2009), and study how an ex-post intervention (FDIC coverage) creates incentives that affect self-fulfilling runs (see also Dávila and Goldstein, 2023; Pancost and Robatto, 2026). In our framework, deposit insurance affects depositors' payoffs and equilibrium withdrawal strategies, linking coverage to the run hazard and banks' portfolio and payout decisions.

The treatment of deposit flows connects our model to Bolton et al. (2025), who study dy-

namic banking when banks cannot freely adjust their deposit base, and Fleckenstein et al. (2026), who show how depositor inattention shapes deposit values, interest-rate exposure, and runoff risk. We also distinguish ordinary deposit flows from a run, a discrete jump on banks' deposit base. Banks take normal inflows and outflows as given, while their balance sheets affect the probability of a coordinated withdrawal. The inability to shrink deposits immediately after losses in securities makes capitalization shocks a persistent source of run exposure and affect the value of hedging them.

Finally, our paper builds on the empirical finance literature on banks' interest-rate exposure. Drechsler et al. (2021) show how deposit spreads can offset the interest-rate exposure of long assets. DeMarzo et al. (2025) show that negative franchise duration is not guaranteed once operating costs and lending income are included. Our mechanism concerns hedging deposit cash flows rather than matching the duration of franchise market value. Jiang et al. (2024) document banks' mark-to-market losses and the role of uninsured funding in run vulnerability, motivating our solvency measure. Haddad et al. (2023) use a related measure of mark-to-market equity normalized by assets and emphasize the non-linear interest-rate exposure arising from depositor relationships. We document an additional fact: long-bond holdings are non-monotonic in market-value solvency and concentrated among banks with intermediate solvency buffers. We match this cross-sectional demand for long bonds through the interaction of cash-flow hedging and run risk.

Layout. The remainder of this paper is organized as follows. Section (2) presents the model. Section (3) describes the data, maps the model's balance-sheet objects into Call Report variables, and documents the cross-sectional demand for long bonds that disciplines the model. Section (4) presents the calibration, the model's fit, and a validation exercise based on insured deposits. Section (5) uses the model to evaluate limits on long-bond holdings. Section (6) concludes.

2 Model

2.1 Environment

Time is continuous, indexed by $t \geq 0$, and the horizon is infinite. The domestic economy is populated by a deposit insurance fund, a continuum of risk-neutral depositors (indexed by h) of measure $H > 1$, a continuum of banks (indexed by i) of measure one, each owned by a banker who has preferences over dividend payouts c_{it}, paid in units of a

consumption good. The banker has a utility function of the form:

$$u(c_{it}) = \frac{(Y + c_{it})^{1-\gamma} - Y^{1-\gamma}}{1-\gamma} \tag{1}$$

where $Y \geq 0$ is a utility shifter that sets utility to zero at zero consumption, and γ is the coefficient of relative risk aversion. A concave utility for bankers is a reduced form approach to capture the fact that firms, and banks in particular, smooth dividends over time. We interpret Y as bankers' external source of income (Heaton and Lucas, 2000; Herranz et al., 2015), which guarantees a bounded payoff to bankers' under zero dividend payouts, and allows for equity issuances ($c_{it} > -Y$).

The supply of the consumption good is exogenous, and such that its price P_t grows at a constant inflation rate ι. Through the paper we assume away inflation risk, which allows us to isolate banks' exposure to interest rate movements. We denote by the short term nominal rate by r_t, which makes the real short rate equal to $r_t - \iota$.

An outside investor prices traded assets through the stochastic discount factor (SDF) process

$$\frac{dM_t}{M_t} = -r_t\, dt + \varsigma\, dB_t, \tag{2}$$

where B_t is a standard Brownian motion and ς is the (constant) price of aggregate risk. There are two traded assets. The first is a short bond with instantaneous return r_t, so that

$$\frac{dP_t^S}{P_t^S} = r_t\, dt.$$

The nominal short rate follows an exogenous mean-reverting process in the spirit of Vasicek (1977).

$$dr_t = \theta_r(\bar{r} - r_t)\, dt + \sigma_r\, dB_t, \tag{3}$$

with $\theta_r > 0$. Importantly, the same aggregate shock dB_t drives both the SDF and the short rate. The second asset is a long-duration security:

Proposition 1 (Long-bond return)**.** *Let $P_t^L(\mathcal{H}) \equiv L(r_t, \mathcal{H})$ be the price of a zero-coupon bond maturing in a horizon of $\mathcal{H}$ periods. The return of such bond is:*

$$\frac{dL}{L} = \Big(r_t + \varsigma\sigma_r \mathcal{D}(\mathcal{H})\Big)\, dt - \sigma_r \mathcal{D}(\mathcal{H})\, dB_t, \tag{4}$$

Where $\mathcal{D}$ is given by:

$$\mathcal{D}(\mathcal{H}) = \frac{1 - e^{-\theta_r \mathcal{H}}}{\theta_r}$$

Proof. Appendix (A.1). □

First notice that longer bonds (higher $\mathcal{H}$) have higher duration $\mathcal{D}(\mathcal{H})$, and therefore higher exposure to the dB_t shock. The diffusion term is negative: when $dB_t > 0$ (a rate-hike shock), the long bond earns a *low* return (because of its duration). If $dB_t > 0$ is bad news in (2), investors would require compensation to hold the long bond, generating a positive term premium [2]. Through the paper, we will consider a long bond with a maturity of $\mathcal{H} \to \infty$ to represent an interest-rate risk factor, in Section (4) we will calibrate the return of the long bond to match the average five-year term premium in the data (Begenau et al., 2026, Begenau et al., 2025), and will omit it from the notation for simplicity from now on. Define:

$$\pi \equiv \varsigma \sigma_r / \theta_r, \qquad \sigma \equiv \sigma_r / \theta_r. \tag{5}$$

2.2 Bank balance sheets

Asset side. Banks are indexed by their individual state $(n_{it}, x_{it}, \ell_{it})$, where n_{it} is the bank's net worth, x_{it} denotes uninsured deposits, both in real units, and $\ell_{it} \in [0, 1]$ is the share of assets invested in loans. We will denote the distribution of active banks at time t by g_t. Total assets are financed with net worth and uninsured deposits, so

$$\text{Total Assets}_{it} = n_{it} + x_{it}. \tag{6}$$

The asset side is split between loans and liquid securities. A bank i has a loan share $\ell_{it} = \ell_i$, fixed over time.

$$\text{Total Loans}_{it} = \ell_i (n_{it} + x_{it}),$$

We interpret this as a bank specific technology determining the scale of a bank's lending operations. In Appendix (B.9) we show that the loan share is stable over time and across banks. The remaining share $1 - \ell_i$ is invested in liquid securities,

$$\text{Liquid Assets}_{it} = (1 - \ell_i)(n_{it} + x_{it}).$$

[2] In Appendix (B.8) we show that the average five-year term premium is negative in our sample, which maps to the constant term π in our model.

Within liquid securities, the bank chooses a share α_{it} to long bonds and a share $1 - \alpha_{it}$ to short bonds. Therefore, the total amount invested in long bonds is

$$\text{Long bonds}_{it} = \alpha_{it}(1 - \ell_i)(n_{it} + x_{it}),$$

and the total assets invested in short bonds is

$$\text{Short bonds}_{it} = (1 - \alpha_{it})(1 - \ell_i)(n_{it} + x_{it}).$$

The short bond earns the instantaneous return r_t. The return process for long bonds is given by (4). Loans are illiquid assets and earn a flow return

$$r_t + \xi,$$

where ξ is a parameter representing the loan spread. This loan spread is part of the bank's franchise value: an operating bank has access to a loan technology that generates excess returns. A run destroys this part of the franchise. We capture this by assuming that the loan share evolves according to

$$d\ell_i = -(1 - J_{it})\ell_i \, dJ_{it}. \tag{7}$$

When a run occurs, $dJ_{it} = 1$, deposits are withdrawn and the bank loses its ability to operate the loan franchise, so ℓ_i jumps to zero. Here J_{it} records the run event, whose intensity is derived below.

Uninsured deposits. The bank finances assets with net worth and uninsured deposits. Deposits are valuable because they allow the bank to lever its equity and expand its asset portfolio at a low funding cost. Depositors are paid

$$r_t^x = \beta r_t, \qquad \beta \in (0, 1),$$

so the bank earns a funding spread $r_t - r_t^x = (1 - \beta)r_t$ on each unit of deposit funding. This funding spread is part of the bank's franchise value. While the bank is operating normally ($J_{it} = 0$), deposits are constant $x_{it} = x_i$. A run ($dJ_{it} = 1$) is a jump on the amount of deposits in the bank:

$$dx_{it} = (1 - J_{it-})[-x_{it-} \, dJ_{it}], \tag{8}$$

where x_{it-} denotes deposits immediately before a jump. Once a bank suffers a run it has zero deposits forever.

2.3 Depositors

Each bank has a continuum of atomistic, risk-neutral depositors indexed by h, and as long as there are no runs, they behave according to (8). Those depositors get coordination opportunities that arrive at Poisson rate $\lambda_0 > 0$. At each opportunity, the bank's balance sheet is fixed at assets $n + x$, and depositors simultaneously choose whether to request withdrawal or stay. Let $\mathcal{W} \in [0, 1]$ denote the fraction requesting withdrawal.

Information. At a coordination opportunity, banks have draw a shock η_{it} which captures an additional access to funds through under short notice. In practice, banks can borrow against their assets from the Federal Home Loan Banks or the discount window, borrow in repo markets, or issue equity, and the terms of these sources vary across stress episodes [3]. After the additional funding shock, the bank's ability to meet withdrawals is given by:

$$z_{it} = \frac{n_{it}}{x_{it}} + \sigma_\eta \eta_{it}, \qquad \sigma_\eta > 0, \tag{9}$$

A depositor h observes a private signal about bank i:

$$s_{hit} = z_{it} + \sigma_\varepsilon \varepsilon_{hit}, \tag{10}$$

where $\sigma_\varepsilon > 0$, and the errors ε_{hit} are independent and uniform on $[-1, 1]$. with η_{it} independent of the private errors and independently redrawn at each opportunity. Conditional on public bank information, z_{it} has a continuously differentiable, strictly positive density f_z. Depositors do not observe z directly, but know the prior distribution f_z. The FDIC observes z when applying the closure rule after requests have been submitted. We omit the subscripts h, i, and t where they are unnecessary.

Failure and payments. Securities are liquid and can be sold at par, while loans are sold at a fire sale discount $\delta \in (0, 1)$ per dollar. At the coordination opportunity, the bank's liquidation capacity is

$$x[1 - \ell(1 - \delta)](1 + z). \tag{11}$$

[3] For instance, Silicon Valley Bank announced a capital raise on March 8, 2023, which failed the next day, and the bank was closed on March 10. First Republic received $30 billion in deposits from large banks on March 16, 2023, borrowed heavily from the Federal Reserve and the Federal Home Loan Banks, and was not closed until May 1.

When $\eta = 0$, this equals $(1-\ell)(n+x) + \delta\ell(n+x)$. Depositors request withdrawal simultaneously, and before any withdrawal is executed, the bank fails if and only if

$$z < \underline{z} \quad \text{or} \quad \mathcal{W} > [1 - \ell(1-\delta)](1+z), \tag{12}$$

where $\underline{z} \in (0,1)$ is a net worth floor beyond which closure happens regardless of withdrawal requests, that is, for a sufficiently low solvency, the FDIC shuts the bank down. Above that floor, failure depends on withdrawals relative to capacity. If neither condition holds, requests can be paid in full and the bank continues. Upon failure, none of the withdrawal requests is executed before resolution, leaving the balance sheet intact.

In resolution, we assume the banker retains assets worth n, taken proportionally from securities and loans, which he can hold without a forced sale. The remaining assets have market value x and loan share ℓ. Remaining assets yield $[1 - \ell(1-\delta)]x$[4]. The insurance fund pays each depositor ζ per dollar of her original claim, whether she requested withdrawal or stayed, and has no claim on the remaining assets. We restrict $0 \leq \zeta < \ell(1-\delta)$, so insurance and liquidation proceeds together fall short of total deposit claims.

The proceeds from the remaining assets pay requesters' remaining $(1-\zeta)\mathcal{W}x$ claims first, and then stayers' remaining $(1-\zeta)(1-\mathcal{W})x$ claims, pro rata within each group. The respective recovery fractions on these remaining claims are

$$\mathcal{R}(\mathcal{W}) = \min\left\{1, \frac{1-\ell(1-\delta)}{(1-\zeta)\mathcal{W}}\right\}, \qquad \mathcal{W} > 0, \tag{13}$$

and

$$\mathcal{S}(\mathcal{W}) = \frac{\max\{0, 1-\ell(1-\delta) - (1-\zeta)\mathcal{W}\}}{(1-\zeta)(1-\mathcal{W})}, \qquad \mathcal{W} < 1. \tag{14}$$

An atomistic requester at $\mathcal{W} = 0$ is paid in full, $\mathcal{R}(0) = 1$; an atomistic stayer at $\mathcal{W} = 1$ receives no payment from the remaining assets, $\mathcal{S}(1) = 0$. Aggregate payments from the remaining assets satisfy

$$\underbrace{(1-\zeta)x\big[\mathcal{W}\mathcal{R}(\mathcal{W}) + (1-\mathcal{W})\mathcal{S}(\mathcal{W})\big]}_{\text{payments to requesters and stayers, not covered by the FDIC}} = \underbrace{[1-\ell(1-\delta)]x}_{\text{remaining assets}}. \tag{15}$$

The banker therefore runs away with their pre-opportunity net worth, the insurance

[4]Notice, the shock η_{it} is active only at the coordination opportunity, and determines whether the bank can survive withdrawals or not. Once it hasn't survived, this additional funding is no longer available.

fund's net expenditure is exactly ζx, and depositors' principal loss is therefore:

$$\begin{aligned} & x - \Big\{\zeta x + (1-\zeta)x\big[\mathcal{W}\mathcal{R}(\mathcal{W}) + (1-\mathcal{W})\mathcal{S}(\mathcal{W})\big]\Big\} \\ &= x - \Big\{\zeta x + [1-\ell(1-\delta)]x\Big\} \\ &= [\ell(1-\delta) - \zeta]x. \end{aligned}$$

Losses from costly liquidation of loans are therefore split among the insurer and deposits according to:

$$\underbrace{[\ell(1-\delta)-\zeta]x}_{\text{depositors' loss}} + \underbrace{\zeta x}_{\text{insurer's net expense}} = \underbrace{\ell(1-\delta)x}_{\text{liquidation loss}} .$$

Insurance shifts part of the liquidation loss from depositors to the insurer. Changing $\mathcal{W}$ changes how the remaining assets are divided between requesters and stayers, while value recovered by depositors and the insurer's expense remain fixed.

Payoffs. We assume that depositors value their relationship with the bank, and moving their deposits reduces the value of each dollar received by a fraction $k \in (0,1)$. This can represent a switching cost, or a utility loss from dropping the relationship with the bank. At survival a stayer preserves the relationship, whereas a requester incurs this cost. When the bank fails, both must establish a new relationship, so the factor $1-k$ applies to both groups' payments. For a claim $\Delta > 0$, net payoffs are

$$\begin{aligned} \frac{U^{\mathcal{S}}(z,\mathcal{W})}{\Delta} &= \begin{cases} 1, & \text{bank survives,} \\ (1-k)\{\zeta + (1-\zeta)\mathcal{S}(\mathcal{W})\}, & \text{bank fails,} \end{cases} \\ \frac{U^{\mathcal{R}}(z,\mathcal{W})}{\Delta} &= \begin{cases} 1-k, & \text{bank survives,} \\ (1-k)\{\zeta + (1-\zeta)\mathcal{R}(\mathcal{W})\}, & \text{bank fails.} \end{cases} \end{aligned} \tag{16}$$

The normalized withdrawal advantage is $\mathcal{G} \equiv (U^{\mathcal{R}} - U^{\mathcal{S}})/\Delta$, or

$$\mathcal{G}(z,\mathcal{W}) = \begin{cases} -k, & \text{bank survives,} \\ (1-\zeta)(1-k)[\mathcal{R}(\mathcal{W}) - \mathcal{S}(\mathcal{W})], & \text{bank fails.} \end{cases} \tag{17}$$

Withdrawal is strictly preferred at failure because requesters have priority, while staying is strictly preferred at survival.

Absent of uncertainty about the banks ability to raise funds at a coordination opportunity

($\sigma_\varepsilon = \sigma_\eta = 0$), the model features multiple equilibria. For $\underline{z} \leq z < \ell(1-\delta)/[1-\ell(1-\delta)]$, the bank can continue if depositors stay, but cannot meet withdrawals from all depositors in case they request. Expectations of others' requests can therefore be self-fulfilling: anticipating failure, each depositor requests withdrawal to obtain priority in resolution, and these collective requests result in the failure. If depositors stay, the transitory disturbance passes without changing the balance sheet or the bank's ongoing lending and deposit relationships. To deal with multiplicity we follow the long global games tradition that introduces payoff uncertainty and private signals as an equilibrium selection device (Carlsson and Van Damme, 1993; Morris and Shin, 1998, 2003).

Proposition 2 (Depositor threshold equilibrium)**.** *Under the information and resolution rules above, define z^* by*

$$\begin{cases} z^* = \underline{z}, & \text{if } \int_0^1 \mathcal{G}(\underline{z}, \mathcal{W})\, d\mathcal{W} \leq 0, \\ \int_0^1 \mathcal{G}(z^*, \mathcal{W})\, d\mathcal{W} = 0, & \text{if } \int_0^1 \mathcal{G}(\underline{z}, \mathcal{W})\, d\mathcal{W} > 0. \end{cases} \tag{18}$$

The second case has a unique solution above $\underline{z}$. Then:

1. *For every $\sigma_\varepsilon > 0$, a symmetric threshold equilibrium exists. Every equilibrium signal threshold lies strictly between $\underline{z} - \sigma_\varepsilon$ and $\ell(1-\delta)/[1-\ell(1-\delta)] + \sigma_\varepsilon$.*
2. *For all sufficiently small $\sigma_\varepsilon > 0$, the equilibrium is unique within symmetric threshold strategies, including when $z^* = \underline{z}$.*
3. *As $\sigma_\varepsilon \to 0$, every sequence of equilibrium signal thresholds converges to z^*. For any fixed $z \neq z^*$, the withdrawal fraction converges to one if $z < z^*$ and to zero if $z > z^*$.*
4. *$\underline{z} \leq z^* < \ell(1-\delta)/[1-\ell(1-\delta)]$. The cutoff is weakly decreasing in k and ζ. At an interior solution, it is strictly decreasing in k, and strictly decreasing in ζ when $z^* < \zeta/(1-\zeta)$; it is independent of ζ within the region $z^* \geq \zeta/(1-\zeta)$. As $k \downarrow 0$, it converges to $\ell(1-\delta)/[1-\ell(1-\delta)]$.*

Proof. See Appendix A.2.5. □

As in Goldstein and Pauzner (2005), our model has no global strategic complementarity, since conditional on failure, an extra withdrawal dilutes the recovery of other depositors. Our proof then uses the single-crossing approach to symmetric threshold equilibria in (Morris and Shin, 2003; Goldstein and Pauzner, 2005). We establish threshold best responses, derive the marginal depositor's limiting uniform belief over withdrawals, and

verify the payoff approximation and monotonicity needed for our resolution rules [5].

Run intensity. At a coordination opportunity, the limiting equilibrium entails failure when $z < z^*$ and survival when $z > z^*$. Above the closure floor, failures in $\underline{z} \leq z < z^*$ are induced by withdrawal requests. Since η is independently redrawn at each opportunity, the failure intensity is

$$\lambda(n, x, \ell; \zeta, k) = \lambda_0 F_\eta \left(\frac{z^*(\ell, \zeta, k) - n/x}{\sigma_\eta} \right). \tag{19}$$

For standard logistic η, let $\lambda_1 = 1/\sigma_\eta$. Then

$$\lambda(n, x, \ell; \zeta, k) = \lambda_0 \left[1 + \exp\left\{ \lambda_1 \left(\frac{n}{x} - z^*(\ell, \zeta, k) \right) \right\} \right]^{-1}. \tag{20}$$

Our baseline calibration consider $k = 0$, and the cutoff becomes $\ell(1-\delta)/[1-\ell(1-\delta)]$, giving

$$\lambda(n, x, \ell; \zeta, 0) = \lambda_0 \left[1 + \exp\left\{ \lambda_1 \left(\frac{n}{x} - \frac{\ell(1-\delta)}{1-\ell(1-\delta)} \right) \right\} \right]^{-1}. \tag{21}$$

We suppress fixed parameters when writing $\lambda(s)$ below. In Section 4, we calibrate λ_0 and λ_1.

2.4 Banks' dynamic problem

Value after a run. By the resolution procedure from Section (2.3), after a run, the banker leaves the bank with n, and can no longer lever at the low deposit funding cost r^x_{it} ($x_{it} = 0$), nor can it continue earning the loan spread as an operating bank ($\ell_i = 0$), but still consumes ($\bar{c}$) and chooses a portfolio share of long bonds ($\bar{\alpha}$). We denote the run payoff $\overline{v}(n, r)$:

$$\rho \overline{v} = \max_{c, \alpha} \left\{ u(c) + \overline{v}_n \left[(r - \iota + \bar{\alpha}\pi)n - \bar{c} \right] + \overline{v}_r \mu_r(r) + \frac{1}{2}\overline{v}_{nn}\bar{\alpha}^2\sigma^2 n^2 + \frac{1}{2}\overline{v}_{rr}\sigma_r^2 - \bar{\alpha}\sigma\sigma_r n \overline{v}_{nr} \right\}.$$

For any bank, define the time at which a run arrives such as:

$$T \equiv \min\{t \in \mathbb{R}_+ : \quad dJ_{it} = 1\}$$

[5] Our uniqueness result concerns symmetric threshold strategies, uniqueness among arbitrary strategies would require an additional argument.

Net worth dynamics. Marked-to-market equity evolves as asset returns minus dividend payouts, deposit interest expenses, operating costs (κ_{it}), and deposit insurance taxes (τ_t):

$$\begin{aligned} dn_{it} = &\Big[(r_t - \iota)\, n_{it} + (r_t - r_t^x)\, x_{it} + \big(\pi\alpha_{it}(1-\ell_i) + \xi\ell_i\big)(n_{it} + x_{it})\Big]dt \\ &- \Big[c_{it} + \kappa_{it} + \tau_t\Big]dt - \sigma\alpha_{it}(1-\ell_i)(n_{it} + x_{it})\, dB_t. \end{aligned} \tag{22}$$

The first line is the return on assets. The second line subtracts dividends, deposit interest expense, franchise costs, the FDIC taxes, and the mark-to-market exposure of long bonds to interest-rate shocks. We will let operating costs depend on the bank's networth ($\kappa_{it} = \kappa(n_{it})$). For compactness, denote banks' individual state by $s = (n, x, \ell)$ and let the aggregate state be denoted by $\Gamma = (r, g)$, omitting the bank and time subscripts.

$$\begin{aligned} \mu_n(\alpha, c; s, \Gamma) \equiv &(r - \iota)\, n + (1-\beta)\, r\, x + \big(\pi\alpha(1-\ell) + \xi\ell\big)(n + x) \\ &- c - \kappa(n) - \tau, \end{aligned} \tag{23}$$

$$\sigma_n(\alpha; s) \equiv \sigma\alpha(1-\ell)(n+x). \tag{24}$$

Then, before a run,

$$dn = \mu_n(\alpha, c; s, \Gamma)\, dt - \sigma_n(\alpha; s)\, dB_{it},$$

Distribution dynamics. The Kolmogorov-Forward equation describes the evolution of the distribution of active banks (n, x, ℓ) at time t. The equation is:

$$\begin{aligned} dg_t(s) = \Bigg[&- \frac{\partial}{\partial n}\Big(\mu_n(s, \Gamma_t) g_t(s)\Big) \\ &+ \frac{1}{2}\frac{\partial^2}{\partial n^2}\Big(\sigma_n(\alpha; s)^2 g_t(s)\Big) + \\ &- \underbrace{\lambda(s) g_t(s)}_{\text{Exit from } s \text{ due runs}} + \underbrace{\mathcal{E}_t(s)}_{\text{Entrants in } (s)}\Bigg] dt \\ &- \frac{\partial}{\partial n}\Big(\sigma_n(\alpha; s)\sigma_r g_t(s)\Big) dB_t. \end{aligned} \tag{25}$$

We assume that banks that suffer runs are replenished according to a distribution of entrants:

$$\mathcal{E}_t(s) = \underbrace{\psi_0(s)}_{\text{distr. of entrants}} \times \underbrace{\int \lambda(\tilde{s}) g_t(\tilde{s})\, d\tilde{s}}_{\text{mass of runs (failures) at } t}.$$

Deposit insurance. At every failed bank, the deposit insurance pays each depositor ζ per dollar of her claim, and has no claim on bank's assets. Those costs are finance through a tax τ_t, charged from operating banks [6]. The deposit insurance budget balances every state, and is given by the following expression:

$$\tau_t \equiv \tau(\Gamma_t) = \zeta \int \lambda(s)\, x\, g_t(s)\, ds, \tag{26}$$

Bank problem. Let $v(s, \Gamma)$ denote the value of an operating bank i (we will suppress the index i in what follows). The bank chooses dividend payouts c_t and the long-bond share α_t:

$$v(s, \Gamma) = \sup_{\{c_t, \alpha_t\}_{t \geq 0}} \mathbb{E}\left[\int_0^T e^{-\rho t} u(c_t)\, dt + e^{-\rho T} \overline{v}(n, r)\right],$$

subject to the short-rate process (3), deposit dynamics (8), loan-share dynamics (7), net worth dynamics (22), and the KFE (25). Write the KFE (25) compactly as $dg = \mu_g(\Gamma)\, dt + \sigma_g(\Gamma)\, dB_t$, where μ_g is the bracketed drift term and $\sigma_g(\Gamma) = \partial_n(\sigma_n\, g)$ is the loading of the distribution on the aggregate shock. The Hamilton–Jacobi–Bellman equation is:

$$\begin{aligned} \rho v(s, \Gamma) = \max_{c, \alpha} \Bigg\{ & u(c) + v_n \mu_n(\alpha, c; s, \Gamma) + \frac{1}{2} \sigma_n(\alpha; s)^2 v_{nn} \\ & + v_r \theta_r(\overline{r} - r) + \frac{1}{2} \sigma_r^2 v_{rr} - \sigma_n(\alpha; s) \sigma_r v_{nr} + \int \frac{\partial v}{\partial g}\, \dot{g}\, d\tilde{s} \\ & + \lambda(s) \Big[\overline{v}(n, r) - v(s, \Gamma)\Big] \Bigg\}. \end{aligned} \tag{27}$$

The term $\partial v / \partial g$ is the functional derivative of v with respect to the distribution: the marginal value to the bank of an additional mass of competitors at state s'. This term appears because the cross-sectional distribution g affects the bank's problem through the deposit insurance tax $\tau(\Gamma)$, and it moves with the same aggregate shock as r and n through the dB_t term of the KFE. Notice that there is no drift term in ℓ because the loan share is constant while the bank operates. Its only movement is the jump to zero at a run, which is already embedded in the transition to the run payoff.

[6] Our goal is to reproduce the Systemic Risk Exception (SRE) clause activated by the FDIC in 2023, use their own funds to cover uninsured deposits in the event of a run.

It is convenient to stack the aggregate state $\Gamma = (r, g)$ with drift and diffusion

$$\mu_\Gamma(\Gamma) \equiv \begin{pmatrix} \theta_r(\bar{r} - r) \\ \mu_g(\Gamma) \end{pmatrix}, \qquad \sigma_\Gamma(\Gamma) \equiv \begin{pmatrix} \sigma_r \\ \sigma_g(\Gamma) \end{pmatrix}, \tag{28}$$

so that $d\Gamma = \mu_\Gamma\, dt + \sigma_\Gamma\, dB_t$, and $v_\Gamma = (v_r, v_g(\cdot))$. Then (27) reads

$$\begin{aligned} \rho v(s,\Gamma) = \max_{c,\alpha} \Big\{ & u(c) + v_n \mu_n(\alpha, c; s, \Gamma) + \frac{1}{2}\sigma_n(\alpha; s)^2 v_{nn} \\ & + v_\Gamma \mu_\Gamma + \frac{1}{2}\sigma_\Gamma' v_{\Gamma\Gamma} \sigma_\Gamma - \sigma_n(\alpha; s)\sigma_\Gamma' v_{n\Gamma} + \lambda(s)\Big[\overline{v}(n, r) - v(s, \Gamma)\Big] \Big\}, \end{aligned} \tag{29}$$

where the products are shorthand for the corresponding lines of (27): $v_\Gamma \mu_\Gamma$ collects the two drift terms, $\sigma_\Gamma' v_{\Gamma\Gamma} \sigma_\Gamma$ collects the variance of r, the variance of g, and twice their covariance, and

$$\sigma_\Gamma' v_{n\Gamma} = \sigma_r v_{nr} + \int v_{ng}(s')\, \sigma_g(s'; \Gamma)\, ds' \tag{30}$$

collects the covariance of net worth with the aggregate state.

Lemma 1 (Optimal long-bond share)**.** *Any interior optimal portfolio satisfies*

$$\alpha^*(s,\Gamma) = \underbrace{-\frac{v_n \times \frac{\pi}{\sigma^2}}{v_{nn}(1-\ell)(n+x)}}_{\textit{myopic demand}} + \underbrace{\frac{1}{\sigma}\frac{\sigma_\Gamma' v_{n\Gamma}}{v_{nn}(1-\ell)(n+x)}}_{\textit{dynamic hedging demand}}. \tag{31}$$

Proof. See Appendix A.3. □

By (30), the hedging demand has two components: an interest-rate hedge, $\frac{\sigma_r}{\sigma}\frac{v_{nr}}{v_{nn}(1-\ell)(n+x)}$, and a cross-sectional hedge, $\frac{1}{\sigma}\frac{\int v_{ng}(s')\sigma_g(s';\Gamma)ds'}{v_{nn}(1-\ell)(n+x)}$, which captures how the marginal value of net worth responds when a rate shock shifts the whole distribution of banks and, through it, the deposit insurance tax. Loans matter because only the liquid securities portfolio, $(1-\ell)(n+x)$, can be allocated between short and long bonds. Therefore, for a given long-bond share α, duration exposure scales with the size of the liquid securities portfolio.

Definition 1 (Recursive equilibrium)**.** *In the limit as $\sigma_\varepsilon \to 0$, a recursive competitive equilibrium consists of a value function $v(s,\Gamma)$, bank policy functions $c(s,\Gamma)$ and $\alpha(s,\Gamma)$, a depositor equilibrium cutoff z^*, the induced run intensity $\lambda(s)$, a tax function $\tau(\Gamma)$, and a law of motion for the aggregate state $\Gamma = (r, g)$ such that:*

1. *The cutoff z^* is the limiting depositor equilibrium cutoff characterized in Proposition 2:*

depositors request withdrawal for $z < z^*$ and stay for $z > z^*$. It induces the run intensity $\lambda(s)$ in (19).

2. *Given $\tau(\Gamma)$, the induced intensity $\lambda(s)$, and the law of motion of Γ, the value function v and the policies $\{c, \alpha\}$ solve the bank's HJB equation (27).*

3. *The tax $\tau(\Gamma)$ balances the deposit insurance budget (26) at every aggregate state.*

4. *The short rate follows (3), and the distribution of active banks g evolves according to the KFE (25) under the policies $\{c, \alpha\}$ and the run intensity $\lambda(s)$. Banks' forecasts of the aggregate state are consistent with this law of motion, that is, μ_Γ and σ_Γ in (28) are the drift and diffusion implied by (3) and (25).*

We solve the model numerically using the distribution approximation of Schaab (2020). The method represents the distribution of active banks with an aggregate moment that tracks expected deposits at banks experiencing runs, and associates each value of this moment with a tilted reference density. We iterate jointly on the bank's value function and the law of motion of the aggregate moment, updating aggregate forecasts from the policies obtained at each iteration. Appendix (A.5) describes the distribution approximation, the construction of the aggregate-state grid, and the numerical solution procedure.

2.5 Discussion of Assumptions

Slow-moving deposits. The model treats deposits as an exogenous state variable rather than as a freely adjustable source of funding, and the baseline calibration considers an extreme case, where the deposit base is constant. This assumption captures the idea that deposits are tied to customer relationships, payment activity, and depositor inertia. In this respect, our formulation is close to Bolton et al. (2025), who emphasize that banks cannot perfectly control deposit flows. In Appendix (C.3) we calibrate the model considering deposit shocks.

In Appendix (A.4), we consider a version of the model with CES demand for deposits, in which the bank can freely choose the amount of deposits subject to the deposit demand schedule. Allowing deposits to adjust endogenously weakens the feedback from market-value solvency to run exposure by generating wild fluctuations in the uninsured deposit base of banks.

Loans. We treat the loan share ℓ_i as a persistent bank characteristic rather than as a per-period portfolio choice. This assumption is motivated by the empirical persistence

of loan shares within banks, documented in Appendix (B.9). One interpretation is that banks differ ability of finding profitable lending opportunities. Banks with better monitoring and screening technologies can originate and manage loans more efficiently and therefore find it optimal to operate with a higher loan share. Banks with weaker lending technologies instead hold a larger share of liquid securities. In this sense, ℓ_i captures persistent heterogeneity in banks' business models.

We also abstract from credit risk on loans. This is not because loan risk is unimportant in general, but because we want to focus on a different margin: how interest-rate and run risk shape banks' duration choices. Equivalently, one can interpret the loan portfolio as being diversified across many borrowers, so that idiosyncratic credit risk is diversified away. Loans still play an important role in the model as they are illiquid: in a run, their liquidations is costly. Thus, the key role of loans is not to expose banks to fundamental default risk, but to make the asset side less liquid and thereby affect run vulnerability.

Operating costs. We model operating costs as a function of net worth rather than on deposits for two reasons. First, since deposits are exogenous in the model, tying costs to deposits would leave the bank with a large share of expenses that it cannot reduce through its choices. Net worth n changes with dividend and portfolio decisions, so the bank can expand or shrink its balance sheet (and with it its operating costs). Making κ depend on n gives the bank a way to reduce these expenses. For example, when franchise costs are high relative to the return on retained earnings, the bank can pay out equity and lower its costs. Second, in papers with deposit-dependent operating costs (Bolton et al., 2025; Mertens et al., 2026), banks choose their deposit base, which in equilibrium is an explicit function of net worth. Operating costs in these settings therefore also depend on equity, through the bank's leverage choice. We make this dependence explicit by writing κ directly as a function of n.

Liquidation process. Our liquidation rule departs from the statutory priority applied in FDIC receiverships, where deposit claims rank ahead of shareholder claims.[7] In our model, the banker keeps their net worth n before the remaining assets are used to pay depositors, but loses future profits coming from credit and deposit spreads. This is a tractable specification that isolates the destruction of franchise value as the banker's cost of a self-fulfilling run, while allocating the liquidation loss between depositors and the insurance fund. This view of the franchise value as an intangible (and illiquid) asset lost

[7] See 12 U.S.C. § 1821(d)(11)(A) and the FDIC's priority of dividends.

on a run is shared by Amador and Bianchi (2024), and Drechsler et al. (2026).

The assumption also captures the fact that shareholders can receive positive payoffs even around bank failure. Institutions such as Lehman Brothers and Bear Stearns paid substantial dividends before their failure or rescue in 2008, at levels comparable to those in preceding years. As documented and analyzed by Acharya et al. (2022) and Acharya, Le and Shin (2017), dividend payments in these circumstances transfer resources from bondholders to shareholders. Credit Suisse's March 2023 rescue agreement likewise provided positive consideration to shareholders while imposing a write-down on some bondholders.

3 Data and Empirics

We use the U.S. bank *Reports of Condition and Income* (Call Reports, forms FFIEC 031 and FFIEC 041), which provide quarterly balance sheets and income statements at the bank level. Our sample covers 2010Q1 to 2025Q2. We keep commercial banks with at least $1.5 billion in total assets and bank-quarter observations in which uninsured deposits exceed 5 percent of total assets.[8] This leaves 910 banks over 62 quarters (the number of observations in the regressions below varies because of missing values). For the variable definitions and accounting conventions, we follow Drechsler et al. (2021) and Jiang et al. (2024) whenever applicable. The Call Report items and the details of the sample construction are in Appendix B.1.

Since net worth n_{it} is measured at market value in the model, we need to adjust the book equity reported in the Call Reports. We do so by adding the unrealized gains and losses on *held-to-maturity* (HTM) securities. We take the difference between their reported market value and amortized cost (which we denote by $\texttt{HTM Unrealized G/L}_{it}$), so that

$$n_{it} \;=\; \texttt{Book Equity}_{it} \;+\; \texttt{HTM Unrealized G/L}_{it}.$$

For *available-for-sale* (AFS) securities, unrealized gains and losses already enter book equity through accumulated other comprehensive income (AOCI). We therefore only add the HTM component.[9]

[8] Commercial banks are identified by charter type 200, and require each institution to appear in at least two quarters. We impose the size threshold because we want to study failures associated with runs by uninsured depositors. Smaller banks typically rely little on uninsured funding (Begenau et al., 2026), so other sources of distress may be more relevant for their failures.

[9] Loans remain at book value in our baseline measure. This is consistent with the model, where they earn a floating return $r_t + \xi$ and are not exposed to interest-rate valuation changes. In Appendix B.6, we

We construct uninsured deposits x_{it} as in Jiang et al. (2024) and use them to scale net worth:

$$\frac{n_{it}}{x_{it}} = \frac{\texttt{Book Equity}_{it} + \texttt{HTM Unrealized G/L}_{it}}{\texttt{Uninsured Deposits}_{it}}.$$

This variable is inspired by Haddad et al. (2023), who show that security losses are more harmful to banks with high uninsured share of deposits, and measures how much net worth the bank has against each dollar of uninsured deposits, so a bank with a lower ratio has a smaller buffer against its runnable funding. This is also the reason for excluding observations with very little uninsured funding: a small denominator can make the ratio large even when the bank has little net worth relative to its assets.

The other variable we need is the long-bond share α_{it}. In the model, banks divide their liquid assets, $(1-\ell_{it})(n_{it}+x_{it})$, between a short bond that earns r_t and a long bond whose price falls when the short rate rises. To construct the liquid assets in the data, we take total assets (with HTM securities at market value) and subtract total loans. Using the Call Report maturity/repricing breakdown, we classify cash, federal funds sold, and securities that mature or reprice within three months as short bonds. We then measure the long-bond share as

$$\alpha_{it} = \frac{\texttt{Securities} > \texttt{3m}_{it}}{\texttt{Liquid Assets}_{it}}.$$

With this cutoff, our baseline measure includes securities with at least some duration exposure. We consider other maturity thresholds in Appendix B.2.

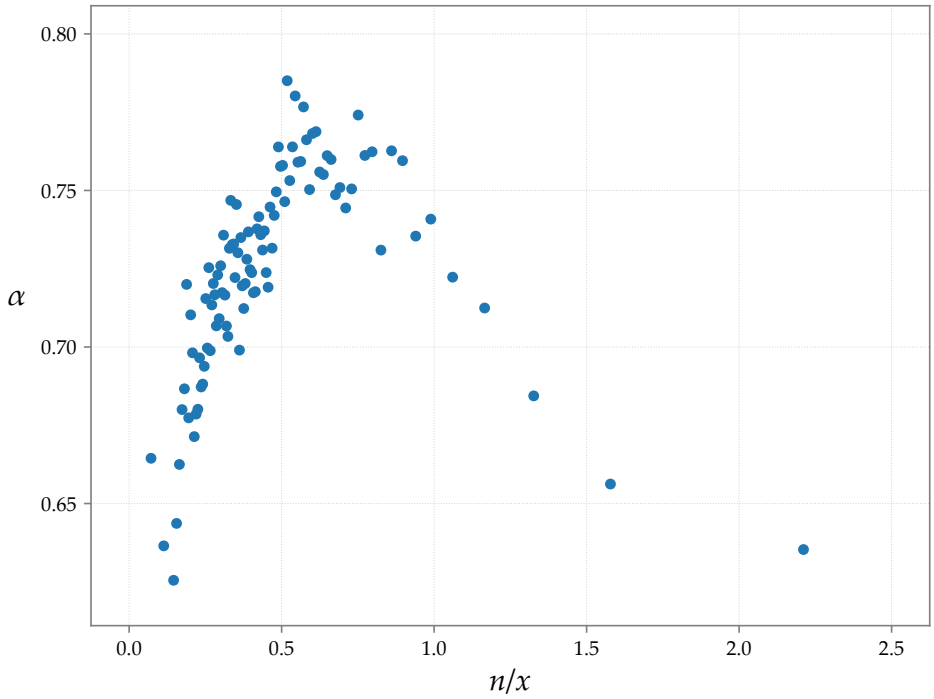
3.1 Cross-sectional demand for long bonds

We start with the relationship between n_{it}/x_{it} and α_{it} in the pooled sample. We sort bank-quarter observations into 100 bins according to their solvency ratio and plot the average long-bond share within each bin.

Figure 1 shows that the relationship is hump-shaped. When banks have little net worth against their uninsured deposits, a higher solvency ratio is associated with a larger long-bond share. For banks with high solvency ratios, the relationship goes in the opposite direction. Long bonds therefore account for the largest share of liquid assets among banks with intermediate solvency. To our knowledge, this relationship between market-adjusted solvency and long-duration securities has not been documented in the existing

consider alternative measures that also impute changes in loan values.

Figure 1: Market-adjusted solvency and long-duration securities



literature.

To see whether the hump remains after accounting for differences across banks and over time, we estimate

$$\alpha_{it} = \beta_0 + \delta_t + \mu_i + \Gamma' X_{it} + \beta_1 \left(\frac{n}{x}\right)_{it} + \beta_2 \left(\frac{n}{x}\right)^2_{it}, \tag{32}$$

where δ_t and μ_i are time and bank fixed effects, and X_{it} contains the balance-sheet controls (size, funding structure, liquidity, and loan composition). We first estimate the pooled regression and then add the fixed effects and controls. These regressions show whether persistent bank characteristics, aggregate conditions, or the observed balance-sheet variables can account for the hump-shaped pattern in the figure. We do not interpret the coefficients as causal effects of solvency on portfolio choice.

In Table 1, the coefficient on n/x is positive and the coefficient on its square is negative in all five columns. The hump remains when we include bank and time fixed effects together with the controls (last column). The coefficients are smaller with bank fixed effects: for example, the linear term falls from 0.17 in the pooled regression to 0.08 when we add bank effects. This suggests that persistent differences across banks account for a significant part of the pooled relationship. At the same time, the signs remain with

Table 1: Solvency and long-duration securities

	Long-bond share α_{it}				
Intercept	0.67^{***}	0.68^{***}	0.69^{***}	0.69^{***}	1.03^{***}
	(0.00)	(0.00)	(0.00)	(0.00)	(0.04)
$\left(\frac{n}{x}\right)_{it}$	0.17^{***}	0.14^{***}	0.08^{***}	0.08^{***}	0.04^{***}
	(0.01)	(0.01)	(0.01)	(0.01)	(0.01)
$\left(\frac{n}{x}\right)^2_{it}$	-0.08^{***}	-0.07^{***}	-0.03^{***}	-0.03^{***}	-0.01^{***}
	(0.00)	(0.00)	(0.00)	(0.00)	(0.00)
Controls					√
Time FE		√		√	√
Bank FE			√	√	√
Observations	28,241	28,241	28,241	28,241	27,629
R^2 (incl. FE)	0.02	0.06	0.72	0.76	0.84
Within R^2	0.02	0.01	0.00	0.00	0.34

bank fixed effects, so the hump is also present in changes within banks. The comparison is suggestive about the sources of the relationship, but does not provide a quantitative decomposition of between-bank and within-bank variation.

There is an additional issue with measuring solvency at the bank level. Uninsured deposits can be concentrated in a particular subsidiary, in which case the deposits reported by another subsidiary may be a poor measure of the relevant funding base of the banking organization. The 5 percent filter helps with these cases. We also repeat the analysis after aggregating the data at the bank-holding-company (BHC) level (Appendix B.4). The fixed-effects coefficients become stronger in that exercise, suggesting a larger within-BHC component, but the overall hump-shaped pattern remains.

Our measure of α_{it} gives the share of liquid assets with duration exposure, but does not measure the duration of these assets. In Appendix B.3, we use an intensive-margin duration measure and the broader asset-side exposure measure from Begenau et al. (2025) as additional checks.

4 Quantitative Results

In Section 4, we estimate (32) using a panel of banks simulated from the model. We choose the internally calibrated parameters to match the average failure rate and the pooled coefficients in Table 1. The fixed-effects coefficients are left untargeted. We use them to check

whether the model reproduces the relationship across banks and within the same bank over time.

4.1 Calibration

Preferences. The corporate finance literature documents that firms (including banks) smooth dividends. Signaling, agency frictions, and the preferences of undiversified shareholders are among the explanations for this behavior. We do not take stands on what are the reasons why banks smooth dividends. Instead, in the model, we give banks a concave utility over dividends, capturing the preference for smooth payouts in reduced form:

$$u(c) = \frac{(Y + c)^{1-\gamma} - Y^{1-\gamma}}{1-\gamma}, \tag{33}$$

where γ is the coefficient of relative risk aversion and $Y \geq 0$ shifts the argument of the utility function. Risk aversion over dividends is then $\gamma/(Y + c)$, so a larger Y weakens the smoothing motive at low payouts, while γ sets its overall strength. We set $\gamma = 2$ and calibrate Y and the discount rate ρ internally.

FDIC coverage and costs from withdrawing. Proposition (2) in Section (2.3) establishes an upper bound on admissible values for ζ. Our baseline calibration will set $\zeta = 0.035$ close to its upper bound and $k = 0$ [10]. In Appendix (D) we have the results of the counterfactuals in the absence of the FDIC coverage $\zeta = 0$, and considering $k = 0.01$ (1% cost of withdrawing/losing the relationship with the bank).

Loan spreads. Banks earn a constant spread ξ over the short rate on their loan book. In the data, we define the return on loans as

$$\texttt{Return on Loans}_{it} = 4 \times \Big(\texttt{Int. Income on Loans/Leases}_{it} - \texttt{Charge offs}_{it} + \texttt{Recoveries}_{it} \Big)$$

[10] As a reference, for the resolutions of SVB and Signature the FDIC estimates $16.7 billion in net resolution losses attributable to protecting uninsured depositors. This is the cost after resolution recoveries (and before the special assessments on surviving banks that finance it). The December 2022 Call Reports record uninsured deposits of $151.6 billion and $79.5 billion, respectively. The implied ratio is $16.7/(151.6 + 79.5) = 0.0723$. It also covers insolvency losses, which the model leaves with the banker, so it is an upper bound for ζ rather than an estimate. See the FDIC's Special Assessment Pursuant to Systemic Risk Determination (updated April 17, 2026) for the loss estimate, and the Congressional Research Service's Silicon Valley Bank and Signature Bank Failures (March 21, 2023) for uninsured deposits reported in the last pre-failure Call Reports.

and compute the *loan spread* by subtracting the Fed Funds rate. We set the model's loan spread to $\xi = 3.4\%$, the average empirical spread over 2010Q1–2025Q4.

Table 2: Baseline parameters.

Parameter	Value	Description	Source
Externally calibrated			
k	0.00	Withdrawal cost	Baseline
ζ	0.035	FDIC coverage	Baseline
γ	2.00	Risk aversion	Standard
$\bar{r}$	0.02	Average rate	Data
θ_r	0.14	Mean reversion of rates	Data
σ_r	0.01	Volatility of rates	Data
ς	-0.01	Price of risk	Data
ι	0.03	Inflation rate	Data
ξ	0.03	Credit spread	Data
β	0.30	Deposit rate sensitivity	Drechsler et al. (2026)
Internally calibrated			
ρ	0.03	Impatience rate	
Υ	0.34	Utility shift	
δ	0.91	Loan sale price	
λ_0	0.01	Level of run-risk	
λ_1	6.78	Slope of run-risk	
κ_1	0.01	Linear franchise cost coefficient	

Short-rate process and the price of risk. We estimate the parameters $(\bar{r}, \theta_r, \sigma_r)$ of the exogenous mean-reverting short-rate process in (3) using quarterly U.S. data. For r_t, we use the nominal three-month Treasury bill rate[11]. We average the three monthly observations in each quarter and convert the annualized yields to decimals. This gives 103 quarterly observations over 2001Q1–2026Q3. We use a nominal rate because the same r_t determines the deposit rate βr_t and the return on the long bond, and the deposit-rate sensitivity β is estimated using nominal rates (Drechsler et al., 2026). The price level enters separately through the inflation rate ι. Since (3) has an exact AR(1) representation at the quarterly frequency, we estimate this AR(1) by OLS (setting $\bar{r}$ to the sample mean) and recover the continuous-time parameters from its coefficients. The mapping is described in Appendix (C.1). We obtain $\bar{r} = 0.0179$ (a long-run short rate of 179 basis points), $\theta_r = 0.145$ (a half-life of 4.8 years), and $\sigma_r = 0.0084$ (an annual innovation volatility of 84

[11] We use the FRED series `TB3MS`, quoted as an annualized yield in percent.

basis points).[12]

With $(\bar{r}, \theta_r, \sigma_r)$ estimated, we obtain the price of risk ς from (5):

$$\varsigma = (-0.0004) \times \frac{\theta_r}{\sigma_r} = -0.0069.$$

Although the stated maturities in our sample are roughly 7–9 years, coupons and especially MBS prepayment make effective duration substantially shorter. We therefore follow Begenau et al. (2025) and use a five-year default-free bond to capture return of the long bonds. We take the 5Y term premium from Adrian et al. (2013), using end-of-quarter observations over 2010Q1–2025Q4, which averages -4 basis points.

Real balances and inflation. The short rate, the deposit rate βr_t, and the long-bond return are nominal, while the balance-sheet states in the model are real. We connect the two using a deterministic price level, $P_t = e^{\iota t}$, with $P_{2010Q1} = 1$ and constant ι. This allows us to write the bank's problem in real terms without adding a stochastic inflation state. We set $\iota = 0.026$, the continuously compounded growth of the CPI between 2010Q1 and 2025Q1, and deflate net worth, uninsured deposits, and dividends by P_t. The net-worth drift in (22) then includes the term $-\iota n$ (the erosion of real equity by inflation). Since net worth and deposits are deflated by the same price level, n/x and all portfolio shares remain unchanged observation by observation.

Deposits and deposit rates. In the baseline each bank's uninsured deposits are constant until a run (when they disappear). This isolates the mechanism from deposit noise, while banks still differ in their deposit level and loan share. In Appendix (C.3), we consider the version with stochastic deposits. For the deposit-β, we follow Drechsler et al. (2026), who use $\beta = 0.3$ for an average bank and estimate betas of 0.22 for insured and 0.33 for uninsured deposits over 2015Q4–2019Q2.

Operating costs. We assume banks pay operating costs that are linear in their net worth:

$$\kappa(n) = \kappa_1 n$$

We calibrate κ_1 internally to match the median n/x in the data.

[12] In Appendix (C.2), we report estimates of the real short rate based on expected and realized inflation and on the one-year Treasury yield.

Entrants distribution. We keep the mass of active banks constant by replacing failed banks with draws from an entrants distribution ψ_0, taken directly from the data. In the benchmark sample (banks with total assets above \$1.5 billion), we define an entrant as a bank that first appears in the sample after 2010Q1. There are 686 such banks over 2010–2024. Only 31 are de novo banks, meaning that they enter the sample within two quarters of their first-ever Call Report (and none of these enters after 2017). The remaining 655 are incumbents that grew past the size threshold. In this sense, growth is what replenishes the population of large banks. We therefore keep all 686 entrants, including those that already operated below the threshold. Since their balance sheets are still adjusting in the first quarter above the threshold, we measure entrants four quarters after entry. Banks that exit or stop reporting before then drop out, leaving 534 banks from which we construct ψ_0.

Table 3: Distribution of n/x: incumbents vs. entrants

Quantile	Incumbents	Entrants
5%	0.17	0.16
25%	0.29	0.28
50%	0.42	0.45
75%	0.58	0.65
95%	0.96	1.51

Table (3) compares the distribution of net worth over uninsured deposits in the full sample with that of entrants (measured four quarters after entry). Entrants have higher solvency ratios in the right tail of n/x. This is not surprising, since an entrant is relatively small compared with the typical incumbent in the sample and is therefore likely to rely less on uninsured depositors (Begenau et al., 2026). Its uninsured-deposit base is then small relative to its equity.

Replacing failed banks with draws from ψ_0 can change the aggregate stock of loans for reasons unrelated to the model. Entrants in the data are smaller and better capitalized than the banks that fail, so using their observed balance sheets directly would destroy loans at every failure. An entrants distribution tilted toward large banks would instead create loans. Since loans are the asset class through which the banking sector serves the real economy, we do not want entry and exit to move aggregate lending mechanically. We therefore require entry to preserve loans: at each replacement, entering banks carry, in expectation, the same loan book $\ell\,(n+x)$ as the banks that just failed.

Internally calibrated parameters. We calibrate $(\rho, \Upsilon, \kappa_1, \lambda_0, \lambda_1, \delta)$ internally. We start from the 2010Q1 distribution in the Call Reports and use the policy functions from the model's solution, together with a sequence of exogenous shocks $\{dB_t\}$, to simulate a panel of banks. We then estimate (32) on this panel and match its coefficients, the average annual failure rate (runs and insolvencies), the median solvency ratio n/x, and aggregate dividends over net worth in the data.

Moment	**Data**	**Model**
Targeted		
Avg. run rate	$< 0.36\%$	0.11%
Agg. c/n	0.07	0.08
Median n/x	0.42	0.44
Table (1), pooled: Intercept	0.67	0.66
Table (1), pooled: MTM solvency ratio	0.17	0.19
Table (1), pooled: MTM solvency ratio^2	-0.08	-0.07
Untargeted		
Table (1), Date FE: MTM solvency ratio	0.14	0.18
Table (1), Date FE: MTM solvency ratio^2	-0.07	-0.07
Table (1), Date + bank FE: MTM solvency ratio	0.08	0.09
Table (1), Date + bank FE: MTM solvency ratio^2	-0.03	-0.07

Table 4: Model fit: targeted and untargeted moments

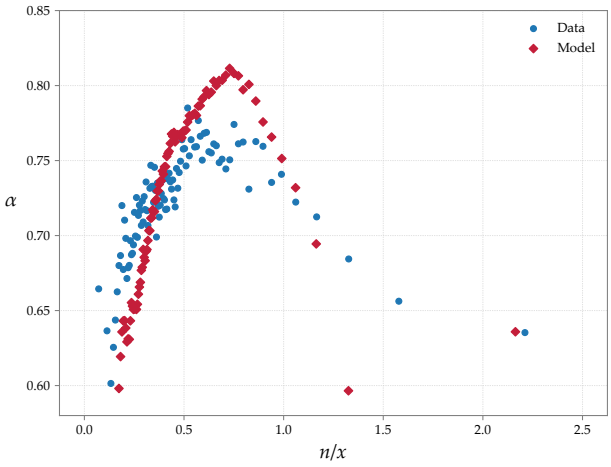
Table (4) reports the fit. The model matches the hump closely: the intercept is 0.66 against 0.67 in the data, the slope is 0.19 against 0.17, and the curvature is -0.07 against -0.08. Figure (2a) compares the portfolios of the simulated banks with those in the data. We also target the median n/x in the data. Figure (2b) shows the full distribution generated by the model (pooling all periods of the simulation).

The average run rate requires some discussion. In the data, we observe bank failures, but cannot directly identify which of them involved runs. The run rate must therefore be below the observed failure rate of 0.36%. If we restrict failures to banks that faced withdrawals $\geq \{5\%, 10\%, 20\%\}$ of uninsured deposits before failure, we obtain rates of $\{0.20\%, 0.10\%, 0.03\%\}$. The average run rate in the model is also consistent with historical estimates of failures with runs range from 0.032% (1993-2024) to 3.5% (1929-1934) (Correia et al., 2026b,c,a).

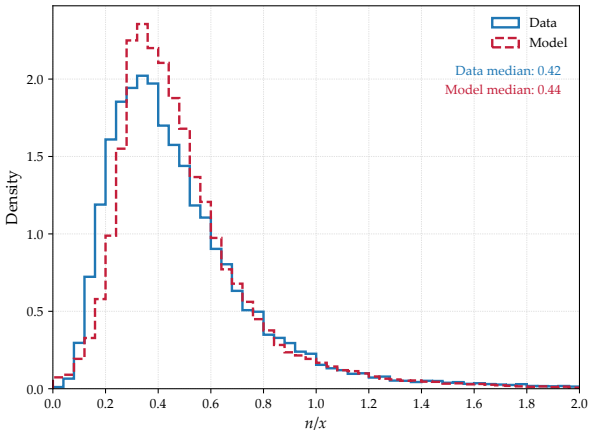
We also report the fixed-effects coefficients as untargeted moments, using the specifications in Table (1). Date fixed effects make little difference to the pooled estimates, as in the data, so conditions common to all banks explain little of the hump. Adding bank fixed

Figure 2: Solvency in the model and in the data

(a) Pooled distribution of n_{it}/x_{it}



(b) n_{it}/x_{it} over time



effects reduces the slope to 0.09 in the model (compared with 0.08 in the data), while keeping it positive and the quadratic term negative. The hump therefore reflects both persistent bank differences and changes in solvency within the same bank, in the model as in the data (with the larger contribution coming from bank-specific characteristics).

4.2 Validation with Insured Deposits

Run risk is what allows our model to generate the hump-shaped pattern observed in the data. To check whether the hump also requires this motive, we use insured deposits in an untargeted exercise (analogous to a placebo test). We replace uninsured deposits in the denominator of the mark-to-market solvency ratio with insured deposits and reestimate the quadratic regression of the long-securities share on this ratio.

$$\frac{n_{it}}{x_{it}^{\text{Insured}}} = \frac{\texttt{Book Equity}_{it} + \texttt{HTM Unrealized G/L}_{it}}{\texttt{Insured Deposits}_{it}}$$

An insured depositor is protected against losses when the bank fails, so the incentive to run that motivates our model is absent. For the corresponding exercise in the model, we set $\lambda_0 = 0$ (switching off runs) and estimate the regression on simulated banks. This gives the portfolio pattern when depositors have no run motive.

The hump disappears in this comparison (Table 5). As net worth relative to insured deposits rises, the long-securities share falls monotonically, both in the model and in the

Table 5: Insured deposits in the data and the model without runs

	Data *insured deposits*	**Model** *runs off* ($\lambda_0 = 0$)
Intercept	0.74	0.95
(n/x^{Insured})	-0.01	-0.62
$(n/x^{\text{Insured}})^2$	-0.27	-0.59

data. Both quadratic coefficients are negative, and the linear coefficient in the data is close to zero. The direction is therefore as implied by our mechanism (the hump requires the run motive). The decline without runs is nevertheless much steeper in the model: the coefficients are -0.62 and -0.59, compared with -0.01 and -0.27 in the data. The model's intercept is also higher, at 0.95 against 0.74.

Without runs, hedging demand decreases with n/x because this ratio measures the bank's equity cushion against the size of its deposit franchise. At low n/x, the bank has more deposits per unit of equity (and hence more deposit-spread income to protect), which strengthens its demand for a hedge. With a higher n/x, the franchise is smaller relative to equity and hedging demand declines. Di Tella and Kurlat (2021) also delivers this relationship, without distinguishing between insured and uninsured depositors. Run risk is what allows us to make this distinction in our model, and match Figure (2a).

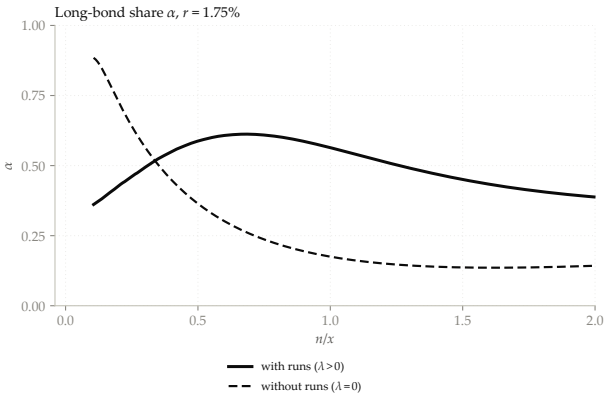
4.3 Exploring Model Mechanism

In this section, we assess our main mechanism using the calibrated model. Figure (3a) shows the policy function for the portfolio with and without runs. The version without runs resembles the results from Section (4.2). With runs, highly capitalized banks have already eliminated run risk, so the dashed and solid lines would converge as $n/x \to \infty$. Low n/x banks face higher run probabilities and want to shield their scarce net worth from a $dB_t > 0$, which would lead them with a very low consumption once a run happens and wipe out their deposits. Still, those banks may never suffer runs, and may keep their franchise despite the low capitalization. In those cases, long bonds are a useful hedge, and that is why the the bottom n/x banks still hold a positive share of long bonds. As banks accumulate net worth, runs get less likely, and the hedging force gets stronger.

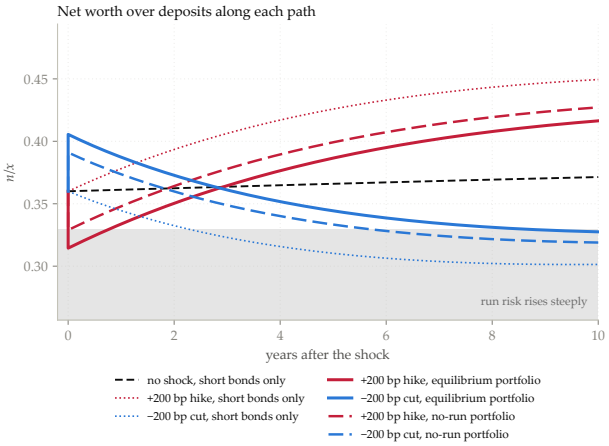
It remains to be understood why intermediate n/x banks hold more long bonds in the presence of runs. The dashed black line in Figure (3b) shows how n/x evolves for one such bank, absent any shocks to short-term rates and assuming a portfolio of short bonds

Figure 3: The hedging demand with and without runs

(a) Long-bond share with and without runs



(b) Evolution of n/x after shocks



only. Next, we consider a 200 bps shock. In case of a hike, the evolution of n/x follows the dotted red line, which increases monotonically after the shock. Without any long bonds in the portfolio, the shock does not generate immediate valuation losses, and higher future deposit spreads increase n/x. Conversely, if this bank faces a rate cut, deposit spreads are lower in the future, reducing the bank's net worth (blue dotted line).

As in Di Tella and Kurlat (2021), the banks in our model are risk averse and use long bonds to transfer resources from states with high return on equity (high rates) to low return on equity (low rates). The dashed lines illustrate the path of n/x under the no-run portfolio. At impact, the bank's net worth jumps due to the price drop (hike) of the long bonds. After that, the dashed lines shift the dotted lines, and the gap between a bank's capitalization 10 years after a hike or a cut shrinks compared with a portfolio that holds short bonds only. We should notice that the immediate effects of a rate hike under the no-run portfolio wouldn't be enough to drag the bank into the gray area (where run risk rises steeply). However, after a rate cut, capitalization would remain in the gray area for 5-10 years after the shock.

Under the optimal portfolio when runs are possible, banks with intermediate n/x increase their holdings of long bonds. This additional exposure allows the bank to avoid the steep run-risk area in Figure (3b) in case of a rate cut (solid blue line), at the expense of briefly increasing run exposure in case of a rate hike.

Put differently, once banks have accumulated enough net worth, they resist $dB_t > 0$ shocks that cut their net worth at impact, but an additional dollar of net worth is highly

dependent on interest rates. Although the immediate effects of rate hikes are not enough to increase run risk considerably, the long-standing effects of a rate cut would push the bank into the run region. This region is reached later when banks hold the optimal portfolio that considers the incidence of runs.

5 Policy Analysis

In this section we use our calibrated model to analyze the results from our policy experiments. In Section (5.1) we study the effects of a modified version of the capital requirements that assigns positive risk weights to long bonds and uninsured deposits, which is equivalent of imposing a floor on capitalization that depends on uninsured deposits, after a rate shock. We study the effects of this policy against a no-policy benchmark (including FDIC coverage).

5.1 Restriction on long bond holdings

Consider Δr be the size of an adverse interest-rate scenario, and let ϕ be a floor on net worth as a fraction of uninsured deposits. The bank's duration exposure is $\alpha_{it}(1-\ell_i)(n_{it}+x_{it})$, so the scenario marks net worth down by $\alpha_{it}(1-\ell_i)(n_{it}+x_{it})\,(\Delta r/\theta_r)$. Suppose a regulator requires net worth to stay above ϕx_{it} after this scenario:

$$\begin{aligned} \frac{n_{it}}{x_{it}} - \alpha_{it}(1-\ell_i)\left(\frac{n_{it}}{x_{it}}+1\right)\frac{\Delta r}{\theta_r} \;&\geq\; \phi \\ \iff \qquad \alpha_{it} \;&\leq\; \frac{\dfrac{n_{it}}{x_{it}} - \phi}{(1-\ell_i)\left(\dfrac{n_{it}}{x_{it}}+1\right)\dfrac{\Delta r}{\theta_r}} \;\equiv\; \bar{\alpha}\big(\phi, \Delta r; n_{it}, x_{it}, \ell_i\big). \end{aligned} \tag{34}$$

We evaluate such policies. We modify the banks' problem with the portfolio choice restricted by (34):

$$\rho v(s,\Gamma) = \max_{c,\; \alpha \leq \bar{\alpha}(\phi,\Delta r; s)} \Big\{ \text{RHS of (27)} \Big\}, \tag{35}$$

so the first-order condition (31) holds only where the cap is slack. Where it binds, the bank holds $\alpha^*(s,\Gamma) = \bar{\alpha}(\phi, \Delta r; s)$. Notice that this is not the same as solving the unconstrained problem and then clipping the portfolio. Because $\bar{\alpha}$ increases in n_{it}/x_{it} (better capitalized banks have a less stringent bound), retained earnings relax the constraint and raises v_n where the cap binds and lowers payouts.

The cap proposed in (35) is not any different from the usual capital requirements used by regulators. To see this rewrite the constraint as a capital requirement:

$$n_t \geq \frac{\Delta r}{\theta_r} \times \underbrace{\alpha_t(1-\ell)(n_t+x_t)}_{\text{Long bonds}} + \phi \times \underbrace{x_t}_{\text{Un. Depositors}} \tag{36}$$

The above equation imposes a risk weight of $(\Delta r/\theta_r)$, on long bonds. This weight is proportional to the size of the adverse interest-rate scenario Δr and the duration of the long-bond $1/\theta_r$. Our policy also puts a risk weight of ϕ on uninsured deposits.

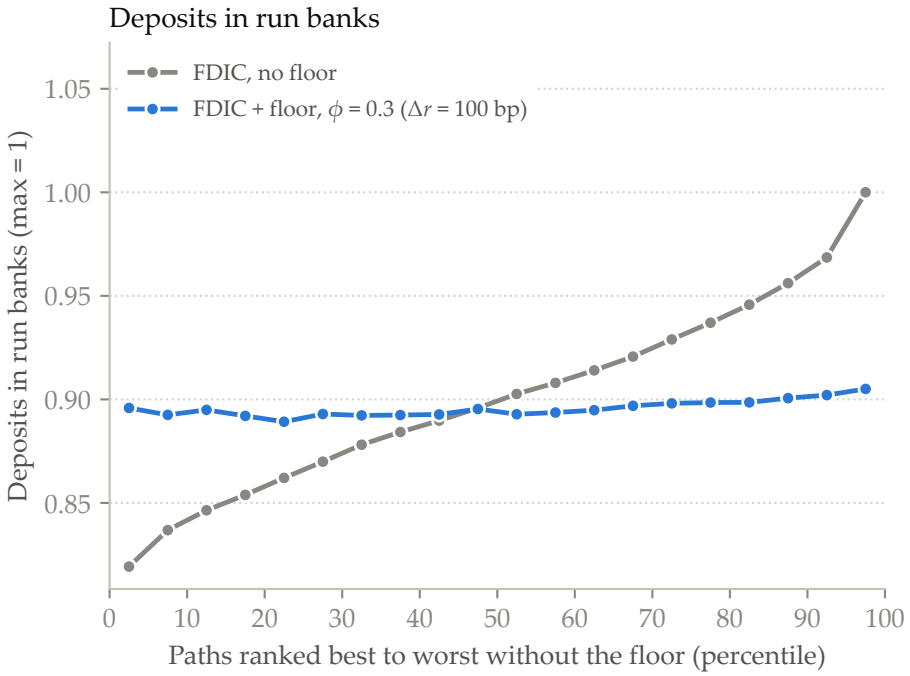
Table 6: Duration restrictions along the realized rate path.

	Deposits in run banks	Sec. losses in 2022 (%)	DIF fee (bp)
FDIC, no floor	1.00	−17.7	1.12
FDIC + floor $\phi = 0.1$	0.99	−17.9	1.11
FDIC + floor $\phi = 0.2$	0.95	−17.1	1.07
FDIC + floor $\phi = 0.3$	0.84	−13.1	0.95
FDIC + floor $\phi = 0.4$	0.79	−7.7	0.89

We start by feeding the realized path of rates to our economy with and without the policy floor mentioned above. Table (6) shows the effect of the floor on deposits in run banks, securities losses, and the deposit-insurance fee along the realized rate path. Without a floor, the deposit-insurance fee is 1.1 basis points of deposits per year over 2022–25, up from 0.8 basis points over 2010–21, because the rate hikes raise fragility. The floor reduces considerably the losses in the securities portfolio in 2022, from 17.7% to 7.7% at $\phi = 0.4$. This attenuates the effect of the rate hikes in 2022, as banks are less exposed to duration. It also cuts deposits in run banks, by 16 percent at $\phi = 0.3$ and 21 percent at $\phi = 0.4$, while $\phi = 0.1$ does almost nothing. Because fewer banks fail, the floor lowers the fee as well, from 1.12 to 0.89 basis points over 2022–25.

The realized path of rates during this period, however, is an extreme event according to the estimated interest rate process, which uses data from a moment when rates were mostly stable, and low (in the zero-lower bound, for a significant period of time). When considering broader scenarios, the effect of the policy is not as clear. Figure (4) considers alternative paths of rates from 2022Q1 onwards, with the implementation of the floor at 2021Q4. We rank each path by the expected deposits of banks that fail between 2022Q1 and 2025Q2 without the floor. The figure shows that for around half of these paths, the

Figure 4: Deposits in run banks on the worst rate paths.



policy increases the deposits in run banks, as it removes the hedge against falling rates. A good and recent example is the rate cut during COVID-19, which would have been damaging to banks with the floor in place.

Next, instead of feeding the model with the realized path of rates until 2022, we start from 2010 and use the estimated parameters to simulate various paths of rates. We then compute the *ex ante* welfare gains from the FDIC coverage as well as the gains from limiting the holdings of long bonds. Welfare of banks is computed considering only the starting cohort of 2010Q1 banks. We compute the welfare of those banks taking into account their failures, but not the welfare of newly entrants. We then convert welfare gains into "dividend equivalent" units. Details on this can be found in Appendix (D.1).

Table (7) shows that adding deposit insurance coverage increases the welfare of depositors, who get an extra ζ coverage. In our baseline parametrization with $k \to 0$ banks have losses, since the FDIC coverage introduces a tax, and changes in bank behavior are not strong enough to reduce runs. Combining the FDIC coverage with an increasing floor increases the welfare of depositors marginally until $\phi = 0.30$, where it starts decreasing it. The last two columns of Table (7) repeat these exercises with a positive cost of moving the banking relationship, $k = 0.01$; Appendix D.2 reports the model fit of this parametrization. With $k > 0$, Proposition (2) gives us a run probability decreasing in

Table 7: Welfare gains: banks vs. depositors, $k = 0$ and $k = 0.01$.

	$k = 0$		$k = 0.01$	
	Banks, CE (bp of div.)	Depositors (bp of dep.)	Banks, CE (bp of div.)	Depositors (bp of dep.)
No FDIC, no floor	0	0	0	0
FDIC, no floor	-11.6	$+13.85$	$+33.9$	$+14.15$
FDIC, floor $\phi = 0.1$	-16.7	$+13.88$	$+28.4$	$+14.20$
FDIC, floor $\phi = 0.2$	-25.8	$+13.93$	$+18.0$	$+14.29$
FDIC, floor $\phi = 0.3$	-43.0	$+13.98$	-0.4	$+14.36$
FDIC, floor $\phi = 0.4$	-69.1	$+13.90$	-28.3	$+14.25$

The 2010Q1 banks, followed until their first run on 2,000 simulated paths of the short rate from 2010Q1 to 2025Q2, with $\zeta = 0.035$. k is the cost of moving the banking relationship; Appendix D.2 describes the economy with $k = 0.01$, where λ_0 is raised to keep the failure rate of Table 4.

the FDIC coverage. In that case deposit insurance also prevents runs on the most liquid banks, raising both banks' welfare ($+33.9$ basis points of dividends). The additional effects of the capitalization floor remain marginally increasing up to $\phi = 0.3$.

Remarks. A FDIC premium that taxes banks according to their riskiness would in principle address the fiscal externality in our model. This increases incentives of poorly capitalized banks to retain earnings, but would also charge more from banks with a high marginal value for an extra dollar of net worth. The result is a negative impact in welfare, as shown in Appendix (D.3). A premium that subsidizes risky banks (the ones with high marginal utility) is more effective in increasing welfare at the expense of perverse incentives: safe banks pay taxes so risky banks can increase their payouts, increasing failures.

In our model runs are extremely costly to the banks, as their franchise is valuable. Policies that restrict banks to hold long bonds cut failures in some states, but reduce their hedge against low rate states. The losses avoided are tiny next to the welfare losses from the lack of the hedge. Under the $k > 0$ parametrization, the one policy that increases welfare in the economy acts on the depositors' side: extra FDIC coverage reduces their incentives to run, reducing run probability and generating welfare gains to banks.

6 Conclusion

Banks' exposure to interest-rate risk has become central to financial stability. Over the last decade, banks increased the maturity of their securities portfolios, strengthening the role of long-duration assets on their balance sheets. Long bonds are useful as they hedge fluctuations in the cash flows coming from the deposit business (deposit spreads). When short-term rates fall, deposit margins are compressed, but this tends to be offset by capital gains on long-duration securities. The same hedge, however, makes banks vulnerable to large mark-to-market losses when rates rise. When those losses interact with a large stock of uninsured deposits, not freely adjustable, banks can become insolvent and start facing run risk, as illustrated by the regional banking crisis of March 2023.

This paper develops a model that serves as laboratory to study the interaction between long-bond holdings, uninsured deposits, and run risk, and the policy implications of capital requirements that assign positive risk weights to long-bonds and uninsured deposits. In the model, banks choose dividends and duration exposure while facing state-dependent run risk that becomes severe when marked-to-market solvency is low. The key result is that run risk endogenously changes banks' hedging demand across the state space. In an intermediate region, where the marginal utility is highly state dependent, banks load more on long bonds. This mechanism generates the hump-shaped relationship between long-bond holdings and solvency observed in the data.

Our calibrated model would suggest that imposing a floor on banks' capitalization, based on their uninsured deposits, would have reduced the losses of banks during the 2022–2023 hiking cycle and reduced the deposits involved in failures by 1-21%. However, the same rule would have reduced banks' profitability along more ordinary paths of rates, increasing the deposits involved in failures for half of them. Our model also shows that FDIC coverage can be beneficial not only for depositors, but also for banks, that face lower taxes to cover failures.

References

Abad, Jorge, Saki Bigio, Salomon Garcia-Villegas, Joël Marbet, and Galo Nuño, "The Heterogeneous Bank Lending Channel of Monetary Policy," Working Paper 35239, National Bureau of Economic Research 2026.

Acharya, Viral V., Hanh T. Le, and Hyun Song Shin, "Bank Capital and Dividend Externalities," *The Review of Financial Studies*, 2017, *30* (3), 988–1018.

_ , Irvind Gujral, Nirupama Kulkarni, and Hyun Song Shin, "Dividends and Bank Capital in the Global Financial Crisis of 2007–2009," *Journal of Financial Crises*, 2022, *4* (2), 1–39.

Adrian, Tobias, Richard K Crump, and Emanuel Moench, "Pricing the term structure with linear regressions," *Journal of Financial Economics*, 2013, *110* (1), 110–138.

Aguirregabiria, Victor, Robert Clark, and Hui Wang, "The geographic flow of bank funding and access to credit: Branch networks, synergies, and local competition," *American Economic Review*, 2025, *115* (6), 1818–1856.

Amador, Manuel and Javier Bianchi, "Bank runs, fragility, and credit easing," *American Economic Review*, 2024, *114* (7), 2073–2110.

Bauer, Michael D and Eric T Swanson, "A reassessment of monetary policy surprises and high-frequency identification," *NBER Macroeconomics Annual*, 2023, *37* (1), 87–155.

Begenau, Juliane and Tim Landvoigt, "Financial Regulation in a Quantitative Model of the Modern Banking System," *The Review of Economic Studies*, 2022, *89* (4), 1748–1784.

_ , Monika Piazzesi, and Martin Schneider, "Banks' risk exposures," Technical Report, National Bureau of Economic Research 2025.

_ , Vadim Elenev, and Tim Landvoigt, "Interest Rate Risk and Cross-Sectional Effects of Micro-Prudential Regulation," Working Paper 34892, National Bureau of Economic Research 2026.

Bolton, Patrick, Ye Li, Neng Wang, and Jinqiang Yang, "Dynamic banking and the value of deposits," *The Journal of Finance*, 2025, *80* (4), 2063–2105.

Carlsson, Hans and Eric Van Damme, "Global games and equilibrium selection," *Econometrica: Journal of the Econometric Society*, 1993, pp. 989–1018.

Corbae, Dean and Pablo D'Erasmo, "Capital buffers in a quantitative model of banking industry dynamics," *Econometrica*, 2021, *89* (6), 2975–3023.

Correia, Sergio, Stephan Luck, and Emil Verner, "Bank Failures: The Roles of Solvency and Liquidity," Working Paper 34853, National Bureau of Economic Research 2026.

_ , _ , and _ , "Bank Runs With and Without Bank Failure," Staff Report 1198, Federal Reserve Bank of New York 2026.

_ , _ , and _ , "Failing Banks," *The Quarterly Journal of Economics*, 2026, *141* (1), 147–204.

Dávila, Eduardo and Itay Goldstein, "Optimal deposit insurance," *Journal of Political Economy*, 2023, *131* (7), 1676–1730.

DeMarzo, Peter M, Arvind Krishnamurthy, and Stefan Nagel, "Interest rate risk in banking," Technical Report, National Bureau of Economic Research 2025.

Drechsler, Itamar, Alexi Savov, and Philipp Schnabl, "The deposits channel of monetary policy," *The Quarterly Journal of Economics*, 2017, *132* (4), 1819–1876.

_ , _ , and _ , "Banking on deposits: Maturity transformation without interest rate risk," *The Journal of Finance*, 2021, *76* (3), 1091–1143.

_ , _ , _ , and Olivier Wang, "Deposit Franchise Runs," *The Journal of Finance*, 2026, *81* (3), 1573–1617.

Ennis, Huberto M. and Todd Keister, "Economic Growth, Liquidity, and Bank Runs," *Journal of Economic Theory*, 2003, *109* (2), 220–245.

_ and _ , "Bank Runs and Investment Decisions Revisited," *Journal of Monetary Economics*, 2006, *53* (2), 217–232.

_ and _ , "Bank Runs and Institutions: The Perils of Intervention," *American Economic Review*, 2009, *99* (4), 1588–1607.

Fleckenstein, Matthias, Shohini Kundu, and Francis A. Longstaff, "Valuing Sticky Deposits," Working Paper 34641, National Bureau of Economic Research 2026.

Goldstein, Itay and Ady Pauzner, "Demand–deposit contracts and the probability of bank runs," *the Journal of Finance*, 2005, *60* (3), 1293–1327.

Groot, Oliver De, "A financial accelerator through coordination failure," *The Economic Journal*, 2021, *131* (636), 1620–1642.

Haddad, Valentin, Barney Hartman-Glaser, and Tyler Muir, "Bank fragility when depositors are the asset," *Available at SSRN 4412256*, 2023.

Heaton, John and Deborah Lucas, "Portfolio choice and asset prices: The importance of entrepreneurial risk," *The journal of finance*, 2000, *55* (3), 1163–1198.

Herranz, Neus, Stefan Krasa, and Anne P Villamil, "Entrepreneurs, risk aversion, and dynamic firms," *Journal of Political Economy*, 2015, *123* (5), 1133–1176.

Ikeda, Daisuke and Hidehiko Matsumoto, "Procyclical leverage and crisis probability in a macroeconomic model of bank runs," *Journal of Political Economy Macroeconomics*, 2026, *4* (3), 613–653.

Jamilov, Rustam and Tommaso Monacelli, "Bewley Banks," *The Review of Economic Studies*, 2026, *93* (3), 1889–1925.

Jiang, Erica Xuewei, Gregor Matvos, Tomasz Piskorski, and Amit Seru, "Monetary tightening and US bank fragility in 2023: Mark-to-market losses and uninsured depositor runs?," *Journal of Financial Economics*, 2024, *159*, 103899.

Jordà, Òscar, "Estimation and inference of impulse responses by local projections," *American Economic Review*, 2005, *95* (1), 161–182.

Krishnamurthy, Arvind and Annette Vissing-Jorgensen, "The aggregate demand for treasury debt," *Journal of Political Economy*, 2012, *120* (2), 233–267.

Mertens, Thomas M, Pascal Paul, and Andres Schneider, "Reaching for Duration," Working Paper 2026-16, Federal Reserve Bank of San Francisco 2026.

Metrick, Andrew, "The failure of silicon valley bank and the panic of 2023," *Journal of Economic Perspectives*, 2024, *38* (1), 133–152.

Miao, Jianjun, Zhouxiang Shen, and Dongling Su, *Long-term securities and banking crises*, Boston University-Department of Economics, 2023.

Morris, Stephen and Hyun Song Shin, "Unique equilibrium in a model of self-fulfilling currency attacks," *American Economic Review*, 1998, pp. 587–597.

_ and _, "Global Games: Theory and Applications," in Mathias Dewatripont, Lars Peter Hansen, and Stephen J. Turnovsky, eds., *Advances in Economics and Econometrics: Theory and Applications, Eighth World Congress*, Vol. 1, Cambridge University Press, 2003, pp. 56–114.

Pancost, N. Aaron and Roberto Robatto, "Bailing out (Firms') Uninsured Deposits: A Quantitative Analysis," 2026. Working paper.

Schaab, Andreas, "Micro and macro uncertainty," *Available at SSRN 4099000*, 2020.

Schneider, Andres, "Banks' Risk Exposures and the Zero Lower Bound," 2026. Working paper, April 21, 2026 version.

Tella, Sebastian Di and Pablo Kurlat, "Why are banks exposed to monetary policy?," *American Economic Journal: Macroeconomics*, 2021, *13* (4), 295–340.

Varraso, Paolo, "Banks' Maturity Choices and the Transmission of Interest-Rate Risk," 2025. Working paper, November 5, 2025.

Vasicek, Oldrich, "An equilibrium characterization of the term structure," *Journal of financial economics*, 1977, *5* (2), 177–188.

Wang, Olivier, "Banks, low interest rates, and monetary policy transmission," *The Journal of Finance*, 2025, *80* (3), 1379–1416.

Wang, Yifei, Toni M Whited, Yufeng Wu, and Kairong Xiao, "Bank market power and monetary policy transmission: Evidence from a structural estimation," *The Journal of Finance*, 2022, *77* (4), 2093–2141.

Whited, Toni M, Yufeng Wu, and Kairong Xiao, "Low interest rates and risk incentives for banks with market power," *Journal of Monetary Economics*, 2021, *121*, 155–174.

A Model Appendix

A.1 Proof of Proposition 1

Let $\mathcal{H} = T - t$ denote the remaining maturity horizon of a zero-coupon bond paying one unit at the fixed date T. As in the main text, write its price as $P_t^L(\mathcal{H}) \equiv L(r_t, \mathcal{H})$. The pricing kernel in (2) implies

$$L(r_t, \mathcal{H}) = \mathbb{E}_t\left[\frac{M_{t+\mathcal{H}}}{M_t}\right], \qquad L(r, 0) = 1.$$

Along the life of the bond, $d\mathcal{H} = -dt$. Because $M_t L(r_t, \mathcal{H})$ is a martingale, Itô's lemma and $dr_t = \theta_r(\bar{r} - r_t)dt + \sigma_r dB_t$ give the pricing equation

$$-L_{\mathcal{H}} + \left[\theta_r(\bar{r} - r) + \varsigma\sigma_r\right]L_r + \frac{\sigma_r^2}{2}L_{rr} - rL = 0. \tag{37}$$

Indeed, the term $\varsigma\sigma_r L_r$ comes from the quadratic covariation between the pricing kernel and the bond price.

Guess the affine form

$$L(r, \mathcal{H}) = \exp\{A(\mathcal{H}) - \mathcal{D}(\mathcal{H})r\}, \qquad A(0) = \mathcal{D}(0) = 0.$$

Substitution into (37) yields

$$\begin{aligned}
\mathcal{D}'(\mathcal{H}) &= 1 - \theta_r\mathcal{D}(\mathcal{H}), \\
A'(\mathcal{H}) &= -\left(\theta_r\bar{r} + \varsigma\sigma_r\right)\mathcal{D}(\mathcal{H}) + \frac{\sigma_r^2}{2}\mathcal{D}(\mathcal{H})^2.
\end{aligned}$$

Consequently,

$$\mathcal{D}(\mathcal{H}) = \frac{1 - e^{-\theta_r\mathcal{H}}}{\theta_r}, \qquad \frac{L_r}{L} = -\mathcal{D}(\mathcal{H}).$$

Under the physical measure, the diffusion coefficient of the bond return is $\sigma_r L_r/L = -\sigma_r\mathcal{D}(\mathcal{H})$. The drift follows directly from (37):

$$\frac{dL}{L} = \left[r_t + \varsigma\sigma_r\mathcal{D}(\mathcal{H})\right]dt - \sigma_r\mathcal{D}(\mathcal{H})dB_t.$$

This gives (4) for any remaining maturity horizon $\mathcal{H}$. Since $\theta_r > 0$, $\mathcal{D}(\mathcal{H}) \to 1/\theta_r$ as $\mathcal{H} \to \infty$, recovering the long-maturity return as a special case.

A.2 Depositor game: proof of Proposition 2

Fix the bank's balance sheet at a coordination opportunity and maintain the information, closure, payment, and parameter restrictions of Section 2.3. The prior density f_z is continuously differentiable and strictly positive; it is distinct from the cross-sectional bank density g_t. Write $\mathcal{T}$ for a candidate signal threshold. We first establish the recovery and dominance properties, then derive threshold best responses and the marginal depositor's limiting gain, and finally prove the proposition.

A.2.1 Resolution accounting and withdrawal gains

The gain at a failed bank. The proceeds from the remaining assets cover requesters' remaining claims when $(1-\zeta)\mathcal{W} \leq 1-\ell(1-\delta)$. Then $\mathcal{R}=1$ and

$$\mathcal{G} = (1-\zeta)(1-k)\left[1 - \frac{1-\ell(1-\delta)-(1-\zeta)\mathcal{W}}{(1-\zeta)(1-\mathcal{W})}\right] = (1-k)\,\frac{\ell(1-\delta)-\zeta}{1-\mathcal{W}}. \tag{38}$$

When requests exhaust the proceeds from the remaining assets, $\mathcal{S}=0$ and

$$\mathcal{G} = (1-\zeta)(1-k)\,\frac{1-\ell(1-\delta)}{(1-\zeta)\mathcal{W}} = (1-k)\,\frac{1-\ell(1-\delta)}{\mathcal{W}}. \tag{39}$$

Thus, at failure,

$$\mathcal{G}(z,\mathcal{W}) = (1-k)\begin{cases} \dfrac{\ell(1-\delta)-\zeta}{1-\mathcal{W}}, & 0 \leq \mathcal{W} \leq \dfrac{1-\ell(1-\delta)}{1-\zeta}, \\ \dfrac{1-\ell(1-\delta)}{\mathcal{W}}, & \dfrac{1-\ell(1-\delta)}{1-\zeta} < \mathcal{W} \leq 1. \end{cases} \tag{40}$$

At the kink, both branches of (40) give

$$\begin{aligned} \lim_{\mathcal{W}\uparrow\frac{1-\ell(1-\delta)}{1-\zeta}} \mathcal{G}(z,\mathcal{W}) &= \lim_{\mathcal{W}\downarrow\frac{1-\ell(1-\delta)}{1-\zeta}} \mathcal{G}(z,\mathcal{W}) \\ &= \mathcal{G}\left(z, \frac{1-\ell(1-\delta)}{1-\zeta}\right) = (1-k)(1-\zeta). \end{aligned} \tag{41}$$

Thus the failure payoff is continuous in $\mathcal{W}$.

The failure payoff in (40) has endpoint limits

$$\begin{aligned}\lim_{\mathcal{W}\downarrow 0} \mathcal{G}(z,\mathcal{W}) &= (1-k)[\ell(1-\delta)-\zeta] > 0,\\ \lim_{\mathcal{W}\uparrow 1} \mathcal{G}(z,\mathcal{W}) &= (1-k)[1-\ell(1-\delta)] > 0.\end{aligned} \tag{42}$$

Figure 5 illustrates the withdrawal gain at a fixed state, including the jump at closure and the dilution of recovery after the kink.

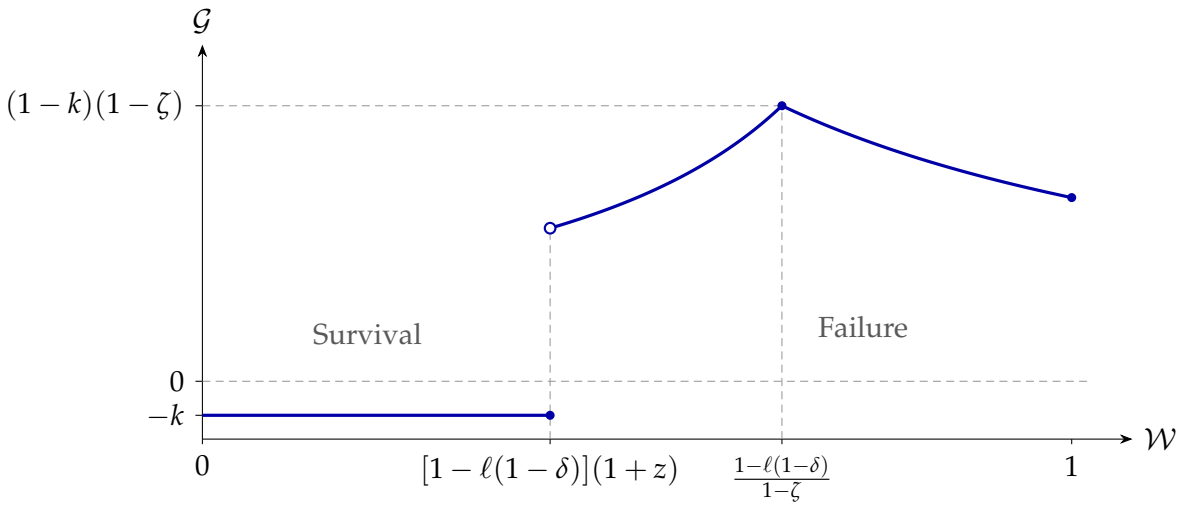


Figure 5: Schematic withdrawal gain at a fixed state $\underline{z} \le z < \zeta/(1-\zeta)$. The open point denotes the limit from failing states. Beyond the recovery kink, dilution reduces the gain while it remains positive.

A.2.2 Dominance regions

Lemma 2 (Strict dominance regions)**.** *Under the parameters and resolution rules of Section 2.3:*

1. *If $z < \underline{z}$, withdrawal strictly dominates staying for every $\mathcal{W}$.*
2. *If $z \ge \frac{\ell(1-\delta)}{1-\ell(1-\delta)}$, staying strictly dominates withdrawal for every $\mathcal{W}$.*
3. *If $\underline{z} \le z < \frac{\ell(1-\delta)}{1-\ell(1-\delta)}$, staying is strictly preferred when $\mathcal{W} \le [1-\ell(1-\delta)](1+z)$ and withdrawal is strictly preferred when the inequality is reversed.*

Proof. If $z < \underline{z}$, closure is compulsory and the gain is given by (38) or (39), both strictly positive because $\zeta < \ell(1-\delta)$. If $z \ge \ell(1-\delta)/[1-\ell(1-\delta)]$, then $z \ge 0 > \underline{z}$ and $[1-\ell(1-\delta)](1+z) \ge 1 \ge \mathcal{W}$, so neither failure clause applies and $\mathcal{G} = -k < 0$. In

between, the bank survives exactly when requests are within capacity, which gives $-k$, and fails otherwise, which gives a strictly positive gain. □

Signals. The posterior of z given s_h is supported on $[s_h - \sigma_\varepsilon, s_h + \sigma_\varepsilon]$. A signal $s_h < \underline{z} - \sigma_\varepsilon$ reveals closure and strictly favors withdrawal; a signal $s_h \geq \ell(1-\delta)/[1-\ell(1-\delta)] + \sigma_\varepsilon$ reveals the upper region and strictly favors staying. Both signal regions are nonempty for every $\sigma_\varepsilon > 0$. There is no region of indifferent states: the gain is strictly positive at every failed bank and $-k$ at every surviving one. We keep the convention that a depositor who is exactly indifferent requests withdrawal; it matters only at a single signal.

A.2.3 Best responses to threshold strategies

Against a candidate signal threshold $\mathcal{T}$, depositors request withdrawal when $s_h < \mathcal{T}$. The continuum law of large numbers gives

$$\mathcal{W}_{\mathcal{T}}(z) = F_\varepsilon\left(\frac{\mathcal{T}-z}{\sigma_\varepsilon}\right) = \begin{cases} 1, & z \leq \mathcal{T} - \sigma_\varepsilon, \\ \dfrac{\mathcal{T}+\sigma_\varepsilon - z}{2\sigma_\varepsilon}, & \mathcal{T}-\sigma_\varepsilon < z < \mathcal{T}+\sigma_\varepsilon, \\ 0, & z \geq \mathcal{T}+\sigma_\varepsilon, \end{cases} \tag{43}$$

which is continuous and nonincreasing in z. Equilibrium claims below refer to symmetric threshold strategies.

Lemma 3 (Posterior gains and optimality)**.** *Define*

$$\Psi_{\mathcal{T}}(s) = \int_{s-\sigma_\varepsilon}^{s+\sigma_\varepsilon} \mathcal{G}(z, \mathcal{W}_{\mathcal{T}}(z)) f_z(z)\, dz. \tag{44}$$

Withdrawal is strictly preferred if $\Psi_{\mathcal{T}}(s) > 0$, staying is strictly preferred if $\Psi_{\mathcal{T}}(s) < 0$, and the depositor is indifferent if $\Psi_{\mathcal{T}}(s) = 0$.

Proof. Conditional on z, the signal density at s is $\frac{1}{2\sigma_\varepsilon}\mathbf{1}\{|s-z| \leq \sigma_\varepsilon\}$. Bayes' rule gives the posterior density

$$f(z \mid s) = \frac{\mathbf{1}\{|s-z| \leq \sigma_\varepsilon\} f_z(z)}{\int_{s-\sigma_\varepsilon}^{s+\sigma_\varepsilon} f_z(u)\, du}, \tag{45}$$

so that

$$\mathbb{E}[\mathcal{G} \mid s; \mathcal{T}] = \frac{\Psi_{\mathcal{T}}(s)}{\int_{s-\sigma_\varepsilon}^{s+\sigma_\varepsilon} f_z(u)\, du}. \tag{46}$$

The denominator is strictly positive and $\Delta > 0$, so the expected payoff difference has the sign of $\Psi_{\mathcal{T}}(s)$. □

A depositor who observes a signal $s_h = s$ knows that $z \in [s - \sigma_\varepsilon, s + \sigma_\varepsilon]$, and computes the expected gains of withdrawing considering the range of possible values for z.

Lemma 4 (One sign change in the state)**.** *Against a threshold $\mathcal{T}$, there is a state boundary $\widetilde{z}_{\mathcal{T}}$ satisfying*

$$\underline{z} \leq \widetilde{z}_{\mathcal{T}} \leq \frac{\ell(1-\delta)}{1-\ell(1-\delta)} \tag{47}$$

such that the bank fails at every $z < \widetilde{z}_{\mathcal{T}}$ and survives at every $z \geq \widetilde{z}_{\mathcal{T}}$. Along the induced withdrawal profile, $\mathcal{G}(z, \mathcal{W}_{\mathcal{T}}(z))$ is strictly positive below this boundary and equals $-k$ at and above it.

Proof.

Step 1: requests relative to capacity. Fix the opponents' threshold $\mathcal{T}$. By (43), increasing z shifts every depositor's signal upward and weakly reduces the fraction requesting withdrawal. Thus $\mathcal{W}_{\mathcal{T}}(z)$ is continuous and nonincreasing, including where it equals zero or one. Liquidation capacity $[1-\ell(1-\delta)](1+z)$ is strictly increasing because $1-\ell(1-\delta) > 0$. Consequently, excess requests

$$\mathcal{W}_{\mathcal{T}}(z) - [1-\ell(1-\delta)](1+z)$$

is continuous and strictly decreasing:

$$\underbrace{\mathcal{W}'_{\mathcal{T}}(z)}_{\leq 0} - \underbrace{[1-\ell(1-\delta)]}_{>0} < 0$$

Step 2: an upper bound on failure states. At $z = \ell(1-\delta)/[1-\ell(1-\delta)]$, capacity is

$$[1-\ell(1-\delta)]\left(1 + \frac{\ell(1-\delta)}{1-\ell(1-\delta)}\right) = 1.$$

Since $\mathcal{W}_{\mathcal{T}}(z) \leq 1$, excess requests are nonpositive there. This state is above $\underline{z}$, so neither clause of (12) applies. The bank survives there and at every higher state.

Step 3: locating the boundary relative to compulsory closure. All states $z < \underline{z}$ fail by compulsory closure. At and above $\underline{z}$, failure occurs exactly when excess requests are strictly positive. There are two cases.

If

$$\mathcal{W}_{\mathcal{T}}(\underline{z}) \leq [1 - \ell(1-\delta)](1 + \underline{z}),$$

the bank can meet all requests at $\underline{z}$. Strict decrease of excess requests implies that it can also meet them at every higher state. Set $\widetilde{z}_{\mathcal{T}} = \underline{z}$: failure occurs strictly below this boundary and survival occurs at and above it.

If instead

$$\mathcal{W}_{\mathcal{T}}(\underline{z}) > [1 - \ell(1-\delta)](1 + \underline{z}),$$

excess requests are positive at the floor and nonpositive at the upper state from Step 2. Continuity gives a zero between them, and strict decrease makes it unique. Denote it by $\widetilde{z}_{\mathcal{T}}$, so

$$\mathcal{W}_{\mathcal{T}}(\widetilde{z}_{\mathcal{T}}) = [1 - \ell(1-\delta)](1 + \widetilde{z}_{\mathcal{T}}).$$

For $\underline{z} \leq z < \widetilde{z}_{\mathcal{T}}$, requests exceed capacity and the bank fails; for $z > \widetilde{z}_{\mathcal{T}}$, capacity exceeds requests and the bank survives. At the boundary itself, requests equal capacity and $z > \underline{z}$. The strict failure inequalities in (12) therefore imply survival at equality. Combining this with compulsory closure below the floor proves the claimed boundary and its bounds in both cases.

Step 4: from failure and survival to the sign of the gain. At failure, both branches of (40) are strictly positive: $1 - k > 0$, $\ell(1-\delta) - \zeta > 0$, $1 - \ell(1-\delta) > 0$, and their denominators are positive on their respective domains. At survival, (17) gives $\mathcal{G} = -k < 0$. Hence

$$\mathcal{G}\big(z, \mathcal{W}_{\mathcal{T}}(z)\big) \begin{cases} > 0, & z < \widetilde{z}_{\mathcal{T}}, \\ = -k < 0, & z \geq \widetilde{z}_{\mathcal{T}}. \end{cases}$$

The gain changes sign by a jump at the boundary; it need not pass through zero. □

Next lemma shows that for a given threshold $\mathcal{T}$, if a signal s generates zero expected gains from withdrawing, this signal must be close enough to the threshold $\tilde{z}_{\mathcal{T}}$.

Lemma 5 (A unique threshold best response)**.** *Against any threshold $\mathcal{T}$, $\Psi_{\mathcal{T}}$ has exactly one zero. If $\Psi_{\mathcal{T}}(s) = 0$, then*

$$\widetilde{z}_{\mathcal{T}} - \sigma_\varepsilon < s < \widetilde{z}_{\mathcal{T}} + \sigma_\varepsilon. \tag{48}$$

The gain is positive below this zero and negative above it. The best-response threshold is continuous on $\mathcal{T}$.

Proof.

Lower and upper signals. If $s \leq \widetilde{z}_{\mathcal{T}} - \sigma_\varepsilon$, the posterior window contains only failing states, except possibly one endpoint, so $\Psi_{\mathcal{T}}(s) > 0$. If $s \geq \widetilde{z}_{\mathcal{T}} + \sigma_\varepsilon$, all posterior states survive and $\Psi_{\mathcal{T}}(s) < 0$.

Absolute continuity. The payoff bounds in (17) and (40) give

$$\int_{\mathbb{R}} \left|\mathcal{G}\left(z, \mathcal{W}_{\mathcal{T}}(z)\right)\right| f_z(z)\, dz \leq \max\{k, (1-k)(1-\zeta)\} < \infty.$$

Write

$$\begin{aligned}\Psi_{\mathcal{T}}(s) = &\int_{-\infty}^{s+\sigma_\varepsilon} \mathcal{G}\left(z, \mathcal{W}_{\mathcal{T}}(z)\right) f_z(z)\, dz \\ &- \int_{-\infty}^{s-\sigma_\varepsilon} \mathcal{G}\left(z, \mathcal{W}_{\mathcal{T}}(z)\right) f_z(z)\, dz.\end{aligned}$$

Each cumulative integral is absolutely continuous, hence so is $\Psi_{\mathcal{T}}$, with

$$\begin{aligned}\Psi'_{\mathcal{T}}(s) = &\mathcal{G}\left(s+\sigma_\varepsilon, \mathcal{W}_{\mathcal{T}}(s+\sigma_\varepsilon)\right) f_z(s+\sigma_\varepsilon) \\ &-\mathcal{G}\left(s-\sigma_\varepsilon, \mathcal{W}_{\mathcal{T}}(s-\sigma_\varepsilon)\right) f_z(s-\sigma_\varepsilon)\end{aligned}$$

almost everywhere. For signals in (48), the upper endpoint survives and the lower endpoint fails. Therefore,

$$\Psi'_{\mathcal{T}}(s) = -k f_z(s+\sigma_\varepsilon) - \mathcal{G}\left(s-\sigma_\varepsilon, \mathcal{W}_{\mathcal{T}}(s-\sigma_\varepsilon)\right) f_z(s-\sigma_\varepsilon) < 0 \tag{49}$$

Dependence on the opponents' threshold. For each $\mathcal{T}$, changing the threshold changes the integrand in (44) continuously except at the single state boundary. Bounded gains and dominated convergence give joint continuity of $(\mathcal{T}, s) \mapsto \Psi_{\mathcal{T}}(s)$. The gains at signals just below and just above the unique zero have opposite strict signs. They retain these signs for nearby opponents' thresholds, so the nearby zero remains between these signals. This proves continuity of the best-response threshold. □

A.2.4 Equilibrium threshold and uniqueness

The marginal depositor. At $s = \mathcal{T}$, equation (43) can be inverted:

$$\mathcal{W} = \frac{\mathcal{T} + \sigma_\varepsilon - z}{2\sigma_\varepsilon} \quad \Longleftrightarrow \quad z = \mathcal{T} + \sigma_\varepsilon(1 - 2\mathcal{W}), \qquad dz = -2\sigma_\varepsilon \, d\mathcal{W}. \tag{50}$$

The lower state endpoint corresponds to $\mathcal{W} = 1$ and the upper endpoint to $\mathcal{W} = 0$; reversing the limits cancels the minus sign:

$$\frac{\Psi_{\mathcal{T}}(\mathcal{T})}{2\sigma_\varepsilon} = \int_0^1 \mathcal{G}(\mathcal{T} + \sigma_\varepsilon(1 - 2\mathcal{W}), \mathcal{W}) \, f_z(\mathcal{T} + \sigma_\varepsilon(1 - 2\mathcal{W})) \, d\mathcal{W}. \tag{51}$$

Lemma 6 (Uniform posterior over withdrawals)**.** *For any fixed threshold $\mathcal{T}$, conditional on $s_h = \mathcal{T}$, the posterior distribution of $\mathcal{W}$ converges to the uniform distribution on $[0, 1]$ as $\sigma_\varepsilon \to 0$. If the prior is constant over the posterior interval, this posterior is exactly uniform at positive noise.*

Proof. By (46), the expected normalized gain is $\Psi_{\mathcal{T}}(\mathcal{T})$ divided by the prior mass of compatible states. Applying the same change of variables as in (51) to this denominator gives

$$\int_{\mathcal{T}-\sigma_\varepsilon}^{\mathcal{T}+\sigma_\varepsilon} f_z(z) \, dz = 2\sigma_\varepsilon \int_0^1 f_z\big(\mathcal{T} + \sigma_\varepsilon(1 - 2u)\big) \, du.$$

The factor $2\sigma_\varepsilon$ cancels between numerator and denominator. Her posterior density over withdrawals is consequently

$$\frac{f_z(\mathcal{T} + \sigma_\varepsilon(1 - 2\mathcal{W}))}{\int_0^1 f_z(\mathcal{T} + \sigma_\varepsilon(1 - 2u)) \, du}, \qquad 0 \le \mathcal{W} \le 1. \tag{52}$$

We now show that this density converges to one. Let $z = \mathcal{T} + \sigma_\varepsilon(1 - 2\mathcal{W})$. Notice that

$$|z - \mathcal{T}| = \sigma_\varepsilon |1 - 2\mathcal{W}| \le \sigma_\varepsilon,$$

The mean value theorem then gives:

$$\begin{aligned} |f_z(z) - f_z(\mathcal{T})| &\le |z - \mathcal{T}| \sup_{v \in [\mathcal{T}-\sigma_\varepsilon, \mathcal{T}+\sigma_\varepsilon]} |f_z'(v)| \\ &\le \sigma_\varepsilon \sup_{v \in [\mathcal{T}-\sigma_\varepsilon, \mathcal{T}+\sigma_\varepsilon]} |f_z'(v)|. \end{aligned}$$

The same bound applies to the normalizing integral:

$$\begin{aligned}&\left|\int_0^1 f_z\big(\mathcal{T}+\sigma_\varepsilon(1-2u)\big)\,du - f_z(\mathcal{T})\right| \\ &\quad\le \int_0^1 \left|f_z\big(\mathcal{T}+\sigma_\varepsilon(1-2u)\big) - f_z(\mathcal{T})\right|\,du \\ &\quad\le \sigma_\varepsilon \sup_{v\in[\mathcal{T}-\sigma_\varepsilon,\mathcal{T}+\sigma_\varepsilon]} |f_z'(v)|.\end{aligned}$$

We can now bound the gap between the posterior density and one for every $\mathcal{W} \in [0,1]$. Adding and subtracting $f_z(\mathcal{T})$, the triangle inequality gives

$$\begin{aligned}&\left|f_z\big(\mathcal{T}+\sigma_\varepsilon(1-2\mathcal{W})\big) - \int_0^1 f_z\big(\mathcal{T}+\sigma_\varepsilon(1-2u)\big)\,du\right| \\ &\quad\le \left|f_z\big(\mathcal{T}+\sigma_\varepsilon(1-2\mathcal{W})\big) - f_z(\mathcal{T})\right| \\ &\qquad + \left|\int_0^1 f_z\big(\mathcal{T}+\sigma_\varepsilon(1-2u)\big)\,du - f_z(\mathcal{T})\right|.\end{aligned}$$

Both terms on the right satisfy the bounds above. For $0 < \sigma_\varepsilon \le 1$, all posterior states lie in the fixed interval $[\mathcal{T}-1, \mathcal{T}+1]$. Dividing by the positive normalizing integral therefore yields, for every $\mathcal{W} \in [0,1]$,

$$\begin{aligned}&\left|\frac{f_z(\mathcal{T}+\sigma_\varepsilon(1-2\mathcal{W}))}{\int_0^1 f_z(\mathcal{T}+\sigma_\varepsilon(1-2u))\,du} - 1\right| \\ &\quad\le 2\sigma_\varepsilon \frac{\sup_{v\in[\mathcal{T}-1,\mathcal{T}+1]} |f_z'(v)|}{\min_{v\in[\mathcal{T}-1,\mathcal{T}+1]} f_z(v)} \longrightarrow 0.\end{aligned}$$

The supremum is finite and the minimum is positive, independently of σ_ε and $\mathcal{W}$. The bound thus forces the posterior density to converge to one at every $\mathcal{W} \in [0,1]$. This is the uniform distribution on $[0,1]$: its probability density is constant and equal to one throughout the interval. □

Let's define the largest withdrawal fraction compatible with survival, given the signal $s_h = \mathcal{T}$, observed by the marginal depositor.

Survival requires both $\mathcal{W} \leq [1-\ell(1-\delta)](1+z)$ and $z \geq \underline{z}$. Substituting $z = \mathcal{T} + \sigma_\varepsilon(1-2\mathcal{W})$ from (50) into the capacity constraint gives

$$\begin{aligned} & \mathcal{W} \leq [1-\ell(1-\delta)]\big[1+\mathcal{T}+\sigma_\varepsilon-2\sigma_\varepsilon\mathcal{W}\big] \\ \iff \quad & \mathcal{W}\big[1+2\sigma_\varepsilon[1-\ell(1-\delta)]\big] \leq [1-\ell(1-\delta)](1+\mathcal{T}+\sigma_\varepsilon) \\ \iff \quad & \mathcal{W} \leq \frac{[1-\ell(1-\delta)](1+\mathcal{T}+\sigma_\varepsilon)}{1+2\sigma_\varepsilon[1-\ell(1-\delta)]}. \end{aligned}$$

Avoiding compulsory closure similarly requires

$$\begin{aligned} z \geq \underline{z} \quad \iff \quad & \mathcal{T}+\sigma_\varepsilon-2\sigma_\varepsilon\mathcal{W} \geq \underline{z} \\ \iff \quad & \mathcal{W} \leq \frac{\mathcal{T}+\sigma_\varepsilon-\underline{z}}{2\sigma_\varepsilon}. \end{aligned}$$

Both upper bounds must hold, together with $\mathcal{W} \leq 1$. The survival cutoff, set to zero when the survival region is empty, is therefore

$$\overline{\mathcal{W}}_{\mathcal{T}} = \max\left\{0, \min\left\{1, \frac{[1-\ell(1-\delta)](1+\mathcal{T}+\sigma_\varepsilon)}{1+2\sigma_\varepsilon[1-\ell(1-\delta)]}, \frac{\mathcal{T}+\sigma_\varepsilon-\underline{z}}{2\sigma_\varepsilon}\right\}\right\}. \tag{53}$$

The minimum imposes both survival constraints and the upper bound of one; the outer maximum keeps the cutoff nonnegative. The marginal gain is exactly

$$\begin{aligned} \frac{\Psi_{\mathcal{T}}(\mathcal{T})}{2\sigma_\varepsilon} = & -k\int_0^{\overline{\mathcal{W}}_{\mathcal{T}}} f_z(\mathcal{T}+\sigma_\varepsilon(1-2\mathcal{W}))\,d\mathcal{W} \\ & + (1-\zeta)(1-k)\int_{\overline{\mathcal{W}}_{\mathcal{T}}}^1 \big[\mathcal{R}(\mathcal{W})-\mathcal{S}(\mathcal{W})\big] \\ & \qquad \times f_z(\mathcal{T}+\sigma_\varepsilon(1-2\mathcal{W}))\,d\mathcal{W}. \end{aligned} \tag{54}$$

A threshold is an equilibrium if and only if this expression is zero.

We first take the small-noise limit of the marginal depositor's expected gain. We then separate survival costs from failure gains and determine when the resulting expression has an interior zero.

Lemma 7 (The marginal depositor's limiting gain)**.** *For fixed $\mathcal{T} \neq \underline{z}$,*

$$\lim_{\sigma_\varepsilon \to 0} \mathbb{E}[\mathcal{G} \mid s_h = \mathcal{T}; \mathcal{T}] = \int_0^1 \mathcal{G}(\mathcal{T}, \mathcal{W})\,d\mathcal{W}. \tag{55}$$

Proof. Equations (46) and (51) give

$$\begin{aligned}&\mathbb{E}[\mathcal{G} \mid s_h = \mathcal{T}; \mathcal{T}] \\ &\quad = \int_0^1 \mathcal{G}\big(\mathcal{T} + \sigma_\varepsilon(1-2\mathcal{W}), \mathcal{W}\big) \frac{f_z(\mathcal{T} + \sigma_\varepsilon(1-2\mathcal{W}))}{\int_0^1 f_z(\mathcal{T} + \sigma_\varepsilon(1-2u))\, du}\, d\mathcal{W}.\end{aligned}$$

By Lemma 6 and its proof, the density ratio converges uniformly to one. For fixed $\mathcal{T} \neq \underline{z}$ and small noise, the posterior window lies entirely above or entirely below the compulsory-closure floor. The change in capacity is bounded by

$$\begin{aligned}&\big|[1-\ell(1-\delta)]\big[1+\mathcal{T}+\sigma_\varepsilon(1-2\mathcal{W})\big] - [1-\ell(1-\delta)](1+\mathcal{T})\big| \\ &\quad = [1-\ell(1-\delta)]\sigma_\varepsilon|1-2\mathcal{W}| \leq [1-\ell(1-\delta)]\sigma_\varepsilon \longrightarrow 0.\end{aligned}$$

The survival outcome can therefore differ only when

$$|\mathcal{W} - [1-\ell(1-\delta)](1+\mathcal{T})| \leq [1-\ell(1-\delta)]\sigma_\varepsilon,$$

an interval of length at most $2[1-\ell(1-\delta)]\sigma_\varepsilon$. Outside it, the failure or survival outcome agrees, and so do the gains: the survival gain is $-k$, and the failure gain depends only on $\mathcal{W}$. A switch between the two outcomes changes the gain by at most $k + (1-k)(1-\zeta)$. Hence

$$\begin{aligned}&\left|\int_0^1 \big[\mathcal{G}\big(\mathcal{T}+\sigma_\varepsilon(1-2\mathcal{W}), \mathcal{W}\big) - \mathcal{G}(\mathcal{T}, \mathcal{W})\big]\, d\mathcal{W}\right| \\ &\quad \leq \int_0^1 \big|\mathcal{G}\big(\mathcal{T}+\sigma_\varepsilon(1-2\mathcal{W}), \mathcal{W}\big) - \mathcal{G}(\mathcal{T}, \mathcal{W})\big|\, d\mathcal{W} \\ &\quad \leq 2[1-\ell(1-\delta)]\sigma_\varepsilon\big[k + (1-k)(1-\zeta)\big] \longrightarrow 0.\end{aligned}$$

The posterior density is uniformly bounded for small noise. Together with the density ratio's uniform convergence to one, this justifies replacing the gain's state argument by $\mathcal{T}$ and gives (55). □

At $\mathcal{T} = \underline{z}$, the posterior window straddles compulsory closure. The integral evaluated at $\underline{z}$ below is its extension from above; it need not equal the small-noise expected gain at a threshold fixed exactly at the floor.

Lemma 8 (Survival costs and failure gains). *For $\underline{z} \leq \mathcal{T} \leq \ell(1-\delta)/[1-\ell(1-\delta)]$, the integral in (55) is*

$$\begin{aligned}\int_0^1 \mathcal{G}(\mathcal{T},\mathcal{W})\,d\mathcal{W} = &-k[1-\ell(1-\delta)](1+\mathcal{T}) \\ &+(1-\zeta)(1-k)\int_{[1-\ell(1-\delta)](1+\mathcal{T})}^1 \big[\mathcal{R}(\mathcal{W})-\mathcal{S}(\mathcal{W})\big]\,d\mathcal{W}.\end{aligned} \tag{56}$$

Below $\underline{z}$, every withdrawal fraction leads to failure and the integral is strictly positive. At and above $\ell(1-\delta)/[1-\ell(1-\delta)]$, it equals $-k$.

Proof. For $\underline{z} \leq \mathcal{T} \leq \ell(1-\delta)/[1-\ell(1-\delta)]$, the bank survives when $\mathcal{W} \leq [1-\ell(1-\delta)](1+\mathcal{T})$ and fails otherwise. Under uniform beliefs, the probability of survival is therefore $[1-\ell(1-\delta)](1+\mathcal{T})$. Multiplying this probability by the survival gain $-k$ gives the first term of (56). Integrating the failure gain $(1-\zeta)(1-k)[\mathcal{R}(\mathcal{W})-\mathcal{S}(\mathcal{W})]$ over the remaining withdrawal fractions gives the second term.

To evaluate the failure term, compare capacity with the recovery kink:

$$[1-\ell(1-\delta)](1+\mathcal{T}) \leq \frac{1-\ell(1-\delta)}{1-\zeta} \quad\Longleftrightarrow\quad \mathcal{T} \leq \frac{\zeta}{1-\zeta}.$$

For $\underline{z} \leq \mathcal{T} \leq \zeta/(1-\zeta)$, the failure region contains both branches of (40). Thus

$$\begin{aligned}\int_0^1 \mathcal{G}(\mathcal{T},\mathcal{W})\,d\mathcal{W} = &\underbrace{\int_0^{[1-\ell(1-\delta)](1+\mathcal{T})}(-k)d\mathcal{W}}_{-k[1-\ell(1-\delta)](1+\mathcal{T})} \\ &+(1-k)[\ell(1-\delta)-\zeta]\int_{[1-\ell(1-\delta)](1+\mathcal{T})}^{\frac{1-\ell(1-\delta)}{1-\zeta}}\frac{d\mathcal{W}}{1-\mathcal{W}} \\ &+(1-k)[1-\ell(1-\delta)]\int_{\frac{1-\ell(1-\delta)}{1-\zeta}}^1\frac{d\mathcal{W}}{\mathcal{W}}.\end{aligned}$$

The two integrals are

$$\begin{aligned}\int_{[1-\ell(1-\delta)](1+\mathcal{T})}^{\frac{1-\ell(1-\delta)}{1-\zeta}}\frac{d\mathcal{W}}{1-\mathcal{W}} &= \ln\frac{(1-\zeta)\{1-[1-\ell(1-\delta)](1+\mathcal{T})\}}{\ell(1-\delta)-\zeta}, \\ \int_{\frac{1-\ell(1-\delta)}{1-\zeta}}^1\frac{d\mathcal{W}}{\mathcal{W}} &= \ln\frac{1-\zeta}{1-\ell(1-\delta)},\end{aligned} \tag{57}$$

using $1-[1-\ell(1-\delta)]/(1-\zeta)=[\ell(1-\delta)-\zeta]/(1-\zeta)$. Substituting gives

$$\begin{aligned}\int_0^1 \mathcal{G}(\mathcal{T},\mathcal{W})\,d\mathcal{W} = &-k[1-\ell(1-\delta)](1+\mathcal{T})\\ &+(1-k)[\ell(1-\delta)-\zeta]\ln\frac{(1-\zeta)\{1-[1-\ell(1-\delta)](1+\mathcal{T})\}}{\ell(1-\delta)-\zeta}\\ &+(1-k)[1-\ell(1-\delta)]\ln\frac{1-\zeta}{1-\ell(1-\delta)}.\end{aligned} \tag{58}$$

For $\zeta/(1-\zeta)\le\mathcal{T}<\ell(1-\delta)/[1-\ell(1-\delta)]$, every failure exhausts the proceeds from the remaining assets. Only the second failure branch is integrated:

$$\begin{aligned}\int_0^1 \mathcal{G}(\mathcal{T},\mathcal{W})\,d\mathcal{W} = &-k[1-\ell(1-\delta)](1+\mathcal{T})\\ &+(1-k)[1-\ell(1-\delta)]\int_{[1-\ell(1-\delta)](1+\mathcal{T})}^1\frac{d\mathcal{W}}{\mathcal{W}}.\end{aligned}$$

Hence

$$\begin{aligned}\int_0^1 \mathcal{G}(\mathcal{T},\mathcal{W})\,d\mathcal{W} = &-k[1-\ell(1-\delta)](1+\mathcal{T})\\ &+(1-k)[1-\ell(1-\delta)]\ln\frac{1}{[1-\ell(1-\delta)](1+\mathcal{T})},\end{aligned} \tag{59}$$

The two expressions agree at $\mathcal{T}=\zeta/(1-\zeta)$, where the first logarithm in (58) vanishes.

For $\mathcal{T}<\underline{z}$, every withdrawal fraction leads to compulsory closure. Integrating both failure branches over $[0,1]$ gives

$$(1-k)\left\{[\ell(1-\delta)-\zeta]\ln\frac{1-\zeta}{\ell(1-\delta)-\zeta}+[1-\ell(1-\delta)]\ln\frac{1-\zeta}{1-\ell(1-\delta)}\right\}. \tag{60}$$

which is strictly positive. At and above $\ell(1-\delta)/[1-\ell(1-\delta)]$, capacity is at least one, every withdrawal fraction leads to survival, and the integral is $-k$. □

Lemma 9 (A unique zero of the limiting gain)**.** *On $[\underline{z},\infty)$, the integral $\int_0^1 \mathcal{G}(\mathcal{T},\mathcal{W})\,d\mathcal{W}$ is continuous. It is strictly decreasing on $[\underline{z},\ell(1-\delta)/[1-\ell(1-\delta)]]$ and equals $-k$ thereafter. Consequently, it has a zero above $\underline{z}$ if and only if its value at $\underline{z}$ is positive, and that zero is unique.*

Proof. In (56), increasing $\mathcal{T}$ raises capacity and replaces a range of positive failure gains with the survival gain $-k$. The failure payoff itself depends only on $\mathcal{W}$ and is continuous

at the recovery kink. Differentiating the integral at $\underline{z} < \mathcal{T} < \ell(1-\delta)/[1-\ell(1-\delta)]$ therefore gives

$$\begin{aligned}
&\frac{d}{d\mathcal{T}}\int_0^1 \mathcal{G}(\mathcal{T},\mathcal{W})\,d\mathcal{W} \\
&\quad = [1-\ell(1-\delta)]\Big\{-k-(1-\zeta)(1-k)\Big[\\
&\quad \underbrace{\mathcal{R}\big([1-\ell(1-\delta)](1+\mathcal{T})\big)-\mathcal{S}\big([1-\ell(1-\delta)](1+\mathcal{T})\big)}_{\geq 0,\text{since the requesters have priority}}\Big]\Big\} < 0.
\end{aligned} \tag{61}$$

The inequality follows from the strictly positive failure gain. The integral in (56) is continuous in its lower limit, so the gain is continuous throughout this interval, including at $\mathcal{T} = \zeta/(1-\zeta)$. At the upper endpoint,

$$\int_0^1 \mathcal{G}\left(\frac{\ell(1-\delta)}{1-\ell(1-\delta)},\mathcal{W}\right)d\mathcal{W} = \int_0^1 (-k)\,d\mathcal{W} = -k < 0.$$

The gain joins the constant survival gain continuously. Strict decrease and the intermediate value theorem then give the claimed condition for an interior zero and its uniqueness. □

A sufficient condition for $\int_0^1 \mathcal{G}(\underline{z},\mathcal{W})\,d\mathcal{W} > 0$ is

$$\boxed{\frac{k}{1-k} < \frac{1}{1+\underline{z}}\ln\frac{1-\zeta}{1-\ell(1-\delta)}.}$$

Evaluating (58) at $\mathcal{T} = \underline{z}$ gives

$$\begin{aligned}
\int_0^1 \mathcal{G}(\underline{z},\mathcal{W})\,d\mathcal{W} = &-k[1-\ell(1-\delta)](1+\underline{z}) \\
&+(1-k)[\ell(1-\delta)-\zeta]\ln\frac{(1-\zeta)\{1-[1-\ell(1-\delta)](1+\underline{z})\}}{\ell(1-\delta)-\zeta} \\
&+(1-k)[1-\ell(1-\delta)]\ln\frac{1-\zeta}{1-\ell(1-\delta)}.
\end{aligned}$$

Since $\underline{z} < 0$ and $\zeta \geq 0$,

$$\begin{aligned}
&(1-\zeta)\{1-[1-\ell(1-\delta)](1+\underline{z})\}-[\ell(1-\delta)-\zeta] \\
&\quad = [1-\ell(1-\delta)]\{\zeta-(1-\zeta)\underline{z}\} > 0.
\end{aligned}$$

The first logarithm therefore has an argument greater than one. Dropping this positive term and factoring out $[1-\ell(1-\delta)]$ gives

$$\int_0^1 \mathcal{G}(\underline{z},\mathcal{W})\,d\mathcal{W} \geq [1-\ell(1-\delta)]\left[(1-k)\ln\frac{1-\zeta}{1-\ell(1-\delta)} - k(1+\underline{z})\right].$$

The condition makes this lower bound strictly positive. Since $\zeta < \ell(1-\delta)$, the logarithm is positive, so sufficiently small k always guarantees positivity.

A.2.5 Proof of Proposition 2

Proof.

Step 1: existence and bounds. At $\mathcal{T} = \underline{z} - \sigma_\varepsilon$ the marginal posterior window is $[\underline{z} - 2\sigma_\varepsilon, \underline{z}]$. All states except one endpoint are compulsory closures, so

$$\Psi_{\underline{z}-\sigma_\varepsilon}(\underline{z}-\sigma_\varepsilon) > 0. \tag{62}$$

At $\mathcal{T} = \ell(1-\delta)/[1-\ell(1-\delta)] + \sigma_\varepsilon$, every posterior state is in the upper dominance region and

$$\Psi_{\mathcal{T}}(\mathcal{T}) = -k\int_{\frac{\ell(1-\delta)}{1-\ell(1-\delta)}}^{\frac{\ell(1-\delta)}{1-\ell(1-\delta)}+2\sigma_\varepsilon} f_z(z)\,dz < 0. \tag{63}$$

Continuity implies a zero between the bounds, and Lemma 5 makes it a threshold equilibrium. Outside these bounds a threshold would prescribe the wrong action at strictly dominant signals.

Step 2: uniqueness among thresholds. For $0 < \sigma_\varepsilon \leq 1$, all candidate equilibrium thresholds and their posterior states lie in the fixed compact interval $[\underline{z}-2,\ \ell(1-\delta)/[1-\ell(1-\delta)]+2]$, by Step 1. Recall that $\overline{\mathcal{W}}_{\mathcal{T}}$ is the largest withdrawal fraction for which the bank survives: if $\overline{\mathcal{W}}_{\mathcal{T}} = 0$, any positive withdrawal fraction is enough to cause a bank's failure; and if $\overline{\mathcal{W}}_{\mathcal{T}} = 1$ the bank survives for any withdrawal fraction. At an equilibrium threshold, it must be the case that $\overline{\mathcal{W}}_{\mathcal{T}} \in (0,1)$. Wherever this boundary is interior, it is continuous and piecewise differentiable, so the outer bounds of zero and one in (53) do not bind.

$$\frac{d\overline{\mathcal{W}}_{\mathcal{T}}}{d\mathcal{T}} \in \left\{\frac{1-\ell(1-\delta)}{1+2\sigma_\varepsilon[1-\ell(1-\delta)]},\ \frac{1}{2\sigma_\varepsilon}\right\}. \tag{64}$$

The second slope is strictly larger than the first, and both are greater than zero, which means that as $\mathcal{T}$ increases, the bank can survive to more withdrawals. Divide (54) by

$\int_0^1 f_z(\mathcal{T}+\sigma_\varepsilon(1-2u))\,du$ to get the expected gain conditional on the signal. The numerator and denominator of the posterior density converge uniformly to $f_z(\mathcal{T})$, and their derivatives to $f_z'(\mathcal{T})$, by uniform continuity of f_z'. The quotient rule therefore gives

$$\begin{aligned}&\frac{\partial}{\partial\mathcal{T}}\left[\frac{f_z(\mathcal{T}+\sigma_\varepsilon(1-2\mathcal{W}))}{\int_0^1 f_z(\mathcal{T}+\sigma_\varepsilon(1-2u))\,du}\right]\\ &\qquad\longrightarrow \frac{f_z'(\mathcal{T})f_z(\mathcal{T})-f_z(\mathcal{T})f_z'(\mathcal{T})}{f_z(\mathcal{T})^2}=0.\end{aligned}\tag{65}$$

uniformly. The marginal depositor's expected gain is

$$\begin{aligned}&\mathbb{E}[\mathcal{G}\mid s_h=\mathcal{T};\mathcal{T}]\\ &\quad=-k\int_0^{\overline{\mathcal{W}}_\mathcal{T}}\frac{f_z(\mathcal{T}+\sigma_\varepsilon(1-2\mathcal{W}))}{\int_0^1 f_z(\mathcal{T}+\sigma_\varepsilon(1-2u))\,du}\,d\mathcal{W}\\ &\qquad+(1-\zeta)(1-k)\int_{\overline{\mathcal{W}}_\mathcal{T}}^1\left[\mathcal{R}(\mathcal{W})-\mathcal{S}(\mathcal{W})\right]\times\frac{f_z(\mathcal{T}+\sigma_\varepsilon(1-2\mathcal{W}))}{\int_0^1 f_z(\mathcal{T}+\sigma_\varepsilon(1-2u))\,du}\,d\mathcal{W}.\end{aligned}$$

The payoffs are bounded, and their failure values do not depend on $\mathcal{T}$. Applying Leibniz's rule to these integrals gives, away from the possible switch of boundary slopes,

$$\begin{aligned}&\frac{d}{d\mathcal{T}}\mathbb{E}[\mathcal{G}\mid s_h=\mathcal{T};\mathcal{T}]\\ &=-\underbrace{\left\{k+(1-\zeta)(1-k)\left[\mathcal{R}(\overline{\mathcal{W}}_\mathcal{T})-\mathcal{S}(\overline{\mathcal{W}}_\mathcal{T})\right]\right\}}_{\geq k}\\ &\qquad\times\frac{f_z(\mathcal{T}+\sigma_\varepsilon(1-2\overline{\mathcal{W}}_\mathcal{T}))}{\int_0^1 f_z(\mathcal{T}+\sigma_\varepsilon(1-2u))\,du}\frac{d\overline{\mathcal{W}}_\mathcal{T}}{d\mathcal{T}}+o(1).\end{aligned}\tag{66}$$

It is important to highlight that the above expression moves both: the marginal signal $s_h=\mathcal{T}$, and the threshold played by all depositors $\mathcal{T}$. The terms from differentiating the posterior density are uniformly $o(1)$ by (65) and boundedness of the payoffs. The posterior density converges uniformly to one. Increasing $\mathcal{T}$ expands the survival region

and replaces a positive failure gain with $-k$, reducing the gain by at least k. Together with the lower bound on the boundary's slope in (64), this gives

$$\begin{aligned}
&\frac{d}{d\mathcal{T}}\mathbb{E}[\mathcal{G} \mid s_h = \mathcal{T}; \mathcal{T}] \\
&\quad \leq -k\,\frac{1-\ell(1-\delta)}{1+2\sigma_\varepsilon[1-\ell(1-\delta)]}[1-o(1)] + o(1) \\
&\quad \overset{\sigma_\varepsilon \to 0}{=} -k[1-\ell(1-\delta)] + o(1) < 0.
\end{aligned} \tag{67}$$

The equality uses the small-noise limit $\sigma_\varepsilon \to 0$, with vanishing terms included in $o(1)$. The leading term is strictly negative for fixed $k > 0$, and the error vanishes uniformly. Hence the expected gain strictly decreases wherever the boundary is interior for sufficiently small positive noise. The set where the boundary is interior is an interval, since both entries in (53) increase strictly with $\mathcal{T}$.

Step 3: convergence of thresholds and state boundaries. We first strengthen Lemma 7 slightly so that we can work with $\int_0^1 \mathcal{G}(\mathcal{T}, \mathcal{W})\, d\mathcal{W}$ along a sequence of equilibrium thresholds.[13] Fix a compact interval $[a, b]$ with $a > \underline{z}$. For sufficiently small noise, every posterior window for $\mathcal{T} \in [a, b]$ lies above the closure floor. The bounds in the proof of the lemma then apply uniformly over this interval: replacing $\mathcal{T} + \sigma_\varepsilon(1 - 2\mathcal{W})$ by $\mathcal{T}$ changes the bank's liquidation capacity per dollar of deposits by at most $[1 - \ell(1-\delta)]\sigma_\varepsilon$, and therefore can reverse the inequality for excess withdrawal requests only when

$$|\mathcal{W} - [1-\ell(1-\delta)](1+\mathcal{T})| \leq [1-\ell(1-\delta)]\sigma_\varepsilon. \tag{68}$$

This set has length $O(\sigma_\varepsilon)$, and gains are bounded. Together with the $O(\sigma_\varepsilon)$ bound in the proof of Lemma 6, this yields

$$\mathbb{E}[\mathcal{G} \mid s_h = \mathcal{T}; \mathcal{T}] = \int_0^1 \mathcal{G}(\mathcal{T}, \mathcal{W})\, d\mathcal{W} + O(\sigma_\varepsilon) \tag{69}$$

uniformly for $\mathcal{T} \in [a, b]$.

Now take any sequence $\sigma_{\varepsilon,j} \to 0$ and an equilibrium threshold $\mathcal{T}_j$ at each noise level. The bounds from Step 1 ensure that every subsequence has a convergent subsequence, whose limit $\overline{\mathcal{T}}$ is at least $\underline{z}$. Consider such a convergent subsequence, keeping the index j.

[13] Lemma 7 fixes $\mathcal{T}$ and then lets σ_ε go to zero. Here we need the approximation error to vanish uniformly over a compact interval of thresholds, since the equilibrium threshold itself changes with noise.

If $\overline{\mathcal{T}} > \underline{z}$, the thresholds eventually lie in a compact interval strictly above the floor. Since the marginal depositor is indifferent at each equilibrium, (69) gives

$$\begin{aligned} 0 &= \mathbb{E}[\mathcal{G} \mid s_h = \mathcal{T}_j; \mathcal{T}_j] \\ &= \int_0^1 \mathcal{G}(\mathcal{T}_j, \mathcal{W})\, d\mathcal{W} + O(\sigma_{\varepsilon,j}), \end{aligned}$$

and continuity of the integral implies

$$\int_0^1 \mathcal{G}(\overline{\mathcal{T}}, \mathcal{W})\, d\mathcal{W} = 0.$$

By Lemma 9, this zero is unique, so $\overline{\mathcal{T}} = z^* > \underline{z}$.

If $\overline{\mathcal{T}} = \underline{z}$, we must instead be in the first case of (18). To see why, suppose the integral at $\underline{z}$ were positive. The same approximation applied to the capacity rule alone would give a positive expected gain for thresholds near the floor and sufficiently small noise. Compulsory closure can only raise this gain, replacing $-k$ with a positive failure gain. This contradicts marginal indifference. Thus the integral at the floor is nonpositive, and $\overline{\mathcal{T}} = z^* = \underline{z}$.

Every convergent subsequence therefore has the same limit z^*, so the whole sequence satisfies $\mathcal{T}_j \to z^*$. Finally, (48) gives

$$|\widetilde{z}_{\mathcal{T}_j} - \mathcal{T}_j| < \sigma_{\varepsilon,j} \tag{70}$$

at equilibrium, so the state failure boundaries converge to z^* too.

Step 4: bounds and comparative statics. Lemma 9 gives $\underline{z} \le z^* < \ell(1-\delta)/[1-\ell(1-\delta)]$ and a strictly negative slope at every interior root. The limiting gain strictly decreases with k: survival contributes $-k$, while each positive failure term is multiplied by $1-k$. For $\mathcal{T} < \zeta/(1-\zeta)$, differentiating (58) gives

$$\frac{\partial}{\partial \zeta} \int_0^1 \mathcal{G}(\mathcal{T}, \mathcal{W})\, d\mathcal{W} = -(1-k) \ln \frac{(1-\zeta)\{1-[1-\ell(1-\delta)](1+\mathcal{T})\}}{\ell(1-\delta)-\zeta} < 0. \tag{71}$$

At and above this boundary the derivative is zero, by (59). The implicit function theorem gives the stated comparative statics; the floor preserves weak monotonicity. As $k \downarrow 0$, the limiting gain is positive at every fixed state below the upper bound and equals $-k$ at that bound. Its unique root therefore converges to the bound. □

For any fixed $z \neq z^*$, equation (43) implies that $\mathcal{W}_{\mathcal{T}_j}(z) \to 1$ if $z < z^*$ and $\mathcal{W}_{\mathcal{T}_j}(z) \to 0$ if $z > z^*$. The state failure boundary determines the limiting failure probability at each coordination opportunity. The continuous distribution of η assigns zero probability to the boundary, so dominated convergence gives

$$\Pr(z < z^* \mid n/x) = F_\eta\left(\frac{z^* - n/x}{\sigma_\eta}\right).$$

Multiplying this probability by the opportunity arrival rate λ_0 gives (19) and, for logistic η, (20).

A.3 Proof of Lemma 1

Proof. Fix (s, Γ) and write $a = (1-\ell)(n+x) > 0$ for the bank's liquid securities holdings. An individual bank takes the aggregate coefficients μ_Γ and σ_Γ as given: its portfolio choice does not change the law of motion of the aggregate distribution. At the given state, the run intensity $\lambda(s)$, the run payoff, and the current insurance tax also do not vary with the bank's instantaneous choice of α.

By (23) and (24), the terms in the HJB (29) that depend on α are

$$\mathcal{H}(\alpha) = \pi a v_n \alpha + \frac{1}{2}\sigma^2 a^2 v_{nn}\alpha^2 - \sigma a \alpha\, \sigma_\Gamma' v_{n\Gamma}. \tag{72}$$

The last term reflects the negative loading of the bank's net worth on the aggregate shock. All value-function derivatives in (72) are evaluated at (s, Γ). Differentiating with respect to α, the first-order condition for an interior optimum is

$$0 = \pi a v_n + \sigma^2 a^2 v_{nn}\alpha^* - \sigma a\, \sigma_\Gamma' v_{n\Gamma}. \tag{73}$$

Moreover,

$$\mathcal{H}''(\alpha) = \sigma^2 a^2 v_{nn} < 0,$$

so the Hamiltonian is strictly concave in the portfolio share and the stationary point is the unique optimum whenever it is admissible and interior. Solving (73) gives

$$\alpha^* = -\frac{\pi v_n}{\sigma^2 a v_{nn}} + \frac{\sigma_\Gamma' v_{n\Gamma}}{\sigma a v_{nn}}.$$

Substituting $a = (1-\ell)(n+x)$ yields (31). The first term is the myopic demand; the second is the dynamic hedging demand, whose interest-rate and distribution components

follow from (30). □

A.4 CES Deposits

Depositors. Depositors derive utility from the liquidity services of deposits and allocate a constant amount of money (D_t) among differentiated deposit goods, aggregated according to a standard CES:

$$D_t = \left(\int_0^1 d_t(i)^{\frac{\epsilon-1}{\epsilon}} di \right)^{\frac{\epsilon}{\epsilon-1}} \tag{74}$$

Depositor's pay a deposit spread $s_t(i) = r_t - r_t^d(i)$ for deposits and solve the following problem

$$\min_{d_t(i)} \int_0^1 s_t(i) d_t(i) di \tag{75}$$

subject to:

(74)

The solution for the above problem yields the standard CES demand:

$$s(d_t) = S_t \left(\frac{D_t}{d_t} \right)^{1-\epsilon} \quad \Longrightarrow \quad r^d(d_t) = r_t - S_t \left(\frac{D_t}{d_t} \right)^{1-\epsilon} \tag{76}$$

Were

$$S_t \equiv \left(\int_0^1 s_t(i)^{1-\epsilon} di \right)^{\frac{1}{1-\epsilon}}$$

Discussion. It is useful to emphasize two simplifications at this stage. First, the aggregate spread index S_t and the aggregate quantity of deposit services D_t are treated as exogenous parameters. This keeps the bank's problem tractable and isolates the bank-side tradeoff between interest-rate risk, portfolio choice, and run exposure. In a general-equilibrium extension, S_t would be pinned down endogenously by the joint behavior of banks and depositors in the deposit market, and D_t would arise from the depositor's optimal allocation between consumption and deposits. Second, the implied deposit "revenue" term for a bank, $d\,s(d)$, is strictly increasing in d: marginal revenue is always positive. As a result, absent additional constraints, a bank would want to expand deposit issuance without bound.

Banks. Each bank has (marked-to-market) equity n_t and funds itself with deposits d_t. Deposits are differentiated goods that provide liquidity services to depositors. Given the deposit demand system, a bank that issues d_t units of deposits must pay an equilibrium deposit rate pinned down by the inverse demand schedule (76) where S_t and D_t are taken as given in partial equilibrium. The bank earns a flow "deposit franchise" revenue equal to the deposit spread times quantity, $s_t(d_t)\, d_t$.

A bank chooses *(i)* a consumption/dividend flow c_t; *(ii)* a portfolio share α_t invested in the long bond (the remainder $1 - \alpha_t$ is invested in the short bond); and *(iii)* the scale of deposit issuance d_t. The bank invests total assets $(n_t + d_t)$ in the short and long bonds. Throughout, we restrict deposit issuance using a leverage constraint,

$$0 \leq d_t \leq \phi n_t,$$

which prevents unbounded deposit growth.[14]

Combining short- and long-bond returns, the bank's equity evolves as

$$dn_t = \Big[\big(r_t + \alpha_t \pi\big)(n_t + d_t) - c_t - r_t^d(d_t)\, d_t\Big]dt - \alpha_t \sigma (n_t + d_t)\, dB_t. \tag{77}$$

Banks face the possibility of runs that destroy the continuation value of the deposit franchise. The Poisson shock with state-dependent intensity $\lambda(n_t, d_t)$, is the same as in the main text.

$$\lambda(n, d) \equiv \frac{\lambda_0}{1 + e^{-\lambda_1 (d - n)}} \tag{78}$$

where λ_0, λ_1 are parameters to be calibrated[15].

Let $v(n, r)$ denote the bank value function when equity is n and the short rate is r. The

[14] Under the CES inverse demand above, the flow revenue term $s_t(d)\, d$ is increasing in d (marginal revenue is always positive). Absent additional constraints, a bank would therefore prefer to issue arbitrarily large deposits. The leverage constraint can be interpreted as a parsimonious reduced-form representation of regulatory leverage limits, deposit franchise capacity, or other balance-sheet constraints that discipline deposit scale in a richer environment.

[15] Notice that $\lim_{\lambda_1 \to \infty} \lambda(n, d) = \lambda_0 \mathbb{1}_{\{n < d\}}$. To facilitate the numerical solution, we use a functional form such as (78) to avoid a discontinuous arrival rate of the run shock.

bank solves

$$\rho\, v(n,r) = \max_{c,\alpha,\, d\in[0,\phi n]} \Big\{ u(c) + v_n(n,r)\Big(\big(r+\alpha\pi\big)(n+d) - c - r^d(d)\, d \Big) + v_r(n,r)\mu_r(r) + \frac{1}{2}\big(\alpha\sigma(n+d)\big)^2 v_{nn}(n,r) + \frac{1}{2}(\sigma_r r)^2 v_{rr}(n,r) - \big(\alpha\sigma(n+d)\big)(\sigma_r r)\, v_{nr}(n,r) + \lambda(n,d)\big(\bar{v} - v(n,r)\big) \Big\}, \tag{79}$$

where $\mu_r(r) = \theta(\bar{r} - r)$.

We can interpret the run technology as an endogenous "death shock" that shortens the bank's effective planning horizon. A run destroys future profits, and move the bank's continuation value from v to $\bar{v}$, making the bank behave as if it were more impatient when runs are likely. When equity is low relative to deposits, run intensity is high and the bank has a small probability of surviving to receive future profits. Accumulating equity is then difficult, since the bank remains exposed to termination while trying to recover. For well-capitalized banks (with high equity relative to deposits), the run hazard is negligible and the effective horizon is longer.

A.5 Numerical solution with an aggregate distribution state

We use the approximation of Schaab (2020) to represent the distribution of active banks with a finite-dimensional aggregate state. In the notation of the presentation, z is the individual bank state, consisting of net worth n, deposits x, and the loan share ℓ. We approximate the distribution by

$$\hat{g}_t(z) = F(\omega_t)(z) \approx g_t(z). \tag{80}$$

With this approximation, we write the bank's problem as

$$v(z,r,g) \approx v(z,r,\omega). \tag{81}$$

The bank therefore needs to forecast ω_t, whose law of motion is

$$d\omega_t = \mu_\omega(r_t,\omega_t)dt + \sigma_\omega(r_t,\omega_t)dB_t. \tag{82}$$

The aggregate state. We take as the aggregate moment the expected flow of deposits at banks experiencing runs:

$$\omega = \int \lambda(z) x g_t(z)\, dz, \tag{83}$$

$$d\omega = \int \lambda(z) x\, dg_t(z)\, dz. \tag{84}$$

Deposits at each individual state are weighted by the run intensity. As banks move across states, the distribution changes, and with it the aggregate moment (and the tax associated with deposit insurance).

The reference density and its tilted versions. We start by choosing a reference density $g_0(z)$ and computing its moment:

$$\omega_0 = \int \lambda(z) x g_0(z)\, dz. \tag{85}$$

We use this moment as the center of the aggregate-state grid,

$$\omega_w \in [\omega_0 - h_w, \omega_0 + h_w]. \tag{86}$$

At each gridpoint, we tilt the reference density as follows:

$$\hat{g}(z; \omega_w) = \frac{g_0(z) \exp\{\theta(\omega_w)\lambda(z)x\}}{\int g_0(\tilde{z}) \exp\{\theta(\omega_w)\lambda(\tilde{z})\tilde{x}\}\, d\tilde{z}}. \tag{87}$$

The parameter $\theta(\omega_w)$ changes the weight on each individual state, and the denominator normalizes the density. We choose the parameter so that the resulting moment equals the gridpoint:

$$\omega_w = \int \lambda(z) x \hat{g}_{\theta(\omega_w)}\, dz. \tag{88}$$

For each ω_w, we then have a density $\hat{g}(z; \omega_w)$ with which to evaluate the aggregate objects in the bank's problem. In particular, the tax in the algorithm is

$$\tau(\omega_w) = \int \lambda(z) x \hat{g}(z; \omega_w)\, dz. \tag{89}$$

The law of motion of the aggregate state. Given a parametric family $\hat{g}$, we obtain the drift and diffusion of ω by integrating the distribution dynamics against the same run-

weighted deposit moment. The expressions in the presentation give

$$\sigma_\omega(r_t, \omega_t) = -\int \lambda(n, x, \ell) x \, \partial_n\big(\sigma_n \hat{g}\big) \, dn \, dx \, d\ell, \tag{90}$$

$$\mu_\omega(r_t, \omega_t) = \int \lambda(n, x, \ell) x \Big[-\partial_n\big(\mu_n \hat{g}\big) - \partial_x\big(\mu_x \hat{g}\big) + \frac{1}{2}\partial_{nn}\big(\sigma_n^2 \hat{g}\big) + \frac{1}{2}\partial_{xx}\big(\sigma_x^2 \hat{g}\big) - \lambda \hat{g} + \mathcal{E}(n, x, \ell) \Big] \, dn \, dx \, d\ell. \tag{91}$$

The drift accounts for banks moving across net worth and deposits, as well as exit through runs and entry. The diffusion describes how the aggregate moment responds to the common shock. Since μ_n and σ_n depend on bank policies, we need to update the aggregate law of motion as those policies change during the solution.

Value-function iteration. After constructing the tilted densities and computing the taxes, we start from a guess v_0 and iterate:

$$v_0 \to v_1 \to \cdots \to v_s.$$

At iteration s, we obtain the policies c^s and α^s, together with μ_n^s and σ_n^s, using the aggregate-law coefficients μ_ω^{s-1} and σ_ω^{s-1} from the preceding iteration. With these policies and the density $\hat{g}(.; \omega_w)$, we update the aggregate dynamics at each gridpoint:

$$\mu_\omega^s(., \omega_w) \qquad \text{and} \qquad \sigma_\omega^s(., \omega_w).$$

We use the updated coefficients in the next value-function iteration and continue until

$$\|v^{s+1} - v^s\| < \text{tol}.$$

At convergence, we obtain v^*, c^*, α^*, μ_ω^*, and σ_ω^*. The policies and aggregate forecasts are therefore determined jointly in the approximate economy: bank choices determine how the aggregate moment evolves, while the forecast of this evolution enters those choices. How well this approximation works depends on whether the family $\hat{g}$ represents the relevant movements in the distribution.

A.5.1 Choice of the reference density

The role of g_0. The procedure above takes g_0 as given. In (87), we form the tilted family departing from g_0. We evaluate the tax (89) on this family and obtain the law of motion

(90)–(91) by integrating the KFE against it. The same distribution enters all the objects the bank uses to forecast the aggregate state. The family $\{\hat{g}(\cdot\,;\omega)\}$ can only reproduce exponential tilts of g_0 in the direction of $\lambda(z)x$. If the model generates a cross-section with a different shape. We then evaluate the perceived law of motion of ω on the wrong density, and the forecasts used in the HJB would not be consistent with the distribution dynamics generated by the policies.

Ad hoc reference densities. We can start from any density with a well defined $\omega_0 = \int \lambda(z)x\, g_0(z)\, dz$. We tried different classes of g_0 distributions. These choices do not perform equally well. We compare those against the rest-point distribution generated by the converged policies. We also compute the rational-expectations gap, taking the difference between the perceived drift μ_ω and the drift obtained by stepping the KFE forward under those policies. Table **??** reports both statistics. We find sizable gaps with ad hoc choices, and their size depends on where g_0 places mass relative to the run threshold. The run intensity λ is steep near this threshold (so even small changes in the location of mass can move the moment substantially).

The model-generated reference density $g_{\mathcal{A}^*}$. Schaab (2020) uses the stationary distribution of the economy without aggregate risk to anchor the family. We cannot take this limit here. Sending $\sigma_r \to 0$ makes both the term premium $\pi = \varsigma\sigma_r/\theta_r$ and the long-bond exposure $\sigma = \sigma_r/\theta_r$ equal to zero, so myopic demand becomes $0/0$ and the portfolio share α is indeterminate. In our model, the long bond's excess return is the aggregate shock itself. Switching it off would therefore remove the object we want to compute.

We use a density generated by the model itself as the reference. Let $\mathcal{A}^*_{(\alpha,c)}$ be the adjoint of the generator of an individual bank (the drift and diffusion terms in the dt bracket of the KFE (25) under given policies (α, c)). We define $g_{\mathcal{A}^*}$ as the unit-mass solution of

$$\mathcal{A}^*_{(\alpha^*,c^*)}\, g_{\mathcal{A}^*} - \lambda(z)\, g_{\mathcal{A}^*} + \psi_0(z) \int \lambda(\tilde{z})\, g_{\mathcal{A}^*}(\tilde{z})\, d\tilde{z} = 0, \qquad \int g_{\mathcal{A}^*}(z)\, dz = 1, \tag{92}$$

where (α^*, c^*) are the converged policies from the full stochastic problem, evaluated at $(\bar{r}, \omega^*)$. We require ω^* to equal the moment of $g_{\mathcal{A}^*}$ itself:

$$\omega^* = \int \lambda(z)\, x\, g_{\mathcal{A}^*}(z)\, dz. \tag{93}$$

Thus, $g_{\mathcal{A}^*}$ is the rest point of the deterministic part of the distribution dynamics, where the KFE drift is zero when the aggregate state is held at its central value and banks use

the policies from the stochastic economy. We keep the policies from the HJB solution with $\sigma_r > 0$ (we do not rederive them), so α^* remains determinate and $\sigma_n = \sigma\alpha^*(1-\ell)(n+x) > 0$ continues to diffuse the cross-section in (92). Also, $g_{\mathcal{A}^*}$ is not the stationary distribution of the stochastic economy. With aggregate risk, the whole cross-section of banks is being hit by aggregate shocks. We use $g_{\mathcal{A}^*}$ as a numerical anchor: the tilts needed to cover the relevant range of ω are then small perturbations of a model-generated density (rather than large deformations of an arbitrary one).

Rest point under constant deposits. In the baseline, deposits are constant ($\bar{x} = \sigma_x = 0$). Holding the short rate at $\bar{r}$, the deterministic part of the distribution dynamics has a rest point, given by $g_{\mathcal{A}^*}$. We compute the law of motion of ω using the converged policies and this anchor. At $\omega^* = 2.48$, the failure rate is 9.2 basis points per year and the median solvency ratio is 0.46. The fee at this point is $\tau^* = 1.8 \times 10^{-3}$ per bank-year, or 0.60 basis points of mean deposits. Over the simulated 2010–25 window, it averages 0.81 basis points per year. The volatility of the moment per unit of the rate shock is $\sigma_\omega = 0.25$. General-equilibrium feedback is inert: levying the fee changes the long-bond share by 8.5×10^{-5} on average in absolute value, and carrying ω as a state adds 3×10^{-5}. The fee has little effect through its level, and even less through its fluctuations.

Since entry is linear in g, (92) is a linear system in the discretized density. On the grid, we have $\left[\mathbf{A}^\top - \mathrm{diag}(\lambda) + \psi_0 \, (\lambda \circ w)^\top\right] g = 0$, where $\mathbf{A}$ is the finite-difference generator used in the HJB and w denotes the cell weights. The system is singular by construction. We close it by replacing one equation with the normalization $\sum_z g(z)w(z) = 1$, so no time marching is needed.

Outer fixed point. The policies in (92) depend on the reference density through the closure. We therefore obtain $g_{\mathcal{A}^*}$ with an outer loop around the value-function iteration:

1. Start from an ad hoc reference density $g_0^{(0)}$ (for instance, a Gaussian). Build the tilted family and the ω-grid around $\omega_0^{(0)} = \int \lambda x \, g_0^{(0)}$.
2. Solve the bank's problem by value-function iteration as above, obtaining (α^*, c^*), μ_ω, σ_ω, and τ on the grid.
3. Initialize ω^* at the zero of $\mu_\omega(\bar{r}, \cdot)$ on the grid. Interpolate the policies at $(\bar{r}, \omega^*)$, solve (92) for $g_{\mathcal{A}^*}$, and update ω^* from (93). Repeat until ω^* no longer changes. We need this inner loop because the rest point of the perceived law of motion equals the moment of $g_{\mathcal{A}^*}$ only at the fixed point.

4. Set $g_0^{(p+1)} = g_{\mathcal{A}^*}$ and recenter the ω-grid at its moment. Return to step 2, using the value function from pass p as the initial guess.

We stop when the anchor moment is self-consistent, $|\omega^* - \omega_0^{(p)}| < \text{tol}$.

B Data Appendix

B.1 Variable Construction

We used data from the US Call Reports, more specifically, we use the FFIEC 031-041 reports[16]. We have quarterly observations from 2001Q1 to 2025Q1. Banks are uniquely identified by the variable "*IDRSSD*" in the *Bulk POR Schedule*, and following Drechsler et al. (2021) we filter only *commercial banks*, that is, the ones with charter type equal 200[17]. We follow the literature to construct our main variables of interest, which will be detailed in the upcoming subsections.

B.1.1 Liabilities

Deposits. In case of deposits, we have two candidates for the series we would use: **RCON2200** and **RCFN2200**. Unlike the other variables, deposits do not have an **RCFD** series. Moreover, as **RCFN** refers to deposits in foreign branches, we use **RCON2200** as our main variable for deposits.

Insured/Uninsured Deposits. This variable is more difficult to construct. We have access to the *Amount of deposit accounts with 250K or more/less* (aggregating over retirement and non-retirement accounts) and *Number of deposit accounts with 250K more/less* (also with a distinction between retirement accounts) in the series **RCONF045-RCONF052**. We will follow Jiang et al. (2024) and define:

$$\begin{aligned}
\text{Ins. Deposit Accounts} &= \text{RCONF045} + \text{RCONF049} \\
\text{Number of Ins. Deposit Accounts} &= \text{RCONF046} + \text{RCONF050} \\
\text{Uns. Deposit Accounts} &= \text{RCONF047} + \text{RCONF051} \\
\text{Number of Uns. Deposit Accounts} &= \text{RCONF048} + \text{RCONF052}
\end{aligned}$$

[16]The FFIEC 031 report collects basic financial data from commercial banks in the form of a balance sheet, an income statement, and supporting schedules for banks with **domestic and foreign offices**. At the same time, the FFIEC 041 is restricted to **domestic offices**.

[17]Since we're not exporting data directly from the WRDS, we had to rely on additional .csv files with charter type variable (RSSD9048). The *Attributes* files from active or closed banks can be found here

The total *Insured Deposits* is thus:

$$\text{Insured Deposits} = \underbrace{\text{Ins. Deposit Accounts}}_{\text{Aggregate deposits over accounts with less than coverage}} \underbrace{+\text{Number of Uns. Deposit Accounts} \times \text{Insurance Coverage}}_{\text{For accounts over coverage, sum insured piece}}$$

The total *Uninsured Deposits* is thus:

$$\text{Uninsured Deposits} = \underbrace{\text{Unins. Deposit Accounts}}_{\text{Total amount in accounts over coverage}} \underbrace{-\text{Number of Unins. Deposit Accounts} \times \text{Insurance Coverage}}_{\text{Subtract the covered money in each of these accounts.}}$$

Total Liabilities. This variable includes deposits, FedFunds purchased and securities sold with agreements to repurchase, other borrowed money, subordinated notes, etc. We use **RCON2948** as the primary source, and use **RCFD2948** whenever the first is not available.

B.1.2 Assets

Total Securities. We get information from banks' security holdings from the Schedule RC-B. Securities can be classified either as Held-to-maturity (HTM)[18] or Available-for-sale (AFS)[19]. From 2018 onwards, equity securities also started being reported.

$$\text{Total Securities} = \text{HTM Securities} + \text{AFS Securities} + \text{Equity Securities}$$

Each of these terms will be detailed.

Held-to-maturity (HTM). Those are reported at amortized costs, or book value, and are not updated as market prices change. In the balance sheet (Schedule RC) HTM securities

[18] If a bank classifies a security as HTM, it should have the intention to hold the security until it matures. However, the HTM classification is not necessarily permanent. A bank may sell a security out of HTM, but doing so risks "tainting" the entire remaining HTM portfolio and forcing a reclassification of all HTM securities into AFS. Under certain conditions a holder can sell HTM securities and avoid tainting. **A bank can also redesignate a security from AFS to HTM under certain conditions, though a similar tainting rule does not exist.**

[19] AFS securities will vary mechanically due to price changes, while HTM securities will be a more reasonable way of keeping track of the *quantity* of securities.

are reported at amortized cost **(1754)**. The variables 1754 (RCON and RCFD) are both reported from 2001-2019. From 2019 onward, HTM securities are reported under the code **JJ34** (RCON and RCFD).

Available-for-sale (AFS). Those are marked to market. Unrealized gains and losses of AFS securities affect book equity as part of the account "accumulated other comprehensive income" (AOCI). In the balance sheet (Schedule RC), AFS securities are reported at fair-value **(1773)**.

Equity Securities not held for trading. Equity securities started to be reported in 2018 under the variables **JA22** (RCON and RCFD). From then on, we start considering it as a component of *Total Securities*.

Securities FV. Although HTM securities enter the balance sheet as amortized cost (face value of the securities), banks also have to report its fair value under the **1771** code. To get the **Securities FV** variable, we sum AFS and HTM securities at fair value.

Securities AC. Although AFS securities are reported in the balance sheet at fair value, banks also report the amortized cost (face value) of the securities bought under the code **1772**. The **Securities AC** is the sum between the Amortized cost of AFS securities and the HTM securities.

Cash. We follow Drechsler et al. (2021) and define **Cash 1** using the series **0010** from the **Schedule RC-A**, the primary variable is **RCON0010** and we use **RCFD0010** whenever the first wasn't available. We define **Cash 2** as the sum of *Noninterest-bearing balances and currency and coin*, reported under the code **(0081)** and *Interest-bearing balances* under the code **(0071)**. [20] **Cash** then takes **Cash 1** as primary variable, and uses **Cash 2** whenever the first was not available.

B.1.3 Interest Expenses

The expenses information comes from the income statement of the FFEIC-031/041 (*Schedule RI*). A notable point is that all these variables are accumulated by year. To obtain quar-

[20] Those items can be further decomposed into *Cash items in process of collection and unposted debits* **(0020)**, *Currency and coin* **(0080)**, *Balances due from depository institutions in the U.S.* **(0082)**, *Balances due from banks in foreign countries and foreign central banks* **(0070)**, and *Balances due from Federal Reserve Banks* **(0090)**.

Table 8: Number of rows with mismatches between RCON and RCFD variables.

Variable	Only RCON	Only RCFD	Both (same)	Both (different)	Description
Liabilities					
2200	633312	-	-	-	Total Deposits
2948	639209	4933	2132	2688	Total Liabilities
Equity					
3210	630313	9589	0	0	Total Equity Capital
B530	630313	9589	0	0	AOCI
Loans					
2122	630313	0	5250	4339	Total Loans
Securities					
1754	630313	4686	4143	760	HTM at Amortized Cost
1771	630313	9589	0	0	HTM at Fair Value
1772	630313	9589	0	0	AFS at Amortized Cost
1773	630313	4686	3437	1466	AFS at Fair Value
Cash					
0010	474439	9660	5318	4342	Total Cash
0071	639209	9753	0	0	Interest-bearing balances
0081	639209	9753	0	0	Currency and coin

Note: Notice that since the RCFD variable accounts for domestic and foreign branches, for variables in which RCON and RCFD are both non-null

terly values of expenses, we calculate the difference between subsequent dates within a year. The complete list of variables used is in Table (**??**)

As in DeMarzo et al. (2025) we define *"Total Non Interest Expenses"* as follows:

$$\begin{aligned}\text{Total Non Interest Expenses} = &\underbrace{\text{Salaries}}_{\text{RIAD4135}} + \underbrace{\text{Expenses of premises and fixed assets}}_{\text{RIAD4217}} \\ &+ \underbrace{\text{Other Non Interest Expenses}}_{\text{RIADB497}}\end{aligned}$$

We also define "Non Interest Income" such as:

$$\text{Non Interest Income} = \underbrace{\text{Service Charges from Deposits}}_{\text{RIAD4080}} + \underbrace{\text{Other Non Interest Income}}_{\text{RIADB497}}$$

B.1.4 Repricing Maturity

We find information on repricing maturity on the *Schedule RC-B*. We use the RCFD series as a primary source since the RCON series is empty for these variables. We use repricing

Table 9: Variables taken from the Income Statement (Schedule RI)

Variable	Code	Period
Expenditure Variables		
Transaction Deposit Expenses	RIAD4508	2001-2025
Savings Expenses	RIAD0093	2001-2025
Small TD Expenses	RIADA518	2001-2016
	RIADHK03	2017-2025
Large TD Expenses	RIADA517	2001-2016
	RIADHK04	2017-2025
Time Deposit Expenses	Large + Small TD Expenses	2001-2016
Total Interest Expenses	RIAD4073	2001-2025
Interest Expenses on Subordinated Debt	RIAD4200	2001-2025
Other Interest Expenses	RIAD4185	2001-2025
Interest Expenses in FFS	RIAD4180	2001-2025
Income Variables		
Total Interest Income	RIAD4107	2001-2025
Net Interest Income	RIAD4093	2001-2025
Non-Interest Income	RIAD4080+RIADB497	2001-2025
Total Non-Interest Expenses	RIAD4135+RIAD4217+RIADB497	2001-2025

Note: Small TD and **Large TD** changed codes from 2017 onwards. The threshold, though, remains the same: 100k dollars. After 2017, there is also a category for over/under 250k dollar TDs.

maturities for MBS and US Treasuries to construct the variable **Securities Maturity**, following Drechsler et al. (2017), and Jiang et al. (2024). First, we sum all securities in each bin. We use the midpoint of each bin, except for the last one, for which we use the minimum value (15Y) to compute the average maturity, weighted by the value of securities held in that specific bin.

B.2 Alternative definitions of long securities

In this section we try alternative definitions for long securities (in the main body of the text, we used $>$ 3-months). We construct four alternative portfolio-share measures based on maturity cutoffs of one, three, five, and fifteen years. For each cutoff h, we define the share of securities above the cutoff as one minus the share of liquid assets held in cash, federal funds sold, and securities with maturity at or below h. Liquid assets are measured as total assets at fair value less total loans, consistent with the baseline construction. Thus, the four outcomes are the shares of liquid assets invested in securities with maturities above one, three, five, and fifteen years.

For each outcome, we estimate a nonparametric binned-scatter relationship with the market-

Table 10: Maturity variables taken from the Balance Sheet Statement (Schedule RC-B)

Variable	Code
Treasuries	
3M-	A549
3M-1Y	A550
1Y-3Y	A551
3Y-5Y	A552
5Y-15Y	A553
15Y+	A554
Mortgage-Backed-Securities	
3M-	A555
3M-1Y	A556
1Y-3Y	A557
3Y-5Y	A558
5Y-15Y	A559
15Y+	A560

adjusted solvency ratio, using 100 bins. Figure (6) plots the resulting within-bin means for the four maturity thresholds. The non-monotonic relationship remains across the alternative definitions, although shifted, (as expected, since we changed the definition of long securities) indicating that the hump is not driven by the particular three-month cutoff used in the baseline measure.

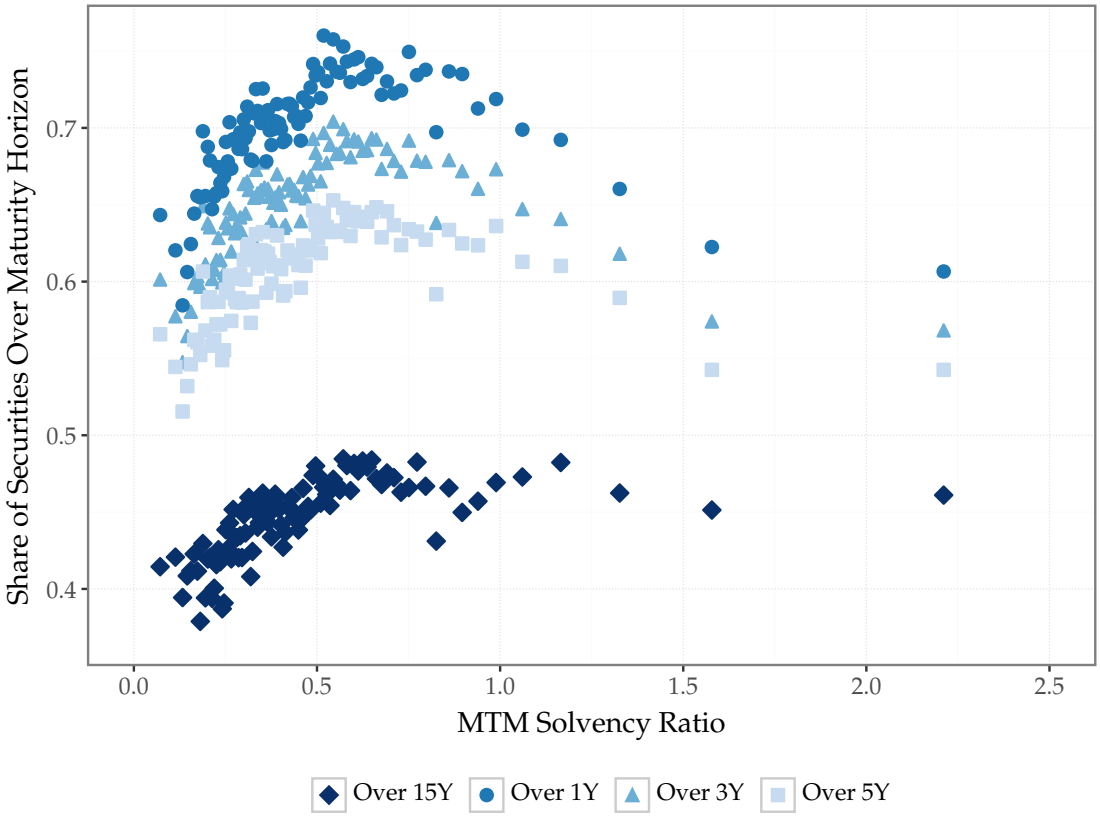
B.3 Alternative measures of duration exposure

B.3.1 Intensive-margin duration exposure

Our model has a portfolio weight as central object. In that case we consider the share of bonds exposed to *any* of duration exposure. This measure cannot distinguish between securities with different maturities above the three-month threshold. For instance, two banks in our model are exactly the same when they hold 1Y vs. 10Y securities. To incorporate an intensive margin, we assign representative maturities to the longer maturity buckets reported in the Call Reports. Specifically, we assign weights of 2, 4, 10, and 15 to securities in the 1–3 year, 3–5 year, 5–15 year, and 15 years or more buckets, respectively. Let S_{it}^{h} denote the value of securities in maturity bucket h. We define the intensive-margin maturity measure as

$$\texttt{Intensive Margin}_{it} = \frac{2S_{it}^{1\text{–}3} + 4S_{it}^{3\text{–}5} + 10S_{it}^{5\text{–}15} + 15S_{it}^{15+}}{S_{it}^{1\text{–}3} + S_{it}^{3\text{–}5} + S_{it}^{5\text{–}15} + S_{it}^{15+}}.$$

Figure 6: Alternative definitions of long securities



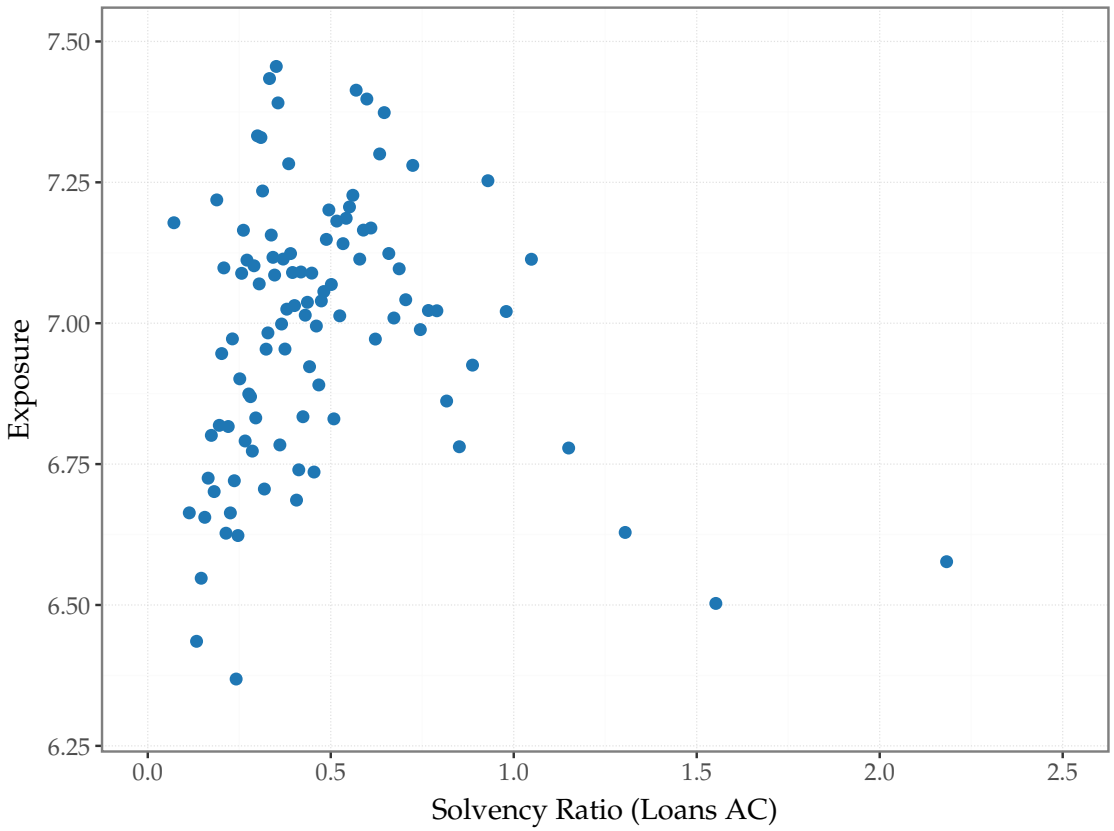
The resulting duration-weighted exposure measure is the product of this intensive-margin maturity measure and the share of liquid assets held outside the shortest securities bucket:

$$\texttt{Total Exposure}_{it} = \texttt{Share of Long Securities}_{it} \times \texttt{Intensive Margin}_{it}.$$

The share component is defined as one minus the share of liquid assets held in securities with maturity below three months, cash, and federal funds sold. Liquid assets are measured as total assets at fair value less total loans. Thus, this measure combines the extensive margin of holding securities beyond the shortest maturity bucket with the intensive margin of maturity within the longer securities portfolio.

We estimate the relationship between this exposure measure and the solvency ratio using the same binned-scatter procedure as in the main text. Plotting within-bin means of $\texttt{Total Exposure}_{it}$ against $\texttt{MTM Solvency Ratio}_{it}$ we get the result shown in Figure (7).

Figure 7: Solvency and duration-weighted exposure



B.3.2 Asset-side interest-rate exposure

We also construct a broader asset-side measure of interest-rate exposure based on the return-loading approach in Begenau et al. (2025). The measure assigns an interest-rate factor loading to each maturity bucket, which we then apply to the bank's position in that bucket. We construct it in four steps.

Step 1: two-factor return regressions. For each fixed-income instrument j (Treasuries, swaps, AAA and BBB corporate bonds, and agency MBS) and maturity m, we estimate the spanning regression of Begenau et al. (2025),

$$r_{jmt} = \alpha_{jm} + \beta_{jm}^{\mathrm{DF}} r_t^{\mathrm{DF}} + \beta_{jm}^{\mathrm{BBB}} r_t^{\mathrm{BBB}} + u_{jmt},$$

where the factors are the quarterly holding-period returns of a five-year default-free bond and a five-year BBB-rated bond. We reproduce their Table A.1 using only public data. Treasury and swap holding-period returns are constructed from FRED constant-maturity yields. For AAA and BBB bonds, we construct returns from a synthetic curve equal to

the Treasury zero curve plus a flat Moody's spread, while MBS returns come from an equal-weighted portfolio of agency-MBS ETFs. Table (11) reports the estimates under the Treasury-proxy factor convention for the full 1990Q2–2024Q1 sample. In Table (12), we use the swap-factor convention, restricting the sample to the shorter period for which FRED swap rates are available.

Step 2: orthogonalization. The BBB spanning return also contains an interest-rate component, so β_{jm}^{DF} alone does not give the instrument's interest-rate exposure. We write $r_t^{\mathrm{BBB}} = a\, r_t^{\mathrm{DF}} + (1-a) f_t^{\mathrm{credit}}$, with f^{credit} orthogonal to r^{DF}, and obtain the pure interest-rate loading as

$$b_{jm}^{\mathrm{IR}} \;=\; \beta_{jm}^{\mathrm{DF}} + a\, \beta_{jm}^{\mathrm{BBB}},$$

where we estimate a by regressing r^{BBB} on r^{DF} by OLS over a "normal-times" sample. We exclude stress quarters (2002Q2–2002Q4, 2008Q1–2009Q4, 2011Q3, and 2020Q1–2020Q2), since credit and rate factors comove during these quarters for crisis-specific reasons. Our estimate ($a \approx 0.68$) is close to the value of 0.6 used in Begenau et al. (2025).

Step 3: mapping loadings to Call Report buckets. We re-estimate the loadings separately for each maturity and value each Call Report repricing-maturity bucket at a single representative maturity. We use 0.25 years for the under-3-month bucket (its holding-period return is known one quarter ahead, so the loading is exactly zero), 0.625 years for 3 months–1 year, and 2, 4, 10, and 15 years for the 1–3, 3–5, 5–15, and over-15-year buckets, respectively. For the open-ended bucket, we use its 15-year lower bound, consistent with the maturity variables in Section (B.1). This understates the exposure of banks holding 20- or 30-year assets.

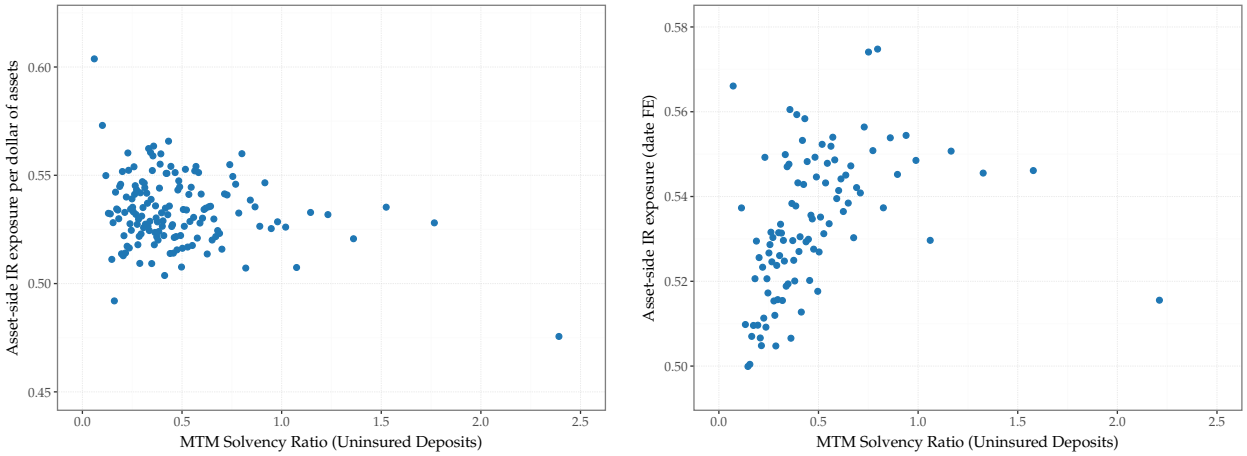
Step 4: bank-level aggregation. We assign a loading curve to each asset class. Treasuries use the Treasury curve, while mortgage-backed securities use the AAA curve (an approximation that ignores prepayment convexity). For residual securities and loans, we use a safe investment-grade proxy given by the midpoint of the AAA and BBB curves. We rescale the security buckets so that they sum to the fair value of total securities, preserving portfolio composition. For each bank-quarter, we multiply the position in each bucket by its interest-rate loading, sum across securities and loans, and normalize by total assets:

$$\texttt{Asset-side IR Exposure}_{it} \;=\; \frac{\sum_m S_{itm} b_m^{\mathrm{IR},S} + \sum_m L_{itm} b_m^{\mathrm{IR},L}}{\texttt{Total Assets}_{it}}.$$

The resulting variable is a duration-weighted dollar-equivalent position in the five-year default-free interest-rate factor per dollar of total assets. It is an asset-side measure: liabilities, interest-rate derivatives, and credit-default swaps are not included.

We relate this exposure measure to the market-adjusted solvency ratio relative to uninsured deposits using binned regressions. Panel A of Figure (8) displays the relationship without fixed effects using 150 bins. Panel B shows the same relationship using 100 bins while partialling out date fixed effects. In both panels, the horizontal axis is the solvency ratio based on market-adjusted equity with loans at amortized cost, divided by uninsured deposits, and the vertical axis is $\texttt{Asset-side IR Exposure}_{it}$.

Figure 8: Asset-side interest-rate exposure and solvency



Panel A: No fixed effects.

Panel B: Date fixed effects.

B.4 BHC aggregation

In this section, we check whether our empirical patterns survive once we aggregate banks across banking holding companies. Figure (9) shows the binned scatter plot of the share of long bonds against the solvency ratio, where we aggregate banks at the BHC level. Table (13) shows similar results as the ones exhibited in Section (3).

B.5 Different asset categories

We split banks in the following asset bins

1. 1.5B-10B
2. 10B-50B

Table 11: Properties of fixed-income returns: Treasury-proxy factor, 1990Q2–2024Q1

Instrument	Maturity	Mean (%)	Vol (%)	β^{IR}	t^{IR}	β^{BBB}	t^{BBB}	R^2	R^2 (1f)	ARCH p	Obs
Treasuries	short	3.76	2.44	0.37	16.98	0.03	0.96	0.81	0.81	0.01	136
Treasuries	medium	5.71	6.63	1.18	95.31	−0.03	−1.82	0.99	0.99	0.03	136
Treasuries	long	7.33	12.62	2.20	24.84	−0.22	−1.96	0.88	0.88	0.39	136
Swaps	short	3.49	2.33	0.35	10.79	0.02	0.52	0.73	0.72	0.95	65
Swaps	medium	6.51	6.74	1.21	29.02	−0.05	−0.81	0.95	0.95	0.89	65
Swaps	long	9.10	13.74	2.47	19.15	−0.37	−2.10	0.88	0.87	0.22	65
AAA	short	5.15	1.96	0.16	6.82	0.18	6.02	0.65	0.55	0.00	136
AAA	medium	7.01	4.89	0.52	13.34	0.44	8.93	0.85	0.76	0.08	136
AAA	long	8.40	9.63	0.80	6.17	0.77	4.71	0.57	0.50	0.20	136
BBB	short	6.14	2.10	−0.01	−0.61	0.42	15.87	0.76	0.31	0.02	136
BBB	medium	8.04	5.23	−0.03	−2.44	1.18	75.46	0.99	0.41	0.11	136
BBB	long	9.49	10.23	−0.39	−4.40	2.35	21.31	0.82	0.22	0.50	136
MBS (proxy)	all	2.45	4.02	0.54	11.39	0.30	5.62	0.80	0.70	0.00	68

Notes: Approximate public-data reproduction of Table A.1 of Begenau et al. (2025). Mean is 400× the mean quarterly return; vol is 200× the standard deviation of quarterly returns. Each row reports the regression $r_{jmt} = \alpha_{jm} + \beta^{IR}_{jm} f^{IR}_t + \beta^{BBB}_{jm} f^{BBB}_t + u_{jmt}$, estimated by OLS with an intercept; β^{IR} corresponds to the paper's β^{swap}. Short is 1–3 years, medium 5–7 years, long 10–15 years. Treasury and swap returns are approximate holding-period returns built from FRED constant-maturity par yields treated as zero-coupon yields. AAA and BBB returns come from a synthetic curve equal to the Treasury zero curve plus a flat Moody's DAAA/DBAA spread over the 10-year Treasury. The MBS proxy is an equal-weighted MBB/VMBS/SPMB ETF return starting in 2007Q2. R^2 (1f) is the R^2 of the one-factor (interest-rate only) regression. ARCH p is the p-value of the Engle ARCH test at 4 lags.

Table 12: Properties of fixed-income returns: swap-factor specification (FRED swap sample)

Instrument	Maturity	Mean (%)	Vol (%)	β^{IR}	t^{IR}	β^{BBB}	t^{BBB}	R^2	R^2 (1f)	ARCH p	Obs
Treasuries	short	2.96	2.15	0.32	11.71	0.02	0.49	0.75	0.75	0.05	65
Treasuries	medium	5.72	6.54	1.11	26.84	0.03	0.56	0.94	0.94	0.94	65
Treasuries	long	7.79	12.84	2.10	14.89	−0.14	−0.73	0.82	0.82	0.54	65
Swaps	short	3.49	2.33	0.36	13.10	0.02	0.45	0.79	0.79	0.69	65
Swaps	medium	6.51	6.74	1.20	81.67	−0.04	−2.04	0.99	0.99	0.05	65
Swaps	long	9.10	13.74	2.42	22.40	−0.34	−2.26	0.91	0.90	0.54	65
AAA	short	4.64	1.71	0.15	4.67	0.14	3.08	0.49	0.41	0.01	65
AAA	medium	7.40	4.68	0.55	8.99	0.37	4.35	0.75	0.67	0.20	65
AAA	long	9.39	9.92	0.90	4.67	0.55	2.04	0.43	0.39	0.77	65
BBB	short	5.76	1.87	−0.03	−1.00	0.40	10.32	0.68	0.12	0.78	65
BBB	medium	8.52	4.80	−0.02	−0.98	1.18	51.89	0.98	0.23	0.28	65
BBB	long	10.48	9.85	−0.33	−2.72	2.31	13.77	0.77	0.08	0.72	65
MBS (proxy)	all	3.86	2.87	0.42	9.05	0.15	2.43	0.74	0.70	0.61	39

Notes: Same construction as Table (11), with the interest-rate factor built from FRED swap rates instead of the Treasury proxy. The sample is restricted to the quarters where FRED swap rates are available (2000Q3–2016Q3), so the swap convention serves as validation of the Treasury-proxy convention used in the bank-level construction rather than as a second headline specification.

3. 50B-250B

4. >250B

Figure 9: Share of long bonds vs. Solvency Ration (BHC level)

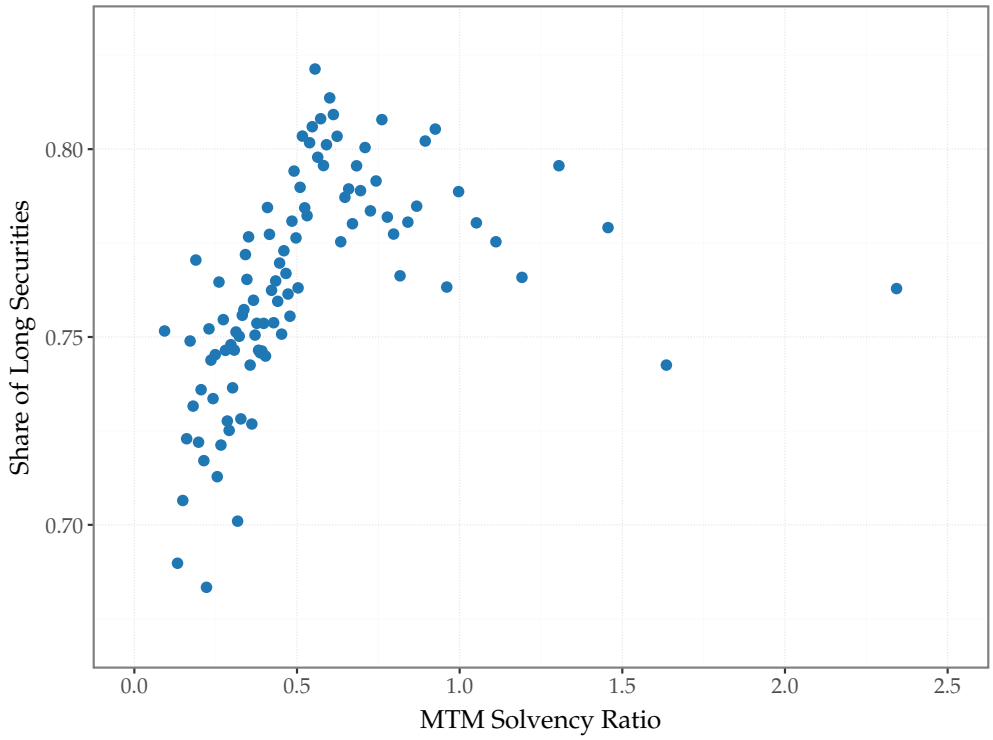


Table 13: Solvency and long-duration securities (BHC level)

	Share of Long Securities		
Intercept	0.731^{***}	0.712^{***}	1.284^{***}
	(0.003)	(0.005)	(0.042)
MTM Solvency Ratio	0.076^{***}	0.133^{***}	0.116^{***}
	(0.005)	(0.012)	(0.014)
MTM Solvency Ratio^2	-0.017^{***}	-0.042^{***}	-0.039^{***}
	(0.004)	(0.005)	(0.005)
Controls			√
Bank FE		√	√
Time FE		√	√
Observations	14,145	14,145	13,995
Banks	379	379	379
R^2	0.02	0.03	0.42

Notes: Standard errors in parentheses. $^{***}p < 0.01$, $^{**}p < 0.05$, $^{*}p < 0.10$. Controls include log assets, log deposits, lag loan share, lag cash share, uninsured deposit share, leverage ratio, and liability maturity. Standard errors are unadjusted.

Figure (10) shows the hump-shaped plot for banks between 1.5-10B USD in total assets (left panel), and 10-50B (right panel). Figure (11) shows that for larger banks, the pattern gets less smooth and converges into a tent shape, with its peak shifting slightly to the left.

Figure 10: Banks with less than 50B USD in total assets

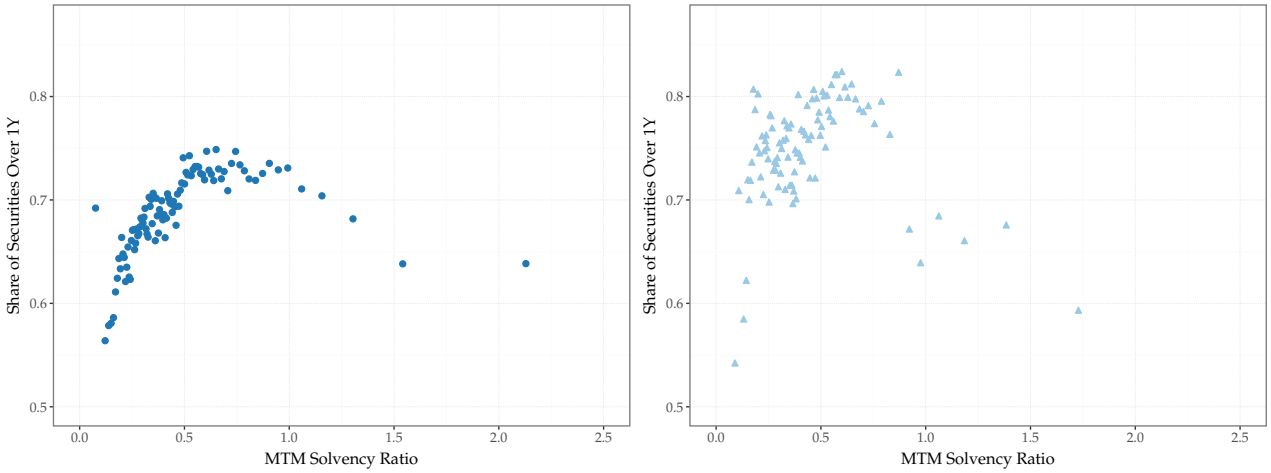
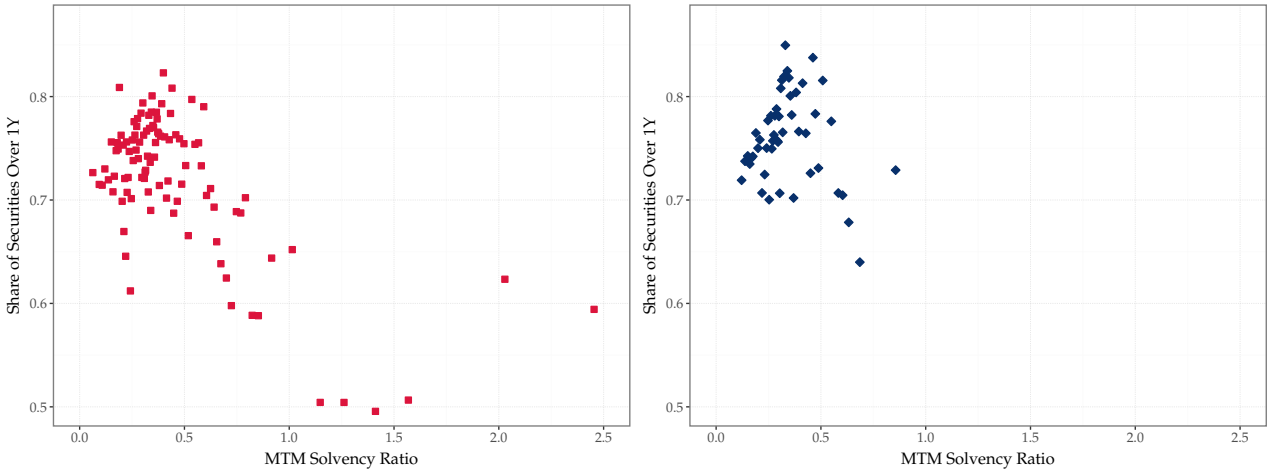


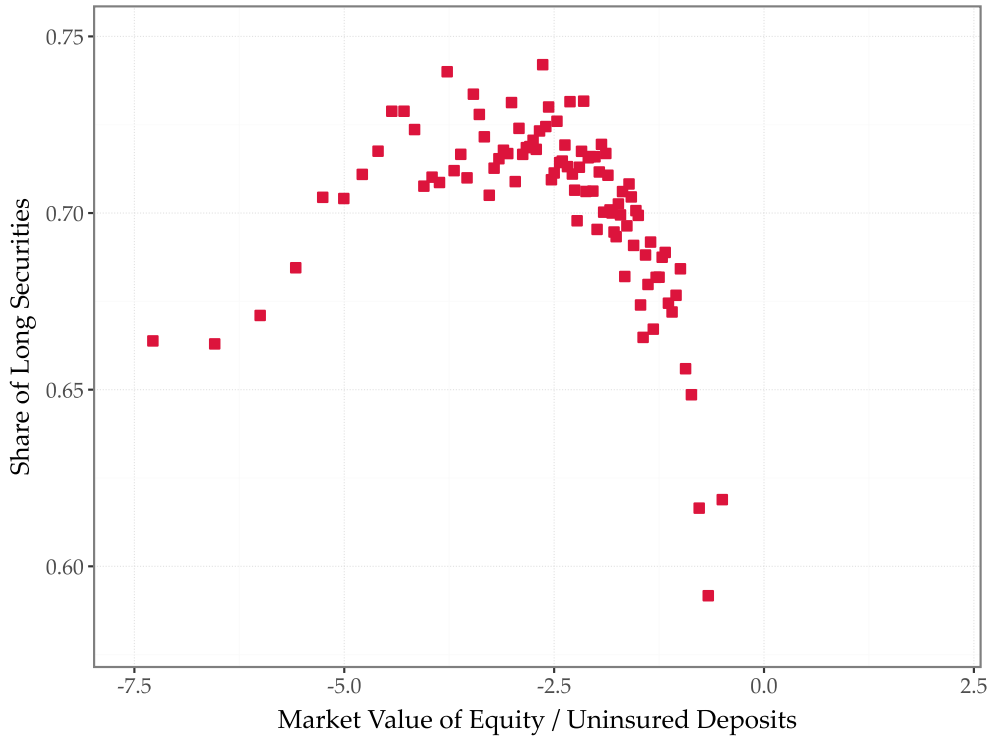
Figure 11: Banks with more than 50B USD in total assets



B.6 Alternative treatments to loans

Our measure of solvency from Section (3) adds unrealized gains/losses to book equity, which accounts for loans at face value. In this section, we consider two alternative treatments: *(i)* assume that since loans are illiquid, their market value is zero; *(ii)* we follow Jiang et al. (2024) and mark loans to market. We start by defining the market value of

Figure 12: Market value of equity excluding loans



equity excluding loans

$$\texttt{MTM Equity (without loans)}_{it} = \texttt{Book Equity}_{it} - \texttt{Total Loans}_{it} + \texttt{Unreal. Gains/Losses HTM}_{it}$$

Figure (12) shows that once we exclude the book value of loans from the bank's equity, the inverse U-shaped curve persists, although all banks have negative equity values.

B.6.1 Marking loans to market.

To impute unrealized gains and losses on bank loan portfolios we follow a Treasury-revaluation procedure in the spirit of Jiang et al. (2024), deliberately abstracting from credit risk so that the only source of mark-to-market variation is the movement in risk-free interest rates.

For each bank-quarter (i, t) we observe the outstanding stock of loans disaggregated by remaining maturity or next repricing date. The buckets are: less than 3 months, 3 months to 1 year, 1 to 3 years, 3 to 5 years, 5 to 15 years, and more than 15 years. We construct each bucket as the sum of the corresponding residential first-lien categories (Schedule RC-C, Part I, items on 1–4 family loans by repricing) and all other loan categories, so that total

loans by maturity cover the full loan book for which repricing information is disclosed. Variable-rate loans appear in the bucket corresponding to their next repricing date, not their contractual maturity, which is the convention in the Call Reports themselves.

We map each maturity bucket to a traded, credit-risk-free Treasury ETF whose effective duration approximates the midpoint of that bucket's repricing horizon. The mapping is: less than 3 months $\rightarrow$ BIL (1–3 month T-bills); 3 months to 1 year $\rightarrow$ SHV (short Treasury); 1–3 years $\rightarrow$ SHY; 3–5 years $\rightarrow$ IEI (3–7 year Treasury); 5–15 years $\rightarrow$ an equal-weighted blend of IEF (7–10 year) and TLH (10–20 year); more than 15 years $\rightarrow$ TLT (20+ year Treasury). We use adjusted closing prices from Yahoo Finance, sampled at the last trading day of each calendar quarter.[21]

For a chosen window of k quarters (our baseline sets $k = 2$, i.e. one semester), we compute the gross return on each proxy index over the window as

$$R_b(t) \;=\; \frac{P_b(t)}{P_b(t-k)},$$

where $P_b(t)$ is the quarter-end level of the ETF proxy for bucket b. The percentage price change is $\Delta_b(t) = R_b(t) - 1$, which is positive when Treasury prices rise (rates fall) and negative when Treasury prices fall (rates rise).

We apply each bucket's price change to the bank's *lagged* loan exposure in that bucket, that is, the book value reported k quarters earlier, rather than the contemporaneous stock. This timing convention ensures that we are reevaluating the portfolio that was actually exposed to the interest-rate moves over the window, and avoids a mechanical look-ahead bias from endogenous portfolio rebalancing during the window. The bucket-level gain or loss is $\mathrm{gl}_b(i,t) = L_b(i,\, t-k)\,\Delta_b(t)$, and the bank-level aggregate is

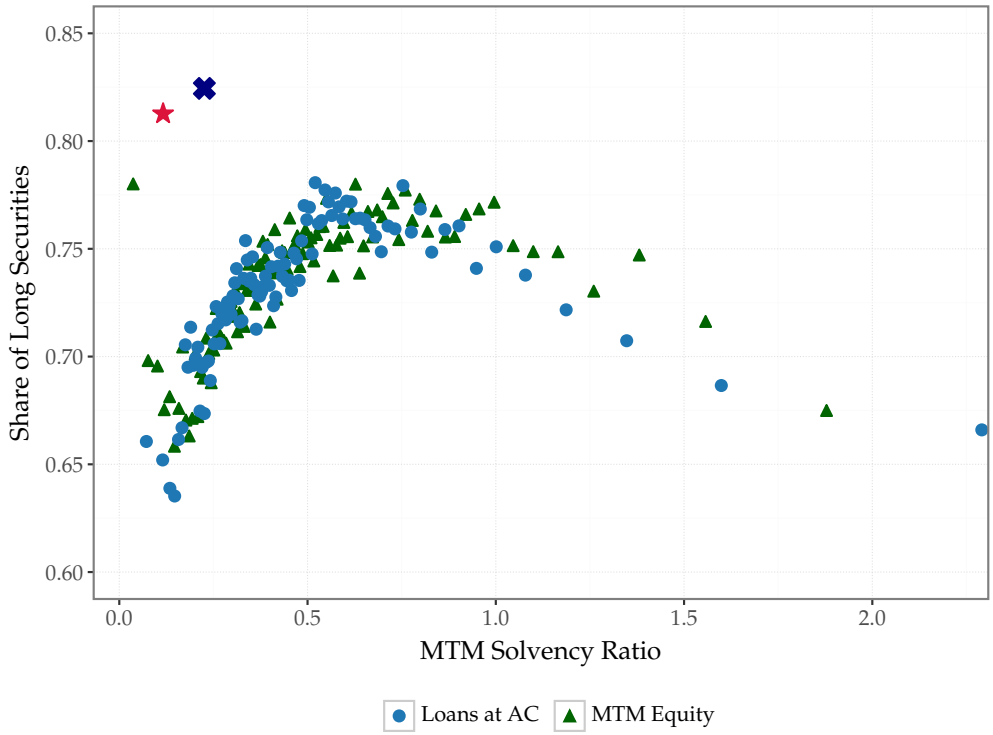
$$\texttt{MTM Loans Gains/Losses}_{i,t} \;=\; \sum_b L_b(i,\, t-k)\;\Delta_b(t), \tag{94}$$

where the sum runs over the six maturity buckets. A positive value indicates an unrealized gain on the loan portfolio (rates fell over the window); a negative value indicates an unrealized loss (rates rose).

This procedure isolates the duration channel: loans that reprice far in the future behave like longer-duration fixed-income claims and experiences larger mark-to-market swings

[21] Coverage varies by ETF inception date. BIL, SHV, and TLH began in 2007; therefore, earlier quarters have partial bucket coverage. We track a coverage share for each bank-quarter and, in the baseline, restrict the sample to observations with full coverage across all six buckets.

Figure 13: Market value of equity excluding loans



when rates move. Two approximations are worth noting. First, by using Treasury proxies, we assume that loan values move one-for-one with credit-risk-free rates of matching maturity, abstracting from credit spread variation. Second, for residential mortgages, prepayment optionality means that the effective duration is typically shorter than that of a non-callable Treasury bond; one can optionally scale the Treasury-based price change with an MBS multiplier (e.g., using the SPMB ETF relative to a duration-matched Treasury) to capture this, but our baseline omits this adjustment for transparency.

Figure (13) compares the relationship between the market value of equity and the share of long securities when loans are accounted at book value or priced according to treasury bonds.

B.7 Long bonds as deposit cash-flow hedge

A prominent explanation in the recent literature for why banks hold long-duration securities is that these positions hedge fluctuations in the cash flows generated by the deposit franchise. This has been emphasized empirically by DeMarzo et al. (2025): because deposit spreads tend to comove positively with short-term interest rates, long-duration securities (whose market values fall when rates rise) provide a natural hedge. In

other words, long bonds can generate valuation gains precisely when deposit cash flows are weak, and valuation losses when deposit cash flows are strong. The model of Section (2) builds in this hedging motive: depositors earn $r_t^x = \beta r_t$, so the deposit spread $r_t - r_t^x = (1-\beta) r_t$ rises with the short rate, while the long bond loses value when the short rate rises. The calibration does not target the evidence in this appendix. Table (4) reports one untargeted moment built from it: the cross-sectional correlation between a bank's deposit-spread sensitivity $1-\beta_i$ and its average long-bond share $\mathbb{E}[\alpha_i]$. We document the hedging relationship in three steps: we first measure the sensitivity of deposit spreads to the federal funds rate, then show that securities' unrealized gains and losses move in the opposite direction, and finally relate banks' deposit-spread sensitivities to their long-security holdings.

B.7.1 Deposit spreads and unrealized gains and losses

We measure deposit cash flow using deposit spreads. Specifically, we define the deposit rate as annualized interest expense on deposits divided by total deposits and define the deposit spread as

$$\texttt{Deposit Spread}_{it} = \texttt{FedFunds Rate}_t - \texttt{Deposit Rate}_{it}.$$

To capture interest-rate-driven valuation changes in the securities portfolio, we construct total unrealized gains/losses as the sum of (i) HTM unrealized gains/losses, measured as market value minus amortized cost, and (ii) AOCI, which primarily reflects unrealized gains/losses on AFS securities.

Following DeMarzo et al. (2025), we first document these offsetting exposures in the aggregate time series. Figure (14), Panel A (left), shows correlations of $\texttt{Deposit Spread}_{it}$ and total unrealized gains/losses with the (quarterly) federal funds rate. On average, deposit spreads comove positively with short rates, whereas unrealized gains/losses comove negatively with short rates. The pattern is consistent with long-duration securities serving as a hedge: when rates decline and deposit spreads compress, bond valuations rise and unrealized gains increase; when rates increase and deposit spreads improve, bond valuations fall and unrealized losses increase.

We estimate the sensitivity of each series to the federal funds rate using regressions of the form

$$s_{it}^j = \mu_i + \beta^j \, \texttt{FedFunds}_t + \epsilon_{it}^j, \qquad j \in \{\texttt{Deposit Spread}, \texttt{Unrealized G/L}\}.$$

Table (14) reports the pooled panel estimates of these sensitivities, including bank fixed effects.

Table 14: Sensitivity to the federal funds rate

	Deposit Spread	**Unrealized Gains/Losses**
Intercept	-0.004^{***}	0.003^{***}
	(0.000)	(0.000)
β	0.72^{***}	-0.40^{***}
	(0.002)	(0.003)
Bank FE	$\surd$	$\surd$
Observations	28,180	28,180
Within R^2	0.86	0.48

Notes: Standard errors in parentheses. $^{***}p < 0.01$, $^{**}p < 0.05$, $^{*}p < 0.10$.

B.7.2 Deposit-spread sensitivity and long securities across banks

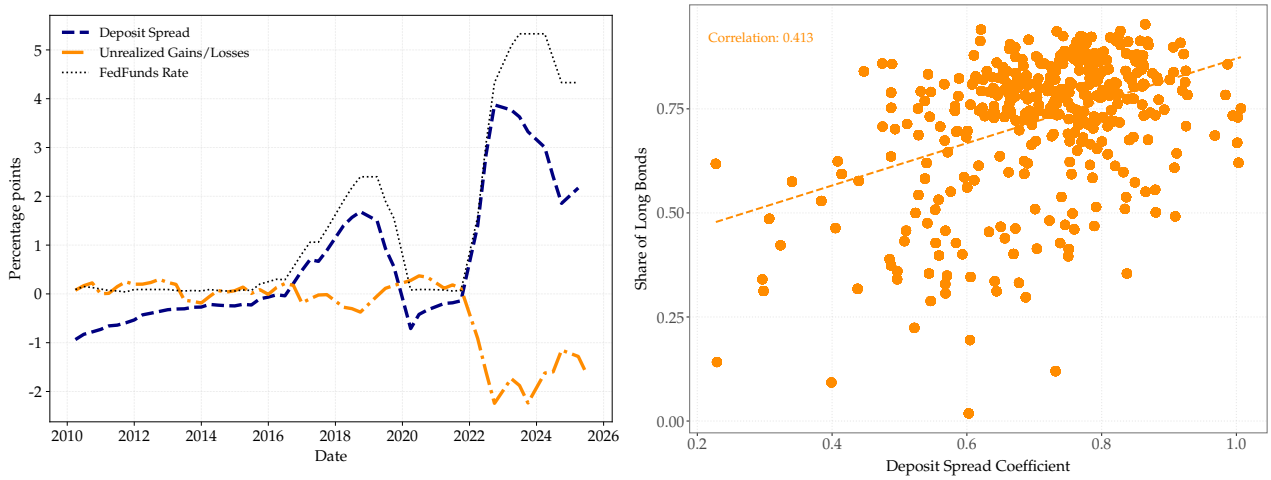
We next show that the same relationship appears at the bank level. We estimate the same regressions separately for each bank with at least 25 quarterly observations. For the deposit spread, the bank-specific slope is the bank's spread sensitivity, the data counterpart of $1-\beta$ in the model, which Table (4) denotes by $1-\beta_i$. Figure (14), Panel B (right), plots the sensitivity of deposit spreads to the federal funds rate against a bank's average share of long securities. Banks whose deposit spreads are more sensitive to short-term rates hold, on average, a larger share of their liquid assets in long securities.

The bank-level sensitivity underlying Panel B is estimated from a levels regression of the deposit spread on the federal funds rate, which mixes genuine deposit pass-through with common low-frequency movements in rates and spreads. In Appendix (B.7.3) we compute alternative deposit-spread sensitivity measures using first differences, distributed lags in levels and in differences, and specifications identified with the high-frequency monetary-policy surprises of Bauer and Swanson (2023). The bank ranking produced by the baseline estimator is largely preserved across the alternatives, and the main pattern of Panel B, a positive cross-sectional correlation between deposit-spread sensitivity and the average share of long securities, remains under every measure.

B.7.3 Alternative measures of deposit-spread sensitivity

Our baseline measure of a bank's deposit-spread sensitivity follows DeMarzo et al. (2025): bank by bank, we regress the *level* of the deposit spread, $s^D_{it} = \texttt{FedFunds Rate}_t - \texttt{Deposit Rate}_{it}$,

Figure 14: Deposit cash-flow hedge and long-duration securities



Notes: Panel A (left) shows correlations of deposit spreads and unrealized gains/losses with the (quarterly) federal funds rate in the aggregate time series. Panel B (right) shows the relationship between banks' deposit-spread sensitivity to the federal funds rate and their time-average holdings of long securities.

on the level of the fed funds rate,

$$s_{it}^{D} = \mu_i + \beta_i^{L0}\, r_t + \varepsilon_{it},$$

so that $\beta_i^{L0} = \partial s_{it}^{D} / \partial r_t$ is the bank-specific spread sensitivity. This section estimates alternative measures of deposit-spread sensitivity, and asks whether the cross-sectional relationship between spread sensitivity and the bank's average share of long securities survives. Every specification below is estimated bank by bank with Newey–West standard errors, and the dependent variable is always the deposit spread, so each coefficient is a spread sensitivity $\partial s_{it}^{D} / \partial r_t$ rather than a deposit-rate pass-through.

Unconditional rate variation. The first set of alternatives uses all observed movements in the fed funds rate:

- **Differences, contemporaneous:**

$$\Delta s_{it}^{D} = a_i + \beta_i^{D0}\, \Delta r_t + u_{it}.$$

- **Levels, cumulative over three lags:**

$$s_{it}^{D} = a_i + \sum_{\ell=0}^{3} \beta_{i,\ell}^{L}\, r_{t-\ell} + u_{it},$$

with the cumulative coefficient $\beta_i^{L,\text{cum}} = \sum_{\ell=0}^{3} \beta_{i,\ell}^{L}$.

- **Differences, cumulative over three lags:**

$$\Delta s_{it}^{D} = a_i + \sum_{\ell=0}^{3} \beta_{i,\ell}^{D} \, \Delta r_{t-\ell} + u_{it},$$

with $\beta_i^{D,\text{cum}} = \sum_{\ell=0}^{3} \beta_{i,\ell}^{D}$.

Identified monetary-policy surprises. Most movements in the policy rate are the endogenous response of policy to the economy. The second set of alternatives replaces Δr_t with the high-frequency monetary-policy surprises of Bauer and Swanson (2023) (FRBSF update), orthogonalized to pre-announcement macroeconomic and financial news and summed within each calendar quarter, $m_t = \sum_{e \in t} m_e$:

- **MP surprise, cumulative over three lags:**

$$\Delta s_{it}^{D} = a_i + \sum_{\ell=0}^{3} \theta_{i,\ell} \, m_{t-\ell} + u_{it},$$

with $\theta_i^{\text{cum}} = \sum_{\ell=0}^{3} \theta_{i,\ell}$.

- **Local projection at horizon four** (Jordà, 2005):

$$s_{i,t+h}^{D} - s_{i,t-1}^{D} = a_{i,h} + \psi_i(h) \, m_t + \Gamma_{i,h}' X_{i,t-1} + u_{i,t+h},$$

where $X_{i,t-1}$ contains two lags of Δs_{it}^{D} and of Δr_t, all strictly lagged.

A surprise is not a rate change: over 2022–2023 the Fed delivered roughly 500 basis points of hikes against about 35 basis points of cumulative surprise. To put the shock-based coefficients in rate units, we estimate the first-stage response of the one-year Treasury yield to the surprise (the maturity matched to the surprise's construction, which is scaled to have unit impact on the fourth eurodollar future) and rescale the estimates to basis points of spread response per 100 basis point impact rise in the one-year Treasury. The surprise sample runs through 2023Q4, and the quarters affected by the 2020 carve-out in the orthogonalized series are dropped rather than treated as zero-shock quarters.

Table (15) reports, for each estimator, the number of banks for which it is available, the mean of the estimated sensitivities, the dispersion of the estimated sensitivities, and the cross-sectional correlation with the bank's average share of long securities. The positive

cross-sectional relationship between spread sensitivity and the average share of long securities survives every estimator, with correlations between 0.14 and 0.43.

Table 15: Deposit-spread sensitivity: alternative estimators

Estimator	Banks	Mean	SD	Corr. with share long sec.
Levels, contemporaneous (baseline)	379	0.71	0.13	0.43
Differences, contemporaneous	369	0.92	0.07	0.32
Levels, cumulative over 3 lags	377	0.63	0.15	0.43
Differences, cumulative over 3 lags	369	0.69	0.15	0.34
MP surprise, cumulative over 3 lags	285	156.00	53.51	0.32
Local projection, horizon 4	321	37.08	46.55	0.14

Notes: Each row is a bank-by-bank estimator of the deposit-spread sensitivity $\partial s_{it}^{D} / \partial r_t$, estimated with Newey–West standard errors. The first four rows are per unit of the fed funds rate; the two surprise-based rows (in red) are in basis points of spread response per 100 basis point impact rise in the one-year Treasury, so their means and dispersion are on a different scale — correlations are scale-free and unaffected. "Corr. with share long sec." is the cross-sectional correlation between the estimated sensitivity and the bank's average share of long securities, computed on every bank for which the estimator is available.

B.8 Term Premium

Figure (15) plots the five-year term premium computed using the Adrian et al. (2013) (ACM) methodology, sampled quarterly at end-of-quarter dates over 2001Q1–2025Q4, the same sample used to estimate the real short-rate process in Section (4). The term premium is the component of the yield that compensates investors for bearing interest-rate risk over the life of the bond, as opposed to the part reflecting expectations of future short rates. The five-year term premium oscilates between positive and negative values through the sample period, and on average is around - 4 basis points. This number pins down the price of risk ς in the benchmark model with a constant term premium.

B.9 Within bank loan shares

In this section, we show data to support our assumption that banks' loan shares are constant across time ($d\ell_t = 0$).

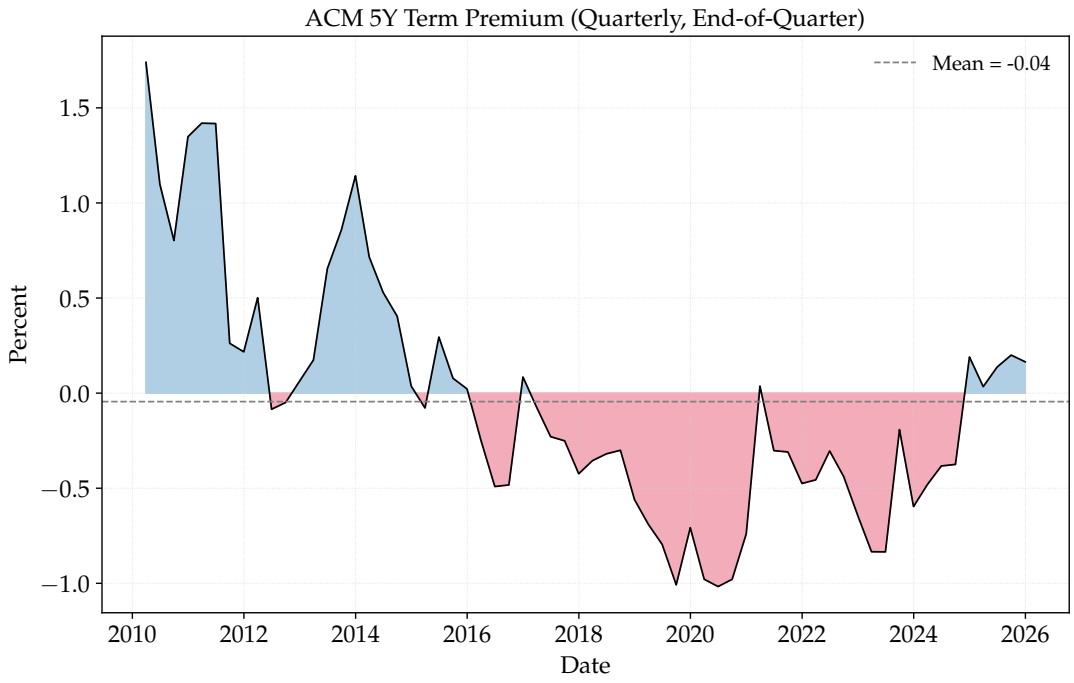


Figure 15: ACM five-year term premium (quarterly, end-of-quarter, 2001Q1–2025Q4).

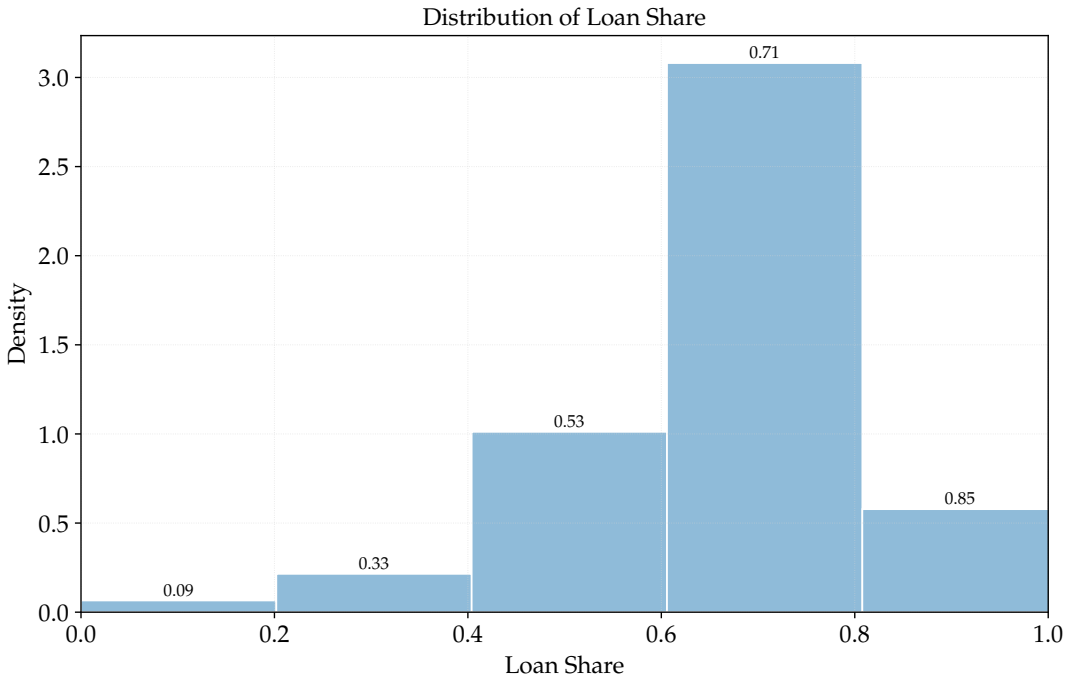


Figure 16: Distribution of loan shares

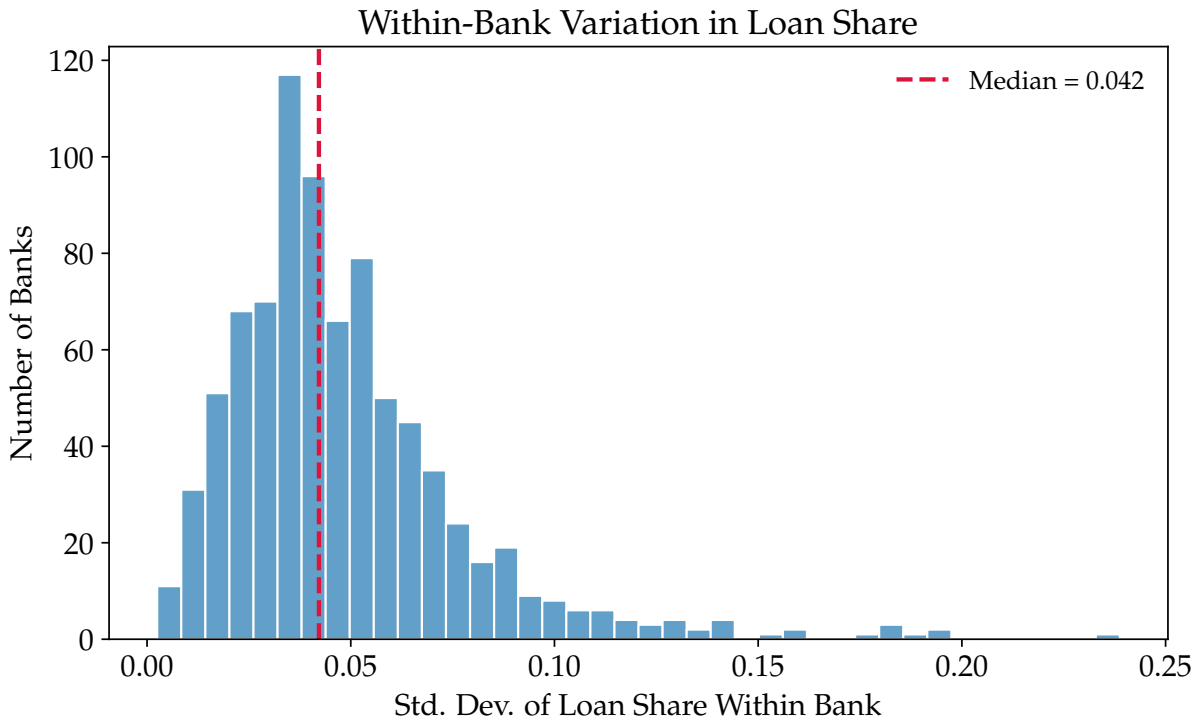


Figure 17: Within-bank variation of loan shares

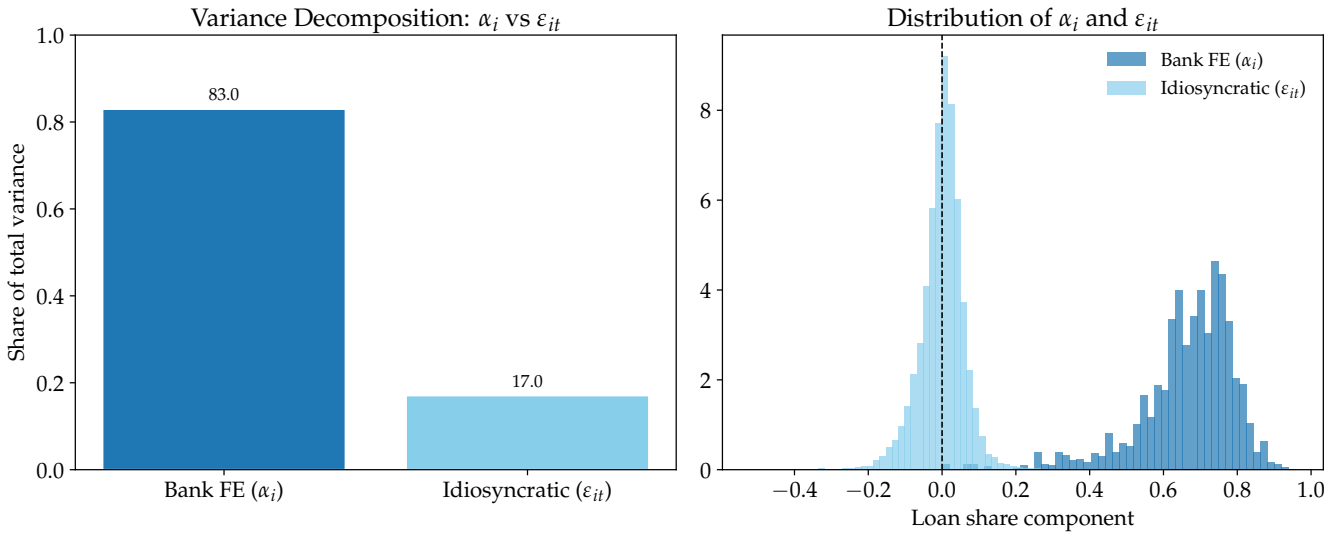


Figure 18: Variance decomposition of loan shares

C Calibration Appendix

C.1 Mapping the quarterly AR(1) into the continuous-time short-rate process

This appendix derives the exact mapping between the continuous-time short-rate process and the quarterly AR(1) used in the estimation. The model assumes that the real short rate follows

$$dr_t = \theta_r(\bar{r} - r_t)\,dt + \sigma_r\,dB_t, \tag{95}$$

where $\theta_r > 0$ and $\sigma_r > 0$. Define deviations from the long-run mean by

$$x_t \equiv r_t - \bar{r}. \tag{96}$$

Since $\bar{r}$ is constant, (95) implies

$$dx_t = -\theta_r x_t\,dt + \sigma_r\,dB_t. \tag{97}$$

Multiplying both sides by the integrating factor $e^{\theta_r t}$ gives

$$d\left(e^{\theta_r t}x_t\right) = \sigma_r e^{\theta_r t} dB_t. \tag{98}$$

Integrating from t to $t+\Delta$,

$$e^{\theta_r(t+\Delta)}x_{t+\Delta} - e^{\theta_r t}x_t = \sigma_r \int_t^{t+\Delta} e^{\theta_r s}\,dB_s. \tag{99}$$

Therefore,

$$x_{t+\Delta} = e^{-\theta_r\Delta}x_t + \sigma_r \int_t^{t+\Delta} e^{-\theta_r(t+\Delta-s)}\,dB_s. \tag{100}$$

Substituting back $x_t = r_t - \bar{r}$, we obtain

$$r_{t+\Delta} = \bar{r} + e^{-\theta_r\Delta}(r_t - \bar{r}) + \varepsilon_{t+\Delta}, \tag{101}$$

where

$$\varepsilon_{t+\Delta} \equiv \sigma_r \int_t^{t+\Delta} e^{-\theta_r(t+\Delta-s)}\,dB_s. \tag{102}$$

The innovation has conditional mean zero. By Itô isometry, its conditional variance is

$$\mathrm{Var}_t(\varepsilon_{t+\Delta}) = \sigma_r^2 \int_t^{t+\Delta} e^{-2\theta_r(t+\Delta-s)}\, ds \tag{103}$$

$$= \sigma_r^2 \int_0^{\Delta} e^{-2\theta_r u}\, du \tag{104}$$

$$= \frac{\sigma_r^2}{2\theta_r}\left(1 - e^{-2\theta_r \Delta}\right). \tag{105}$$

Hence,

$$\varepsilon_{t+\Delta} \sim N\left(0, \frac{\sigma_r^2}{2\theta_r}\left(1 - e^{-2\theta_r \Delta}\right)\right). \tag{106}$$

Because the data are quarterly, we set $\Delta = 1/4$. Then

$$r_{q+1} = \bar{r} + e^{-\theta_r/4}(r_q - \bar{r}) + \varepsilon_{q+1}. \tag{107}$$

This can be written as the AR(1)

$$r_{q+1} = a + b r_q + u_{q+1}, \tag{108}$$

with

$$b = e^{-\theta_r/4}, \qquad a = (1-b)\bar{r}. \tag{109}$$

The variance of the quarterly AR(1) innovation is

$$\sigma_u^2 = \frac{\sigma_r^2}{2\theta_r}\left(1 - e^{-2\theta_r/4}\right) = \frac{\sigma_r^2}{2\theta_r}(1 - b^2). \tag{110}$$

Therefore, the continuous-time parameters are recovered from the quarterly AR(1) coefficients by

$$\theta_r = -4 \log b, \qquad \bar{r} = \frac{a}{1-b}, \qquad \sigma_r = \left(\frac{2\theta_r \sigma_u^2}{1 - b^2}\right)^{1/2}. \tag{111}$$

This mapping is exact and does not rely on an Euler approximation.

C.2 Real rate AR(1) process with alternative maturities

Table (16) reports robustness exercises for the estimation of the short-rate process using alternative empirical proxies for the real safe rate. For the three-month specifications, we use the three-month Treasury bill rate and convert it to a quarterly frequency by averaging observations within each quarter. The ex-ante three-month real rate subtracts the

Survey of Professional Forecasters (SPF) median forecast of next-quarter headline CPI inflation, reported as an annualized quarter-over-quarter rate. The realized three-month specification instead subtracts realized CPI inflation. For the one-year specifications, we use the one-year Treasury yield and deflate it either by SPF one-year-ahead expected CPI inflation or by realized CPI inflation over the subsequent year. All rates are expressed in annual units, and the continuous-time parameters are obtained from the exact quarterly AR(1) mapping described above. The last row reports the price of risk implied by each specification when ς is calibrated, as in the main text, to the average five-year term premium.

Table 16: Robustness: alternative estimates of the real short-rate process

	Three-month Treasury bill		One-year Treasury yield	
Parameter	SPF inflation	Realized inflation	SPF inflation	Realized inflation
$\bar{r}$	−0.004928	−0.007280	−0.002723	−0.005961
θ_r	0.272531	0.599040	0.149765	0.544718
σ_r	0.010383	0.022010	0.007820	0.023889
σ_r/θ_r	0.038098	0.036742	0.052215	0.043856
ς	0.083678	0.086767	0.061055	0.072693

Notes: The table reports estimates of the continuous-time process $dr_t = \theta_r(\bar{r} - r_t)dt + \sigma_r dB_t$ obtained from its exact quarterly AR(1) representation over 2001Q1–2026Q3. SPF inflation denotes survey-based expected CPI inflation. Realized inflation denotes ex-post CPI inflation over the corresponding horizon. All rates are annualized and in decimal units. In every column, $\bar{r}$ is set to the sample mean of the real-rate series and θ_r and σ_r are estimated on the demeaned series; free-intercept estimates of θ_r and σ_r are virtually identical. The ratio σ_r/θ_r is the scale of long-bond exposure in the model. The price of risk $\varsigma = \overline{\mathrm{TP}}_{5y}\,\theta_r/\sigma_r$ is computed in every column from the same average five-year ACM term premium of 32 basis points (Figure (15)), so that each specification reproduces the same average term premium.

The distinction between the three-month and one-year Treasury measures is economically meaningful. Three-month Treasury bills are closer substitutes for money and other very liquid safe assets, and therefore their pecuniary yields may embed a larger liquidity or convenience-yield component than longer short-maturity Treasury securities (Krishnamurthy and Vissing-Jorgensen, 2012). As a result, real rates constructed from three-month bills can have a substantially lower estimated long-run mean $\bar{r}$ than real rates constructed from one-year Treasury yields. We therefore interpret the lower $\bar{r}$ in the three-month specifications not necessarily as evidence of a lower frictionless real short rate, but as reflecting that very short Treasury bills are more money-like. The one-year measure remains a short safe rate, but is less directly tied to the special liquidity services of Treasury bills.

C.3 Model with deposit shocks

The main text holds each bank's uninsured deposits fixed while it operates. This appendix presents the version of the model in which deposits follow a stochastic process, shows how deposit shocks enter the bank's problem and the distribution dynamics, and reports the calibration and the policy results obtained under that specification.

Deposit process. While the bank is operating normally ($J_{it} = 0$), deposits follow

$$dx_{it} = (1 - J_{it-})\Big[\bar{x}\,dt + \sigma_x\,dW^x_{it} - x_{it-}\,dJ_{it}\Big], \tag{112}$$

where x_{it-} denotes deposits immediately before a possible jump. The drift $\bar{x}$ captures the predictable component of deposit flows, and W^x_{it} is a standard Brownian motion that captures idiosyncratic net flows on a bank's deposits. Because deposits can in principle become negative under this specification, the numerical implementation imposes a reflecting barrier that keeps uninsured deposits above a lower bound.

Distribution dynamics. With deposit shocks, the state of an active bank is $s = (n, x, \ell)$ and the Kolmogorov forward equation for the distribution of active banks gains a drift and a diffusion term in x:

$$\begin{aligned} dg_t(s) = \Bigg[& -\frac{\partial}{\partial n}\Big(\mu_n(s,\Gamma_t)g_t(s)\Big) - \frac{\partial}{\partial x}\Big(\bar{x}g_t(s)\Big) \\ & + \frac{1}{2}\frac{\partial^2}{\partial n^2}\Big(\sigma_n(\alpha;s)^2 g_t(s)\Big) + \frac{1}{2}\frac{\partial^2}{\partial x^2}\Big(\sigma_x^2 g_t(s)\Big) \\ & - \underbrace{\lambda(s)g_t(s)}_{\text{Exit from } s \text{ due runs}} + \underbrace{\mathcal{E}_t(s)}_{\text{Entrants in } (s)}\Bigg]dt \\ & - \frac{\partial}{\partial n}\Big(\sigma_n(\alpha;s)\sigma_r g_t(s)\Big)dB_t. \end{aligned} \tag{113}$$

We assume that banks that suffer runs are replenished according to a distribution of entrants:

$$\mathcal{E}_t(s) = \underbrace{\psi_0(s)}_{\text{distr. of entrants}} \times \underbrace{\int \lambda(\tilde{s})g_t(\tilde{s})\,d\tilde{s}.}_{\text{mass of runs (failures) at } t}$$

Bank problem. The bank chooses dividend payouts c_t and the long-bond share α_t subject to the short-rate process (3), the deposit dynamics (112), the loan-share dynamics

(7), the net-worth dynamics (22), and the KFE (113). Write the KFE (25) compactly as $dg(s) = \mu_g(s;\Gamma)\,dt + \sigma_g(s;\Gamma)\,dB_t$, where μ_g is the bracketed drift term and $\sigma_g(s;\Gamma) = \partial_n\big(\sigma_n(\alpha;s)\,g(s)\big)$ is the loading of the distribution on the aggregate shock. The Hamilton–Jacobi–Bellman equation is:

$$\begin{aligned}\rho v(s,\Gamma) = \max_{c,\alpha}\Bigg\{ & u(c) + v_n\mu_n(\alpha,c;s,\Gamma) + v_x\bar{x} + \frac{1}{2}\sigma_n(\alpha;s)^2 v_{nn} + \frac{1}{2}\sigma_x^2 v_{xx} \\ & + v_r\theta_r(\bar{r}-r) + \frac{1}{2}\sigma_r^2 v_{rr} - \sigma_n(\alpha;s)\sigma_r v_{nr} + \int \frac{\partial v}{\partial g}\,\dot{g}\,ds \\ & + \lambda(s)\Big[\overline{v}(n,r) - v(s,\Gamma)\Big]\Bigg\}. \end{aligned} \tag{114}$$

Relative to the fixed-deposit problem, the deposit shock adds the drift term $v_x\bar{x}$ and the diffusion term $\frac{1}{2}\sigma_x^2 v_{xx}$, so that the bank's value depends on the level of deposits through both the expected growth of its funding base and the idiosyncratic risk to that base.

Deposit process parameters. We parameterize real uninsured deposits as an arithmetic Brownian motion,

$$dx_t = \bar{x}\,dt + \sigma_x\,dW_t^x, \tag{115}$$

so that

$$\mu_x(x_t) = \bar{x}, \qquad \sigma_x(x_t) = \sigma_x.$$

This specification implies that innovations to deposits have constant volatility in levels. Consequently, the volatility of deposit growth is decreasing in the size of the deposit base:

$$\frac{dx_t}{x_t} = \frac{\bar{x}}{x_t}\,dt + \frac{\sigma_x}{x_t}\,dW_t^x.$$

Thus, larger banks face lower proportional deposit-flow volatility, since σ_x/x_t is smaller for banks with larger deposit bases. This feature is aligned with the empirical evidence that deposit outflows are less volatile for large banks than for small banks (Corbae and D'Erasmo, 2021, Aguirregabiria et al., 2025).

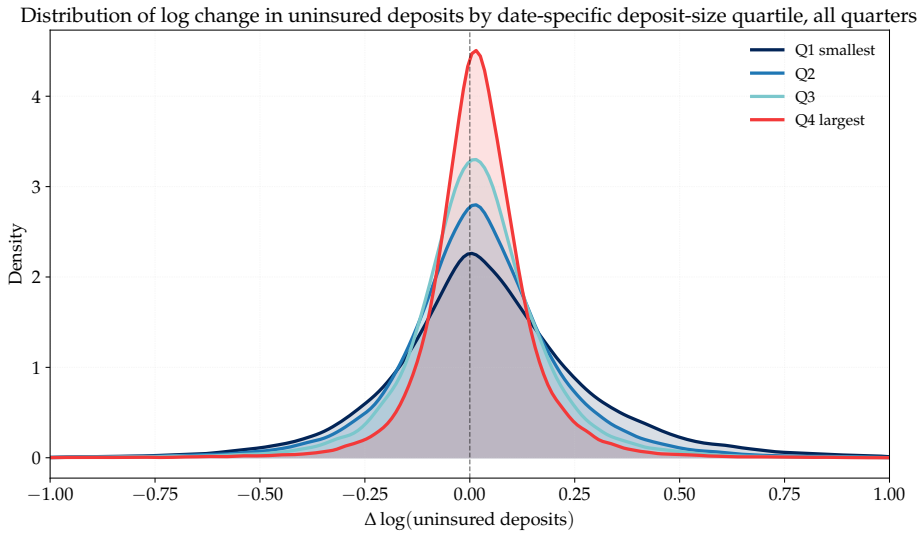
We estimate (115) directly on the real deposit index x_{it} defined above, using its exact quarterly discretization, $x_{i,t+1} - x_{it} = \bar{x}/4 + \sigma_x\,\varepsilon_{it}/2$. The sample has 921 banks and 27,139 consecutive bank-quarter changes over 2010Q1–2025Q1, winsorized at the first and ninety-ninth percentiles. The drift is the pooled mean change and the volatility is the standard deviation of changes after removing quarter means, so that dated aggregate

movements in deposits, such as the 2020–2022 surge and its reversal, do not enter the idiosyncratic volatility:

$$\widehat{\overline{x}} = 8.62 \qquad \widehat{\sigma}_x = 21.26$$

Figure (19) provides direct motivation for the arithmetic specification of deposit dynamics. The figure plots the distribution of quarterly log changes in uninsured deposits, separately by date-specific deposit-size quartiles. The smallest banks display the widest distribution and the fattest tails, while the largest banks display the narrowest distribution. Because quartiles are computed within each quarter, this pattern is not driven by aggregate time variation in deposit conditions, but instead reflects cross-sectional differences in proportional deposit-flow volatility. This evidence supports modeling deposits as an arithmetic Brownian motion, $\mu_x(x) = \overline{x}$ and $\sigma_x(x) = \sigma_x$. With constant volatility in deposit levels, the volatility of deposit growth is approximately σ_x/x, so larger banks face lower proportional deposit volatility.

Figure 19: Geometric vs. Arithmetic Brownian motion



Calibration. Table (18) reports the parameters of the model with deposit shocks. This version predates the baseline calibration of the main text: it uses the deposit drift and volatility estimated above, a deposit-rate sensitivity $\beta = 0.40$, fixed $\gamma = 2$ and $\rho = 0.03$, and it targets the average run rate rather than the failure rate. The policy results in Table (20) and Figure (4) in the main text were computed under this version.

Table 17: Distribution of Deposit Growth by Deposit-Size Quartile

Deposit-size quartile	Observations	Mean	Std. dev.	Median	Banks
Q1 smallest	88,877	0.052	0.287	0.033	3,809
Q2	93,764	0.014	0.230	0.017	4,433
Q3	94,509	0.006	0.200	0.012	4,072
Q4 largest	94,562	0.009	0.173	0.016	3,019

Notes: Summary statistics for quarterly log changes in uninsured deposits by date-specific deposit-size quartile. Quartiles are computed within each quarter using the level of uninsured deposits. "Banks" is the number of distinct banks observed in each quartile over the sample.

Table 18: Baseline parameters: model with deposit shocks.

Parameter	**Value**	**Description**	**Source**
Externally calibrated			
k	0.00	Withdrawal cost	Benchmark
γ	2.00	Risk aversion	Standard
ρ	0.03	Impatience rate	Standard
ζ	0.035	DIF coverage ratio	Baseline
$\overline{r}$	0.0179	Average rate	Data
θ_r	0.15	Mean reversion of rates	Data
σ_r	0.01	Volatility of rates	Data
ς	-0.01	Price of risk	Data
ι	0.026	Inflation rate	Data
$\overline{x}$	8.62	Deposit drift	Data
σ_x	21.26	Deposit volatility	Data
ξ	0.03	Credit spread	Data
β	0.40	Deposit rate sensitivity	Drechsler et al. (2026)
Internally calibrated			
Y	0.74	Utility shift	
δ	0.75	Fire-sale discount	
λ_0	0.012	Level of run-risk	
λ_1	6.70	Slope of run-risk	
κ_1	0.010	Linear franchise cost coefficient	

Internally calibrated parameters. The parameters $(Y, \kappa_1, \lambda_0, \lambda_1, \delta)$ are calibrated internally. We set 2010Q1 as the initial distribution extracted from the Call Reports. We then apply the policy functions from the model's solution, associated with a sequence of exogenous shocks $\{dB_t\}$ to generate a panel of simulated banks. We then run the regression specified in (32) and match its coefficients, the average annual run rate, and the median solvency ratio n/x in the data. Table (19) reports the fit.

Moment	Data	Model
Targeted		
Avg. run rate	0.35%	0.37%
Median n/x	0.42	0.31
Table (1), pooled: Intercept	0.67	0.57
Table (1), pooled: MTM solvency ratio	0.17	0.21
Table (1), pooled: MTM solvency ratio^2	-0.08	-0.04
Untargeted		
Table (1), Date FE: MTM solvency ratio	0.14	0.23
Table (1), Date FE: MTM solvency ratio^2	-0.07	-0.04
Table (1), Date + bank FE: MTM solvency ratio	0.08	0.13
Table (1), Date + bank FE: MTM solvency ratio^2	-0.03	-0.02
Corr$\left(1-\beta_i,\, \mathbb{E}[\alpha_i]\right)$	0.41	0.84

Table 19: Model fit: model with deposit shocks

Table (19) also reports untargeted moments from the fixed-effects versions of the regression in Table (1). Mirroring the empirical evidence, adding date fixed effects leaves the model's coefficients close to the pooled estimates, so aggregate conditions common to all banks account for little of the hump. Adding bank fixed effects lowers both coefficients in the model, as it does in the data, but the linear term remains positive and the quadratic term remains negative. Thus, in the model as in the data, both persistent differences across banks and within-bank movements in solvency contribute to the hump, with bank-specific characteristics doing more of the work.

Policy results. Table (20) repeats the duration-restriction exercise of the main text in the model with deposit shocks.

Table (20) shows the effect of the floor on deposits in run banks and securities losses along the realized rate path. We start by noticing that the policy reduces considerably the losses in the security portfolio in 2022, from 17.3% to 2.3%. This attenuates the effect of the rate hikes in 2022, as banks are less exposed to duration.

Table 20: Duration restrictions along the realized rate path: model with deposit shocks.

	Deposits in run banks	Sec. losses in 2022 (%)
FDIC, no floor	1.00	-17.3
FDIC + floor $\phi = 0.1$	0.99	-16.6
FDIC + floor $\phi = 0.2$	0.94	-11.1
FDIC + floor $\phi = 0.3$	0.89	-5.2
FDIC + floor $\phi = 0.4$	0.87	-2.3

Banks start from the empirical 2010Q1 cross-section and are followed to 2025Q2 along the observed path of the 3-month T-bill rate; $1,000$ panels of 300 banks. Deposit insurance is in place in every row. The floor is based on a rate increase of $\Delta r = +100$bp in (34). Deposits in run banks are the expected deposits of banks that fail between 2022Q1 and 2025Q2, relative to the no-floor row. Securities losses are the 2022 mark-to-market change as a percent of the securities book.

D Policy Appendix

D.1 Computation of banks' welfare

Table 7 reports banks' welfare as a consumption equivalent. This appendix describes how we compute it.

Banks and rate paths. We follow the banks of the empirical 2010Q1 cross-section, each from its initial state $s_{i0} = (n_{i0}, x_{i0}, \ell_{i0}, r_0)$ in the cross-section, until their first run. The short rate starts at its 2010Q1 value and follows the estimated process (3) until $\bar{T} = 2025\text{Q}2$. We draw 2,000 paths of the short rate, the same in every economy. In each economy, every bank follows its own optimal policies (c, α) and pays the fee (26), which balances the insurance fund at every date given all banks operating at that date, entrants included. Entrants pay the fee but do not enter the welfare calculation.

Welfare of a bank. Let T_i be the date of bank i's first run. In each economy, its welfare is

$$W_i = \mathbb{E}\left[\int_0^{T_i \wedge \bar{T}} e^{-\rho t}\, u(c_{it})\, dt + \mathbb{1}_{\{T_i \le \bar{T}\}}\, e^{-\rho T_i}\, \overline{v}\big(n_{iT_i}, r_{T_i}\big) + \mathbb{1}_{\{T_i > \bar{T}\}}\, e^{-\rho \bar{T}}\, v\big(s_{i\bar{T}}, \Gamma_{\bar{T}}\big)\right],$$

where the expectation is over the paths of the short rate and over run dates. Given a path of the short rate, net worth evolves deterministically and the run is a Poisson event with intensity $\lambda(s_{it})$. We therefore compute the expectation over run dates exactly, weighting each date by the survival probability $\exp\{-\int_0^t \lambda(s_{iu})\, du\}$; only the rate paths are simulated. Notice that the tax charged at $\bar{T}$ will be assumed to remain constant for $t > \bar{T}$.

Consumption equivalent. In the benchmark economy, without deposit insurance and without floor, we scale dividends by $1 + \mu$ at every date and state while the bank operates. The extra dividends are paid from outside the bank, so its balance sheet, its policies and its run dates do not change:

$$\begin{aligned} W_i(\mu) = \mathbb{E}\Big[\int_0^{T_i \wedge \bar{T}} & e^{-\rho t}\, u\big((1+\mu)\, c_{it}\big)\, dt + \mathbb{1}_{\{T_i \le \bar{T}\}}\, e^{-\rho T_i}\, \overline{v}\big(n_{iT_i}, r_{T_i}\big) \\ & + \mathbb{1}_{\{T_i > \bar{T}\}}\, e^{-\rho \bar{T}}\, v_\mu\big(s_{i\bar{T}}\big)\Big]. \end{aligned}$$

The continuation value v_μ keeps the benchmark policies and solves the linear equation $(\rho + \lambda - \mathcal{A})\, v_\mu = u\big((1+\mu)\, c\big) + \lambda\, \overline{v}$, where $\mathcal{A}$ is the generator of the state under those

policies. The post-run value $\overline{v}$ is not scaled.

Aggregation. We use one $\bar{\mu}$ for all banks and all rate paths, which solves

$$\sum_i w_i \underbrace{W_i(\bar{\mu})}_{\text{no FDIC, no floor}} = \sum_i w_i \underbrace{W_i}_{\text{policy economy}},$$

and Table 7 reports $10^4\,\bar{\mu}$, in basis points of dividends. Since $Y > 0$, u is not homothetic, so $\bar{\mu}$ is not a ratio of values. We expand $u\big((1+\mu)\,c\big)$ to fourth order in μ, which is exact to numerical precision at the values in our tables, and solve for $\bar{\mu}$. For instance, deposit insurance without a floor gives $\bar{\mu} = -11.6$ basis points: the fee costs the 2010Q1 banks as much as a permanent cut of 0.116% in their dividends.

D.2 A positive cost of moving the banking relationship

The quantitative results in Section 5 set $k = 0$. The run cutoff is then the fire-sale solvency threshold in (21), and deposit insurance affects banks only through the fee τ. This appendix repeats the policy exercises with $k = 0.01$: a depositor who requests withdrawal from a surviving bank, or whose bank fails, loses one cent per dollar received when she moves her banking relationship. The cutoff is then the one characterized in Proposition 2, and the run intensity is (20).

With $k > 0$, Proposition 2 requires $0 \leq \zeta < \ell(1-\delta)$ for every bank. We keep $\zeta = 0.035$, as in Table 7, and compare with the $k = 0$ economy at the same coverage. We keep every other parameter at its calibrated value, except the level of run risk λ_0, which we raise to keep the failure rate (see below). Each economy, with and without deposit insurance and with and without each floor, is solved again with its own cutoff $z^*(\ell, \zeta, k)$ and its own fee (26). We impose no closure floor in these computations ($\underline{z} = -1$), so all failures are induced by withdrawal requests.

Calibration with $k = 0.01$. With every other parameter fixed, a positive relationship cost lowers the run cutoff of Proposition 2, and with it the failure rate, the targeted moment in Table 4: from 0.111% to 0.103% a year. One parameter is enough to restore it. Raising the level of run risk λ_0 by 12.8%, from 0.0103 to 0.0117, brings the failure rate with $k = 0.01$ back to 0.11% a year. Table 21 reports the fit of this economy. The hump is close to the one in Table 4: the intercept is 0.67, the slope 0.18 and the curvature -0.06, against 0.67, 0.17 and -0.08 in the data. The median n/x and aggregate c/n are unchanged. The policy

results below, and the $k = 0.01$ columns of Table 7, use the rescaled λ_0. With λ_0 at its value in Table 2, deposit insurance would raise banks' welfare by 32.1 basis points of dividends instead of 33.9, and no ranking of the policies would change.

Table 21: Model fit with $k = 0.01$ and λ_0 rescaled.

Moment	**Data**	**Model,** $k = 0.01$
Targeted		
Avg. run rate	$< 0.36\%$	0.11%
Agg. c/n	0.07	0.08
Median n/x	0.42	0.44
Table (1), pooled: Intercept	0.67	0.67
Table (1), pooled: MTM solvency ratio	0.17	0.18
Table (1), pooled: MTM solvency ratio^2	-0.08	-0.06
Untargeted		
Table (1), Date FE: MTM solvency ratio	0.14	0.17
Table (1), Date FE: MTM solvency ratio^2	-0.07	-0.06
Table (1), Date + bank FE: MTM solvency ratio	0.08	0.09
Table (1), Date + bank FE: MTM solvency ratio^2	-0.03	-0.07

Design of Table 4. The model has $k = 0.01$, deposit insurance at $\zeta = 0.035$ and $\lambda_0 = 0.0117$; every other parameter is as in Table 2. Only λ_0 is changed, to match the failure rate.

Duration restrictions along the realized path. Table 22 repeats Table 6 at $\zeta = 0.035$ for $k = 0$ and $k = 0.01$. The effect of the floor is unchanged: it reduces deposits in run banks by 16% at $\phi = 0.3$ and by 21% at $\phi = 0.4$, and it reduces the 2022 securities losses by the same amounts as with $k = 0$. With λ_0 rescaled, the level of deposits in run banks over 2022–25 and the deposit-insurance fee are those of $k = 0$: 0.2% higher, and 0.56 basis points without a floor. Deposit insurance now also prevents some runs: without it, deposits in run banks over 2022–25 would be 3.7% higher, whereas with $k = 0$ they are the same with and without insurance.

Welfare. The last two columns of Table 7, in the main text, report welfare with $k = 0.01$. Banks' welfare is a consumption equivalent for the 2010Q1 banks, followed until their first run: the permanent change in dividends, in basis points of dividends, that makes the banks of the economy without deposit insurance or floor as well off as in each row. Depositors' welfare is the fall in the expected discounted losses of these banks' depositors at failure: principal losses $[\ell(1-\delta)-\zeta]x$ and, with $k > 0$, the relationship cost $k[1-\ell(1-\delta)+\zeta]x$, in basis points of the banks' 2010Q1 deposits. Both are averaged over 2,000 simulated paths of the short rate from 2010Q1 to 2025Q2.

Table 22: Duration restrictions along the realized rate path, $k = 0$ and $k = 0.01$.

	$k = 0$			$k = 0.01$		
	Deposits in run banks	Sec. losses in 2022 (%)	DIF fee (bp)	Deposits in run banks	Sec. losses in 2022 (%)	DIF fee (bp)
FDIC, no floor	1.00	−17.7	0.56	1.00	−18.1	0.56
FDIC + floor $\phi = 0.1$	0.99	−17.9	0.55	0.99	−18.3	0.55
FDIC + floor $\phi = 0.2$	0.95	−17.2	0.53	0.95	−17.5	0.53
FDIC + floor $\phi = 0.3$	0.84	−13.2	0.47	0.84	−13.5	0.47
FDIC + floor $\phi = 0.4$	0.79	−7.8	0.44	0.79	−8.0	0.44

Design of Table 6 with deposit insurance at $\zeta = 0.035$. Deposits in run banks over 2022Q1–2025Q2 are relative to the no-floor row of the same k; the no-floor level is 0.2% higher with $k = 0.01$. The fee is the average over 2022Q1–2025Q2, in basis points of deposits per year. With $k = 0.01$, λ_0 is rescaled as in Table 21.

With $k = 0.01$, deposit insurance raises banks' welfare by 33.9 basis points of dividends, against a loss of 11.6 with $k = 0$. The gain comes entirely from the more liquid banks in the model (the ones with the lowest ℓ), about 10% of the 2010Q1 banks. Insurance lowers their cutoff from 0.028 to −0.029, which cuts their run intensity by 18% to 32% across the solvency range. Net of the fee, insurance raises the welfare of these banks by 4.4% of their dividends in consumption-equivalent terms. The banks with higher ℓ only pay the fee, as with $k = 0$, and don't see dramatic reductions on their run risk. Depositors gain 14.2 basis points from insurance, close to the 13.9 with $k = 0$, since their gain is the coverage paid on failing deposits. This gain is sensitive to where ζ sits relative to the band above. Whether insurance improves banks' welfare therefore depends on the size of k and on the fire-sale discount of the most liquid banks.

The floor works as with $k = 0$. Relative to insurance alone, it costs banks between 6 and 62 basis points of dividends and raises depositors' welfare by at most 0.21 basis points of deposits, at $\phi = 0.3$. Its cost to banks is somewhat larger than with $k = 0$ (between 5 and 58 basis points of dividends). At $\phi = 0.3$, the floor costs banks 31.5 basis points of dividends with $k = 0$, 30.9 with $k = 0.01$ for any coverage up to $\zeta = 0.03$, and 34.3 at $\zeta = 0.035$. The last step falls entirely on the banks with less loans, whose runs insurance now prevents: their consumption-equivalent loss from the floor rises from 1.3% at $\zeta = 0.03$ to 1.6%. A plausible reading of the last step is that banks that face fewer runs expect to operate longer, so the restriction on their portfolio weighs on a longer stream of income.

D.3 Deposit-insurance fees that depend on risk

In Section 5 every operating bank pays the same fee τ_t in (26). This appendix lets the fee of bank i depend on its expected claim on the insurance fund, $\zeta\lambda(s_{it})x_{it}$, that is, banks will pay more as they are riskier:

$$\tau_{it} = \tau_t + \vartheta\big(\zeta\lambda(s_{it})\, x_{it} - \tau_t\big).$$

Notice that as we integrate the tax across banks, we have:

$$\int \tau_{it} g(s) dz = (1-\vartheta)\tau_t + \vartheta \int \zeta\lambda(s) x g(s) ds = \tau_t$$

That, is, the total tax charged remains equal to τ_t, and ϑ only shuffles who pays for this bill. Moreover, the only moment we still need keep is ω (deposits at risk). With $\vartheta = 0$ every bank pays the common fee of Section 5, and with $\vartheta = 1$ every bank pays its own expected claim. With $\vartheta = -1$ banks with a high run intensity pay less than the average fee, and safe banks pay more. We keep $\zeta = 0.035$ and report both $k = 0$ and $k = 0.01$, with λ_0 as in Table 7 (rescaled for $k = 0.01$, Appendix D.2). Each economy, with and without each floor, is solved again with its own fees.

Table 23 repeats Table 7 with $\vartheta = -1$. Charging weak banks less raises banks' welfare at every floor. With $\vartheta < 0$, the FDIC premium provides insurance to risky banks, whose additional dollar of networth is extremely valuable. This, however, generates some perverse incentives, as risky banks increase their dividend payouts and fail more, at the expense of safe banks.

Table 23: Welfare gains with risk-based fees: banks vs. depositors, $\vartheta = 0$ and $\vartheta = -1$.

	$\vartheta = 0$ (common fee)		$\vartheta = -1$	
	Banks, CE (bp of div.)	Depositors (bp of dep.)	Banks, CE (bp of div.)	Depositors (bp of dep.)
Panel A: $k = 0$				
No FDIC, no floor	0	0	0	0
FDIC, no floor	-11.6	$+13.85$	-8.3	$+13.79$
FDIC, floor $\phi = 0.1$	-16.7	$+13.88$	-13.5	$+13.82$
FDIC, floor $\phi = 0.2$	-25.8	$+13.93$	-22.3	$+13.87$
FDIC, floor $\phi = 0.3$	-43.0	$+13.98$	-39.1	$+13.92$
FDIC, floor $\phi = 0.4$	-69.1	$+13.90$	-64.2	$+13.84$
Panel B: $k = 0.01$				
No FDIC, no floor	0	0	0	0
FDIC, no floor	$+33.9$	$+14.15$	$+37.0$	$+14.08$
FDIC, floor $\phi = 0.1$	$+28.4$	$+14.20$	$+31.5$	$+14.14$
FDIC, floor $\phi = 0.2$	$+18.0$	$+14.29$	$+21.3$	$+14.22$
FDIC, floor $\phi = 0.3$	-0.4	$+14.36$	$+3.5$	$+14.29$
FDIC, floor $\phi = 0.4$	-28.3	$+14.25$	-23.6	$+14.18$

Design of Table 7, with $\zeta = 0.035$ and λ_0 as in that table; the $\vartheta = 0$ columns repeat its columns for the same k. Without deposit insurance there is no fee, so the No FDIC rows do not depend on ϑ.